UNIVERSITY OF OTTAWA

ENHANCED IEEE 802.11.P-BASED MAC PROTOCOLS FOR VEHICULAR AD HOC NETWORKS

by

YAMEN NASRALLAH

A THESIS

SUBMITTED TO THE FACULTY OF GRADUATE STUDIES

IN PARTIAL FULFILLMENT OF THE REQUIREMENTS FOR THE

DEGREE OF Ph.D IN ELECTRICAL AND COMPUTER ENGINEERING

SCHOOL OF ELECTRICAL ENGINEERING AND COMPUTER SCIENCE

FACULTY OF ENGINEERING

UNIVERSITY OF OTTAWA

OTTAWA, CANADA

MARCH, 2017

Abstract

The Intelligent Transportation System (ITS) is a cooperative system that relies on reliable and robust communication schemes among vehicles and between vehicles and their surroundings. The main objective of the ITS is to ensure the safety of vehicle drivers and pedestrians. It provides an efficient and reliable transportation system that enhances traffic management, reduces congestion time, enables smooth traffic re-routing, and avoids economic losses.

An essential part of the ITS is the Vehicular Ad hoc Network (VANET). VANET enables the setup of Vehicle-to-Vehicle (V2V) as well as Vehicle-to-Infrastructure (V2I) communication platforms: the two key components in the ITS. The de-facto standard used in wireless V2V and V2I communication applications is the Dedicated Short Range Communication (DSRC). The protocol that defines the specifications for the Medium Access Control (MAC) layer and the physical layer in the DSRC is the IEEE 802.11p protocol. The IEEE 802.11p protocol and its Enhanced Distributed Channel Access (EDCA) mechanism are the main focus of this thesis. Our main objective is to develop new IEEE 802.11p-based protocol for V2V and V2I communication systems, to improve the performance of safety-related applications. These applications are of paramount importance in ITS, because their goal is to decrease the rate of vehicle collisions, and hence reduce the enormous costs associated with them. In fact, large percentage of vehicle collisions can be easily avoided with the exchange of relevant information between vehicles and the Road Side Units (RSUs) installed on the sides of the roads.

In this thesis, we propose various enhancements to the IEEE 802.11p protocol to improve its performance by lowering the average end-to-end delay and increasing the average network throughput. We introduce multiple adaptive algorithms to promote the QoS support across all the Access Categories (AC) in IEEE 802.11p. We propose two adaptive backoff algorithms and two algorithms that adaptively change the values of the Arbitrary Inter-Frame Space (AIFS). Then we extend our model to be applied in a large-scale vehicular network. In this context, a multi-layer cluster-based architecture is adopted, and two new distributed time synchronization mechanisms are developed.

Acknowledgements

I would like to sincerely thank my supervisor, Prof. Hussein T. Mouftah, for his encouragement, advices and engagement through the learning and development process of this thesis. I am greatly indebted to him for all the time, efforts, and strong support he provided over the past years.

Beside my supervisor, I must express my sincere gratitude to my co-supervisor, Dr. Irfan Al-Anbagi, for the patient guidance, motivation and continuous support. I have been extremely lucky and honoured to work with him. He cared so much about my work, he spent a significant amount of his time in responding to my queries, discussing my ideas and reading my papers.

Table of Contents

List of Tables

List of Figures

List of Acronyms

Acronym	Definition
AAA	Adaptive AIFS Algorithm
ABA	Adaptive Backoff Algorithm
ABF	Adaptive Broadcast Frame
AC	Access Category
ACK	Acknowledgement
AIFS	Arbitration Inter-Frame Space
AIS	Automatic Identification System
ASDM	Adaptive Space Division Multiplexing
ASTC	Adaptive Service Time Control
BEV	Battery Electric Vehicle
CBMMAC	Clustering Based Multichannel MAC
CCH	Code Division Multiple Access
CRC	Cluster-Range Control
CRD	Cluster-Range Data
CRP	Contention-based Reservation Period
CSMA/CA	Carrier Sense Multiple Access with Collision Avoidance
CTS	Clear To Send
CW	Contention Window
DB	Directional Beam
DCF	Distributed Coordination Function
DCTS	Directional CTS
DDMAC	Dedicated Multi-Channel MAC
DIFS	DCF Inter-Frame Space

DRTS	Directional RTS
DMAC	Directional MAC
DMAC/NT	DMAC with NAVE Table
DTS	Distributed Time Synchronization
DSRC	Dedicated Short Range Communication
ECDSA	Elliptic Curve Digital Signature Algorithm
EPRI	Electric Power Research Institute
EV	Electric Vehicle
GPS	Global Positioning System
HCCA	Hybrid Coordination Function Controlled Channel Access
ICC	Inter-Cluster Control
LM	Location and Mobility-Aware
LTE	Long-Term Evolution
MAC	Medium Access Control
Manet	Mobil Ad hoc Network
MCMAC	Multichannel MAC
MCTRP	Multi-Channel Token-Ring Protocol
NAV	Network Allocation Vector
NS-2	Network Simulator 2
PC	Point Coordination
PCF	Point Coordination Function
PHEV	Plug-in Hybrid Electric Vehicle
QoE	Quality of Experience
QoS	Quality of Service
QDTS	QoS Distributed Time Synchronization
RF	Radio Frequency

RTS	Request To Send
SCH	Service Channel
SDMA	Space Division Multiple Access
SIFS	Short Inter-Frame Space
SPA	Strict Priority Algorithm
TDMA	Time Division Multiple Access
TxOP	Transmission Opportunity
UMTS	Universal Mobile Telecommunication Systems
VANET	Vehicular Ad hoc Network
V2I	Vehicle to Infrastructure
V2G	Vehicle to Grid
V2V	Vehicle to Vehicle
WAVE	Wireless Access for Vehicular Environment
WPCF	WAVE Point Coordination Function

List of Symbols

Symbol	Definition
α	Number of timeslots in a buffer
α_i	Internal collision probability of AC_i
$Area_i$	Contention zone of AC_i
BD	Average buffering delay
$BD[i]$	Average buffer delay in the CH at layer i
β	Total transmission probability of a vehicle
β_i	External transmission probability of AC_i
b_I	Stationary probability at the idle state
$b_{i,j}$	Stationary probability at state (i, j)
b_{Q0}	Stationary probability at the first buffer Q_0
$b(t)$	backoff counter at time t
$s(t)$	backoff stage at time t
CW_i	Size of the contention window at backoff stage i
δ	Propagation delay
D_{cer}	Total delay of the certificate and its signature
$D_{ITS-sgs}$	ITS to smart grid server communication delay
D_{Proc}	Processing delay due to the certificate generation
D_Q	Queuing delay in the RSU
$D_{RSU-ITS}$	RSU to ITS server communication delay
D_{ver}	Time to verify a signature at the destination
η	Average number of vehicles that can select a given timeslot
$E[D_{col}]$	Average end to end delay of a successful transmission after multiple attempts
$E[D_i]$	Average end to end delay of AC i

$E[D_{suc}]$	Average end to end delay after only one transmission attempt
$E_i[backoff]$	Average delay at the backoff stage
$E_i[state]$	Average time spent in each backoff state
$E_i[bloc]$	Average time spent in at the backoff stage due to blocking mechanism
$E_i[N_{block}]$	Average number of time a state i got frozen
$E_i[Retr]$	Average number of packet retransmission
$E[T_I]$	Average idle time of the medium
$E[T_{suc}]$	Average successful transmission time
$E[T_{col}]$	Average failed transmission time
IF_i^j	Increment factor of AC i at the j^{th} backoff phase
l	Number of timeslots in the buffer reserved by a vehicle
λ	Message arrival rate to the RSU queue
L_{cer}	Size of a certificate in Bytes
L_{Header}	Size of the header in Bytes
$L_{payload}$	Size of the payload in Bytes
L_{pk}	Size of a packet in Bytes
L_{sig}	Size of the signature in Bytes
L_{WSM}	Size of a signed WSM message in Bytes
M	Maximum number of times the contention window may be increased
$M+f$	Maximum number of transmission attempts
μ	Service rate of the RSU
N	Number of vehicle in the network
$n_{c,i}^j$	Number of collisions experienced by AC_i at j^{th} phase
n_i	Size of $Area_i$
$n_{s,i}^j$	Number of successful transmission AC_i at j^{th} phase
$n_{t,i}^j$	Total number of packet transmitted by AC_i at j^{th} phase

TS	Time Slot
$\phi[i]$	Number of CH at layer i
p_a	Packet arrival rate probability
P_c	Total external collision probability of a vehicle
p_{ci}	Collision probability of AC_i
p_i	Probability of being at the idle state
$P_i[suc]$	Probability of successful transmission by AC_i
$P[I]$	Probability of the channel being idle
$P[fail]$	Probability of packet transmission failure due to a collision
PF_i^j	Priority factor of AC i at the j^{th} backoff phase
Ψ	Backoff multiplicative factor that depends on p_c
Ψ_i^j	Ψ for AC_i at jth phase
Rat	Quotient of $\frac{/alpha}{T_{SF}}$
Rem	Remainder of $\frac{/alpha}{T_{SF}}$
σ_i	Backoff blocking probability for AC_i
θ_j	Probability of j vehicles trying to access a timeslot
T_{ACK}	Transmission time of ACK message
T_{AIFS}	Duration of an AIFS
T_{CCH}	Size of CCH channel
T_{ci}	Time of a failed transmission due to a collision by AC_i
T_{col}	Time of an unsuccessful transmission
T_{Header}	Transmission time of the header
T_I	Idle time of the medium
T_{Load}	Transmission time of the data packet
Th	Average Throughput of a vehicle
Th_i	Average Throughput of AC_i

T_{SCH}	Size of the SCH channel
T_{SF}	Size of the super frame
T_{sens}	Time of sensing the channel
T_{SIFS}	Duration of an SIFS
T_{si}	Time of a successful transmission by AC_i
T_{suc}	Time of a successful transmission by a vehicle
τ_i	Total internal transmission probability of AC_i
$T_{Timeslot}$	Duration of a time slot
WT	Total wait time (AIFS+Backoff) before sending a packet

Chapter 1

Introduction

1.1 Background

Currently, an increasing number of governments around the world are investing a significant amount of resources to develop an Intelligent Transportation System (ITS). The increasing interest in this field is due to the alarming statistics of vehicles road collisions and injuries. According to the National Highway Transportation Safety Administration (NHSTA), in the United States (US) for 2015 alone, more than 6 million collisions involving vehicles were registered on US roadways which accounted for 2.35 million injuries and 35000 deaths [1]. In Canada, according to the Canadian Motor Vehicle Traffic Collision Statistics (CMVTCS), more than 115,000 collisions took place in 2014 resulting in more than 3000 fatalities and almost 150,000 total injuries [2]. In addition, the economic cost related to collisions and traffic congestions, in terms of time wasted and physical loss, is estimated to be in the billions of dollars. For example, in 2009 the Organization for Economic Co-operation and Development (OECD) reported that Toronto alone incurred congestion costs of 3.3 billion dollars [3].

In 2016, as a measure to improve road safety, the US government approved the FAST Act which provides long-term funding of more than 200 million dollars per year for ITS research to improve the safety of the roads (reduce vehicle collisions), reduce congestions impacts, and provide grants to develop new traffic management technologies [4].

ITS is a cooperative traffic management system that require reliable and robust communication schemes among vehicles and between vehicles and their road surroundings to ensure the safety of vehicle drivers and pedestrians. Enabling this system should increase the efficiency and the reliability of the transportation system. This is achieved by automating vehicle interaction responsiveness with its immediate surroundings and thereby contributing to road-user safety: through

reducing congestion time, enabling smooth traffic re-routing, and over time impact positively the economy.

The backbone of the ITS system is the Vehicular Ad hoc Network (VANET). The main feature of VANET is that it enables the communications between vehicles that are equipped with a network device called On-Board Unit (OBU). The importance of the VANET comes from the fact that it allows the setup of Vehicle-to-Vehicle (V2V) as well as Vehicle-to-Infrastructure (V2I) communication platforms; the two key components in the ITS. VANETs applications can be divided into three classes: road safety, traffic management, and infotainment. In this thesis, we focus on the V2I environment with an emphasis on the road safety-related applications in VANET.

Road safety applications are an integral part of VANET to manage inter-vehicle communications to avoid vehicle collisions. In fact, large percentage of vehicle collisions can be easily avoided with the exchange of relevant information between vehicles and the infrastructure such as Road Side Units (RSUs) that are installed on the side of the roads.

The de facto standard used in wireless inter-vehicle and V2I communication applications is the Dedicated Short Range Communication (DSRC) [5]. DSRC is specifically designed to cope with the highly dynamic environments of vehicular networks. This standard is the only short-range, wireless alternative today that provides the following features: high reliable connection, low delay communication, prioritized service, interoperability, and security and privacy [6].

DSRC consists of two main protocols, namely, the Wireless Access in Vehicular Environment (WAVE) [7] and the IEEE 802.11p protocol [8]. WAVE functions at the network, transport, and application layers while IEEE 802.11p functions at the physical and link layers. This thesis focuses on the IEEE 802.11p standard and its Enhanced Distributed Channel Access (EDCA) mechanism. The latter is based on the Carrier Sense Multiple Access with Collision Avoidance (CSMA/CA) technique and it enables Quality of Service (QoS) support services. The detailed description and analysis of the IEEE 802.11p protocol is presented in Chapter 3.

1.2 Motivation

This work is motivated by the need of a systematic and detailed development of a QoS-based communication system in vehicular environment to meet the conditions and demands set by different services. There is a wide range of V2V and V2I applications that vary considerably in terms of features, requirements and constraints. Each type of application is characterized by different needs and level of service. For example, safety-related applications require minimum response time, traffic management applications require reliable system, and Electric Vehicle (EV) to smart grid communication requires efficient and in some cases real-time interaction.

Based on the literature, the area of QoS-aware Medium Access Control (MAC) protocol in the vehicular environment is still developing, and there is a considerable room for the investigation, design, improvement and development of new protocols to attain enhanced outcomes. More specifically, in the field of V2V and V2I communications related to safety services and other such as EV-smart grid communications.

In the EV-smart grid communication environment, The EV power capacity and the electric grid status information should be collected and exchanged wirelessly to determine better, efficient and economic charging operation of the EVs. The communication pattern and requirements may change based on the charging stations location, accessibility and the availability of power. For example, an alert can be issued to the driver when the battery capacity is below a certain level. This alert triggers the communication process between the EV and the smart grid and it returns with information, to the driver, that includes a list of charging station's location, distance, available power and its cost. Therefore, this service requires a great throughput quality with acceptable delays.

On the other hand, a safety-related service, such as a collision-avoidance service, has its own set of requirements, and the most important one is to have the least possible latency (near real-time communication) with good throughput quality. Because, once a collision occurs, after receiving a notification message from a near-by vehicle, the RSU must broadcast this information to the incoming vehicles in the least possible delay to avoid additional accidents and ensure their safety.

Table 1.1: Latency Requirements for Some VANET Applications

Service	**Requirement**
Intersection Collision Warning	$\leq$ 100 ms
Pre-Crash Sensing	$\leq$ 20 ms
Transit Vehicle Signal Priority	$\leq$ 100 ms
Approaching Emergency Vehicle Warning	$\leq$ 1000 ms
Video Conference	$\leq$ 150 ms
VoIP	$\leq$ 150 ms
Interactive Game	$\leq$ 250 ms

Table. 1.1 shows the maximum end-to-end delay required for some VANET safety and non-safety related applications [9]. The value associated to each service is the delay threshold beyond which the application fails to provide an optimal service. Otherwise, there could be serious consequences, especially in safety-related applications, if the performance of the communication protocol at the link layer introduces further delay that adds up to a total latency exceeding the value in Table. 1.1.

1.3 Objectives

Our main objective in this thesis is to develop new IEEE 802.11p-based protocols for V2V and V2I communication systems. We extend the IEEE 802.11p protocol to support QoS functionalities such as differentiated services. Our target is to provide high system reliability and low end-to-end delay during the communication among vehicles or between the vehicles and the RSU. Various enhancement to the IEEE 802.11p are proposed to improve its performance and to promote the QoS support. Different simulations are made in order to evaluate the different characteristics of VANET and its interaction with the surrounding infrastructure.

One accurate and highly effective way to study the performance of IEEE 802.11p is by developing an analytical model that translates its actual operations and functions, into mathematical equations. Our aim in this thesis, is to develop a comprehensive Markov chain-based analytical model to analyse and evaluate the performance of the new IEEE 802.11p-based protocols. We first, replicate the behaviour of the IEEE 802.11p protocol by considering the real factors that influences its opera-

tion. Then, we expand this model to improve its performance further to achieve a more reliable, efficient and near-real time communication protocols that suit the safety-related applications in VANETs.

Moreover, our objective is to extend the one-hop communication architecture to a multi-hop network architecture. We tackle the synchronization among the vehicles and enable QoS support in the new extended model. In the new architecture we propose multiple algorithms and scenarios to achieve the best results in terms of average end-to-end delay and average throughput per vehicle and per class or Access Category (AC).

1.4 Contributions

The main research contributions of this thesis are as follows:

1. We have developed an accurate Markov-based analytical model that replicates the real behaviour of the IEEE 802.11p protocols by taking into account all aspects that represent its actual operation.

2. We have introduced multiple enhanced and adaptive QoS-based algorithms that improve the performance of IEEE 802.11p protocol in VANET.

3. We have developed a new scalable time synchronization mechanism based on a distributed approach in a multi-hop network architecture.

4. We have developed a QoS-based distributed time synchronization mechanism in a large-scale vehicular network. It enables the time slot distribution based on the AC rather than the vehicles.

5. We have extend the simulation tool Network Simulator 2 (NS2) to fully support the EDCA algorithm and the new enhanced proposed protocols.

6. We have extended our Markov-based model to analytically model our new proposed QoS-based IEEE 802.11p-based protocols.

7. We have provided a comprehensive survey of the available research work in the literature about existing MAC protocols in VANET, and about protocols that aim to improve IEEE 802.11p.

1.5 Evaluation Tools

The main tools used in the process of the design and evaluation of the proposed algorithms are the following:

- Discrete-event Markov chain

  It was used to model the analytical model of our proposed schemes. By deriving the equations of its steady state and by resolving them we were able to determine the performance metrics such as the throughput and the latency of the system.

- MATLAB

  It is a numerical computation tool used to resolve the non-linear set of equations derived form the Markov chain-based models.

- Network Simulator 2

  It is a network simulator environment which was extended to support our proposed algorithms. NS2 validates the findings from the proposed analytical model.

1.6 Thesis Outline

The remainder of this thesis is organized as follows. Chapter 2 surveys the available research contributions and presents the related work. Chapter 3 introduces our accurate Markov-based analytical model of IEEE 802.11p and our first enhanced analytical model: IEEE 802.11p with

finite buffer. Chapter 4 describes our proposed IEEE 802.11p adaptive algorithms: two adaptive backoff algorithms and two AIFS adaptive algorithms. Chapter 5 studies two main subjects related to our enhanced algorithm proposed in Chapter 3. Subject 1: we study the impact of mobility on the V2I communications. Subject 2: we propose a new mechanism based on the finite-buffer model to alleviate the influence of the delay introduced at the RSU queue. Chapter 6 presents our two distributed time synchronization mechanisms for large-scale vehicular networks. Chapter 7 concludes this thesis and envisions future research directions.

List of Publications

1. Y. Y. Nasrallah, I. Al-Anbagi and H. T. Mouftah,"Performance Analysis of IEEE 802.11p Protocol With Finite Buffers". (Submitted)

2. Y. Y. Nasrallah, I. Al-Anbagi and H. T. Mouftah, "A quality of service model for IEEE 802.11p communication protocol in a smart city," *Proceedings of 2014 Global Information Infrastructure and Networking Symposium (GIIS*), Montreal, QC, pp. 1–3, Setp. 2014.

3. Y. Y. Nasrallah, I. Al-Anbagi and H. T. Mouftah, "A realistic analytical model of IEEE 802.11p for Wireless Access in Vehicular Networks," in *Proceedings of 2014 International Conference on Connected Vehicles and Expo (ICCVE)*, Vienna, pp. 1029–1034, Nov. 2014.

4. Y. Y. Nasrallah, I. Al-Anbagi and H. T. Mouftah, "Mobility impact on the performance of electric vehicle-to-grid communications in smart grid environment," *Proceedings 2015 IEEE Symposium on Computers and Communication (ISCC*, Larnaca, pp. 764-769, Jul. 2015.

5. Y. Y. Nasrallah, I. Al-Anbagi and H. T. Mouftah, "Adaptive Service Time Control in Wireless Access for Vehicular Environment," *Proceedings 2015 IEEE International Conference on Ubiquitous Wireless Broadband (ICUWB)*, Montreal, QC, pp. 1–5, Oct. 2015.

6. Y. Y. Nasrallah, I. Al-Anbagi and H. T. Mouftah, "Distributed time synchronization mechanism for large-scale vehicular networks,"*Proceedings 2016 International Conference on Selected Topics in Mobile & Wireless Networking (MoWNeT)*, Cairo, pp. 1–6, Apr. 2016. **(Best Student Paper Award).**

7. Y. Y. Nasrallah, I. Al-Anbagi and H. T. Mouftah, "QoS-based Distributed Time

Synchronization mechanism for high intensity vehicular networks," *Proceedings 2016 IEEE Symposium on Computers and Communication (ISCC)*, Messina, pp. 958–963, June 2016.

8. Y. Y. Nasrallah, I. Al-Anbagi and H. T. Mouftah, "Adaptive Backoff Algorithm for EDCA in the IEEE 802.11p protocol," *2016 International Wireless Communications and Mobile Computing Conference (IWCMC)*, Paphos, pp. 800–805, Sept. 2016.

9. Y. Y. Nasrallah, I. Al-Anbagi and H. T. Mouftah, "Strict Priority and Adaptive AIFS-based Algorithm for EDCA in the IEEE 802.11p protocol," *2017 IEEE 86th Vehicular Technology Conference (VTC2017-Fall)*, Toronto, Canada, Sept. 2017. (submitted)

10. Yamen Y. Nasrallah, Irfan Al-Anbagi, Hussein T. Mouftah, "A Realistic Analtycal Model of IEEE 802.11p for Intelligent Transportation System", a poster presented at 2014 WiSense Workshop, University of Ottawa, Ottawa, Aug. 2014. **(Second Best Poster Award).**

Chapter 2

Survey of Related Work

2.1 Introduction

In this chapter, we review the state-of-the-art in the field of the vehicular communication networks. We review a variety of communication architectures studied for that purpose. We especially pay a closer look to the different approaches proposed to develop Medium Access Control (MAC) protocols suitable for vehicular environment. We focus on the IEEE 802.11p protocol and we present various analytical and mathematical models developed to achieve better performance in terms of throughput and delay. We also present many survey studies about different subjects related to Vehicular Ad hoc Network (VANET)s.

2.2 Mathematical Models of IEEE 802.11p

In this section, we start with a short survey about some IEEE 802.11-based mathematical models, followed with a lengthy survey about Markov-Based analytical model of IEEE 802.11p, and finally we present few papers that study non-Markov base mathematical model of some proposed protocols in VANET.

2.2.1 Mathematical Models of Some IEEE 802.11-based protocols

Many developed analytical models for the IEEE 802.11 MAC protocol family have been based on the well-known Markov chain model proposed by G. Bianchi [10] in 2000. In [11] an analytical model that evaluates the IEEE 802.11 Distributed Coordination Function (DCF) MAC protocol under unsaturated broadcast vehicular network has been proposed. Despite the practical considerations assumed in this study, we think that DCF approach is not suitable for vehicular commu-

nications because it cannot cope with the conditions of this environment and because it does not provide Quality of Service (QoS) support (multiple Access Categories (AC)s) which is an essential design factor of IEEE 802.11p.

Another mathematical model for the IEEE 802.11 DCF has been derived in [12]. It is an extension of the model proposed by Bianchi, it includes the non-saturated traffic conditions, however still it is not useful for vehicular communication for the same reasons explained earlier.

Moreno *et al.* in [13] have evaluated and enhanced the performance and the reliability of the 802.11 Enhanced Distributed Coordination Algorithm (EDCA) broadcast protocol aimed to deliver safety messages in vehicular network. The proposed mathematical model introduces service differentiation scenarios by prioritizing the data traffic and providing each type a differentiated channel access.

In [14], Ma *et al.* have constructed an analytical model for IEEE 802.11a Dedicated Short Range Communication (DSRC)-based communication system that delivers safety messages in a vehicular environment. The developed model has taken into account harsh communication conditions such as the hidden terminal problem, the multi-path fading channel, a high dynamic network and vehicle mobility. However this model is based on one-dimensional discrete even Markov chain that does not consider multiple ACs, and hence does not consider virtual collision among them. It did not consider also the backoff blocking probability in the backoff stage.

2.2.2 Markov-Based Mathematical Models for IEEE 802.11p

In the literature, few papers have proposed stochastic-based model for IEEE 802.11p [15] [16], however the majority have adopted the discrete-event Markov chain model [17–21].

The authors of [22] and [23] have developed a Markov-based analytical model that study the behaviour of the EDCA taking into account the specific conditions of the Control Channel (CCH) in a vehicular network environment. The proposed model is unidimensional, it did not consider the internal competition among ACs, while in our model we derive the equations related to these competitions. He *et al.* in [24] have proposed a two-dimensional discrete event Markov chain to

model the operation of IEEE 802.11p EDCA while exchanging safety messages over the control channel. They have studied the influence of different Arbitration Inter-Frame Space (AIFS) values on the performance. This model has considered immobile vehicles at an urban intersection, and it has not taken into account the unsaturated condition of the traffic. In [25–27] different services were developed based on a Markov-based model of IEEE 802.11p which did not take into account all the required factors such as the saturation, the freezing probability and/or the internal competitions among the ACs.

In [28], the authors have presented an analytical model for the IEEE 802.11p established in a saturated mode of operation. Different EDCA parameters have been associated with different access categories. They have taken into account the internal behaviour of the classes such as the internal contention and collision rates. The saturated mode of operation considered in this paper constitutes a major drawback, because it does not replicate the true performance of the actual Wireless Access for Vehicular Environment (WAVE) scenarios.

A 3-dimensional Markov chain model has been developed to represent the status of a vehicle communicating with the infrastructure using the IEEE 802.11p protocol in [29]. The authors have taken into account the velocity of the vehicles while studying the performance of the protocol, and have included it in the model. They have studied the influence of the vehicle speed on the QoS performance and have proven that high speed commuting vehicle causes severe variations of the communication service. The authors have identified the impacts of the MAC parameters and the vehicle speed on the eventual QoS performance. The model only considers saturated traffic conditions, which does not actually reflect the real behaviour of such applications.

In [30], the authors have developed a system that models the CCH and the Service Channel (SCH) channel management. They have considered various traffic combinations and different traffic classes per combination over control and service channels. To achieve the intended goal, the model has been implemented by combining probabilistic analysis, M/G/1 queuing analysis and Markov chain analysis. The authors have proved that by selecting a balanced channel duty cycle values and

QoS parameters of each class, they can avoid the synchronization of the backoff process which leads to high probability of collision. They have determined the probability distributions for different time phases that the model passes through, such as the backoff time, the frame service time and waiting time in the buffer, and thats for each channel and each traffic class within that particular traffic combination. Although this model has assumed a non-saturated condition, it only focuses on the duty cycle selection between the CCH and SCH channels, and its impact on the collision rate as well as the delay. In our proposed model, we follow a different direction in deriving the system, which tends to have lower complexity without sacrificing the accuracy.

In [31], the authors have established a two dimensional Markov chain to analyse the performance of the EDCA mechanism in IEEE 802.11p MAC sub-layer. They have calculated the normalized throughput and the time delay of the protocol, taking into account the following factors: different Contention Window (CW) sizes, the internal collision that occurs inside the node as a result of the internal contention among the classes, and the frozen mechanism that takes place during the backoff stage when the channel is sensed busy. Their model have proven high accuracy, however it is simulated under saturated traffic conditions, which does not actually reflects the real operation of the IEEE 802.11p. Our model assumes that the vehicle may not have packets to transmit at some periods (unsaturated mode) which replicate the actual vehicular communication environment.

In [32], the authors have tackled the communication among vehicles that handle safety and non-safety messages with priority. To achieve their goal, they have proposed a Markov chain-based model and a queuing model to evaluate the performance. Their model is quite accurate but it lacks the non-saturation assumption which is essential to duplicate the behaviour of IEEE 802.11p.

In [33], an analytical model has been suggested to describe the performance of the IEEE 802.11p MAC sublayer in Vehicle to Vehicle (V2V) safety applications. A Markov chain has been created to show the performance in terms of the mean, deviation and probability distribution of the access delay. Their model have taken into account the non-saturation mode, the internal probability of collision and the probability of finding the channel busy when sensed during the backoff stage.

However the study is limited to only two ACs, AC0 and AC1, while IEEE 802.11p standard defines four ACs. Our model follows the IEEE 802.11p standard, it shows the performance of all ACs described in IEEE 802.11p MAC sub-layer.

The authors of [34] have Proposed a new mathematical model of a two-directional VANET communication system that study that performance of broadcast with enhanced distributed channel access mechanism in IEEE 802.11p MAC layer. They have taken into account the hidden terminal problem and the fact that the messages are described with strict priorities. In order to estimate the broadcast delay of each access categories, an M/M/1 queue model has been used. The proposed analytical model has been validated through simulation using Network Simulator 2 (NS2). Their results have shown that high priority classes experiences the higher packet delivery rate however the delay of the low priority classes will increase but still within the acceptable range.

2.2.3 Non-Markov-Based Mathematical Model

In this section we present few non-Markov-based mathematical model of protocols in VANETs.

In [35], the authors have proposed a communication system that extends the IEEE 802.11p MAC standard to enable real-time applications. Similar to IEEE 802.11, a polling-based collision free communication phase has been appended at the beginning of the super-frame. This phase is controlled by an access point such as a Road Side Unit (RSU), which is dedicated for the high priority vehicles that require real-time coordination with the smart grid. The lower priority classes use the remaining bandwidth available in a contention-based environment. A special real-time scheduling mechanism has been used to reserve the minimum needed bandwidth for the high priority nodes while allowing the maximum possible bandwidth for other low priority nodes.

An end-to-end delay study of IEEE 802.11p protocol for real-time communication in VANET is presented in [36]. The authors have approached the problem from a different perspective. They have studied the impact of the transmission range on the end-to-end delay. They have considered the path length, the queuing delay, the number of hops and the number of contending vehicle. An analytical model has been developed to evaluate the end-to-end delay of the IEEE 802.11p pro-

tocol in vehicular environment as a function of the transmission range and the packet arrival rate. Their findings have proved that if the packet arrival rate increases the transmission range should be shorter to achieve lower end-to-end delay and vice versa.

A cross-layer scheme for IEEE WAVE-based VANETs has been proposed in [37] to tackle the privacy preserving authentication for messages in vehicular safety applications. A modification to the Elliptic Curve Digital Signature Algorithm (ECDSA) has been developed to incorporate ID-based authentication scheme without the need of a trusted third-party certificate and in the absence of any strong mathematical assumption-based signature procedures. They have contributed also in the development of an efficient prioritized verification technique for periodic road safety messages. The priority of the messages are mapped to the MAC layer access categories, and thus a cross-layer message verification scheme based on the MAC traffic class and the traffic intensity is set up to verify every message. Their performance analysis have proved that their authentication and verification approach is secure, reliable, efficient and privacy preserving.

In [38], the authors have studied the performance of the IEEE 802.11p protocol in vehicular communications under Radio Frequency (RF) jamming conditions. In fact, the road safety can be compromised by the RF jamming. The highly changing environment in the vehicular network make it vulnerable to various impacts of jamming. The authors in this paper have tried to identify the main features that are most susceptible to RF jamming damage. They have conducted an experiment that evaluates the performance of the IEEE 802.11p protocol in the presence of RF jamming in an anechoic chamber. They have improvised a new methodology to apply the method used indoor for modelling the performance of IEEE 802.11p network outdoor. And finally they have estimated and evaluated the effect of various RF jamming signals on a vehicular environment by means of measurements. Their work results have shown that RF jamming presents a real threat to VANET applications. They have concluded that there is a need for a new set of protocols and applications that take into account the jamming threat element.

A new WAVE protocol has been proposed in [39] named WAVE Point Coordination Function

(WPCF). Its aim is to provide efficient access and reliable usage of the wireless Vehicular to Infrastructure (V2I) channel by improving the handover. The proposed protocol is a contention-free based access protocol and it has offered pre-ordered transmission opportunities. The proposed scheme has reduced the handover latency and has provided continuous seamless communication for real-time applications. The scheme has been simulated and has been modelled using mathematical derivation, the results have shown that WPCF is more efficient and can support more users than the PCF, the EDCA or the Hybrid Coordination Function Controlled Channel Access (HCCA) for V2I communications.

An enhancement to the physical layer performance of the IEEE 802.11p protocol has been studied in [40]. To enhance the packet error rate of the data transmission, the authors have proposed to integrate a dynamic equalization scheme on top of the current DSRC technology. This scheme uses the information carried by the sub-carriers to update the channel estimate, which lead to a more reliable V2V communication in a changing environment. To demonstrate the viability of their work, they have implemented their scheme in hardware based on a Field-Programmable Gate Array (FPGA). They have extended their scheme to support all data rated defined in the IEEE 802.11p standard. They have shown that their system's performance supersedes a preamble-based scheme at all data rates. And finally they study the relationship and the dependence of the packet length, the data rate and the payload size on the overall performance.

2.3 Vehicular Network Architectures

In this section, we present some hybrid architecture for VANET published in the literature. These architectures include, the integration of different technologies such as IP-based protocols, Wide Wireless Access Network (WWAN) such as Long-Term Evolution (LTE) and Universal Mobile Telecommunications Systems (UMTS) and other short range communication protocols. We review few papers that cover the integration between the Electric Vehicle (EV) and the smart grid.

2.3.1 EV-Smart Grid Communication Systems

Vehicle to Grid (V2G) communication architectures have attracted the attention of the researchers in the recent years, due to the technological advancements in the field of EVs as well as in smart grids. In this section we present few architectures discussed in the literature.

A distributed approach to the integration of the EV into the smart grid has been developed in [41]. The main motivation behind the distributed approach is that a large number of EVs will be participating in the communication with the smart grid. Therefore they have proposed to push the load to the side of EVs, by putting the intelligence needed for the communication in the EVs instead of putting it in the charging stations. As a matter of fact, most of the critical information (such as the EV capabilities, the battery capacity and its current power balance etc.) are already present in the EV, and thus the EV can use these information to get the service it requires. According to this system, the scheduling process and the charging decisions are done locally at the EV. The decision is based on reference information from the smart grid such as the location of the charging stations and the available power. This approach has ensured the scalability and avoids the risk of a single point of failure. To realize their system they have developed an incentive system, an in-vehicle optimizer to create charging schedule and a charging management to actually control the whole process. The results of small-scale field trial have delivered the proof of concept of the proposed system.

The integration of the EV into the smart gird has been the focus of the paper [42]. The authors have been working on the project PowerUp that implements the communication interfaces between the EV and the local recharging controller device, which is connected to the smart grid. They have presented some of the major results of the projects. They involve key features of the smart grid integration aspects for each protocol layer within the V2G communications protocol stack. At the physical level they have described in details the deployment for private recharging stations, the deployment of public charging spots and the deployment for public transport and goods delivery vehicles. At the link layer integration of the V2G interface, they have tested the performance of

a Programmable Logic Controller (PLC) link over a the power line connection with both AC and DC charging systems, and then they have checked the compatibility of with other PLC media in the smart grid to ensure the continuous operation of the link while the EV charging equipment is in use. At the network layer they have described the sequence of two connections: EV to Supply Equipment Communications Controller (SECC) and the Smart Meter (SM) to control center connection. They have finally implemented and tested a prototype and the results have shown an enhanced end-to-end communication performance which makes it prepared for field operational trials.

Rezgui *et al.* in [43] have proposed a new two-way communication scheme for EV charging from the smart grid: the Reliable Broadcast for EV Charging Assignment (REBECA). They have stated that the wireless communication between the EVs and the charging stations is crucial to discover the availability and to make reservations of charging time slots. They have focused their study on two main performance metrics: the latency and the efficiency of the required service. Their main goal has been to determine the number of EVs that can get the service efficiently without overloading the charging station and with lowest delay possible. In addition to REBECCA, the authors have proposed a random access allocation algorithm, a best access allocation algorithm and a power balancing access allocation. The results have shown low service delay and good power balancing in the smart grid.

The communication time requirements of the last mile communication between the smart grid and the EVs have been investigated in [44]. The authors devise scenarios that involve large number of distributed energy sources installed in a low voltage smart grid and EVs trying to charge from them. They have chosen the most delay sensitive functions of the smart grid such as voltage control, congestion control, peak shaving etc. to be able to identify the worst case scenario's time requirements. They have concluded that voltage control is the most essential time sensitive function in the smart grid that necessities very strict communication latency boundary.

A Communication-based Plug-in Hybrid Electric Vehicle (PHEV) load management is proposed

in [45] to control the charging of PHEV from the grid. The authors have assumed that the actual state of the grid and the amount of electrical capacity that every charging station can supply is known and controlled by the Substation Control Center (SCC). The proposed model has enabled the interaction between the smart charging station and the SCC once a PHEV is connected for charging. Based on the amount of energy provisioned for the charging station, the SCC may or may not authorize the power charging through that station. A mathematical analysis of their system has been presented and it has been implemented using a discrete event simulator in C++. Their results have show an improvement in terms of delay, jitter and the charging request blocking ratio.

2.3.2 VANET-WWAN Architectures

In this section, we review some architectures that interconnect a short range communication system in VANET with a wide range communication system.

An architecture of an integrated VANET-UMTS network has been introduced in [46]. The proposed architecture allows the vehicles to get mobile data access any time and anywhere. The main challenges they had to overcome are to merge these two network interfaces as they function in different spectrum, to select an optimal number of gateways that connect to the biggest possible number of vehicles without sacrificing in the performance, and to tackle the arising issues related to the gateway management such as gateway handover mechanism and efficient discovery mechanisms. The proposed architecture assumes that some vehicles are equipped with IEEE 802.11p and 3G UMTS Terrestrial Radio Access Network (UTRAN) interfaces. These vehicles are then selected as gateways to link the vehicular network to the UMTS network. An adaptive mobile gateway management mechanism has been set up to perform service migration between gateways, gateway discovery and advertisement. A simulation has been conducted using NS2 to evaluate the performance of the architecture, and it has showed promising results in terms of packet delivery ratio, packet drop rates and throughput.

Cespedes *et al.* in [47] have proposed a new IP-based communication framework between the vehicles and the smart grid. The aim is to integrate the well-known IP protocol in the vehicles to enable

a ubiquitous and transparent communication in a V2G environment. The authors have described the technologies and the protocols that form the framework and they have specified the main block components essential for IPv6 support in V2G communications. To evaluate the performance, they have simulated their proposed scheme with various types of applications that involve different data rates and channel requirements using Omnet++ and MiXiM simulation tools. Their results have proven the possibility of using IP-based technology as a standard in a vehicular environment.

A video streaming system among vehicles has been proposed in [48]. In this paper an original co-operative V2V communication model to stream video signal among vehicles has been developed. Near-by moving vehicles have been grouped together. The selected vehicle uses the long term evolution system to send requests and receive video from the internet, and then broadcasts or multicasts the received data to the vehicles in the group using IEEE 802.11p protocol. To choose the most suitable sub-carriers for LTE transmission and to improve the quality of the received video, the authors have proposed new resource allocation algorithms for the joint operation of short range V2V communications and long range LTE communications. They have taken into account how to recover errors or lost data from the video signal, and they have also studied and analysed the elements and metrics related to the QoS and the Quality of Experience (QoE) for different video sequences. Their simulation results have shown that collaborative approaches improve the QoS and the QoE compared to traditional non collaborative approaches.

Huang *et al.* in [49] have tackled the problem of streaming multimedia services with an improved QoS in a fleet-based vehicular network. The vehicles, formed in a k-hop range, cooperate to download a video requested by one vehicle using their own 3G/3.5G network. Each vehicle contributes by downloading a portion of the requested video and then they forward them to the destination vehicle using IEEE 802.11p protocol. The key elements of the proposed system are to select the appropriate vehicles within k-hop coverage to download the video, to set up a suitable schedule of data streaming among the involved vehicles (taking into account that vehicles may leave/join the network at any moment) and to be able to recover lost chunk of video during the download or the

transmission process.

2.4 MAC Protocols for VANETs

In this section we review the MAC protocols proposed in the literature for VANET in general. We classify MAC protocols in this section to how the channel is shared: Time schedule-based protocols, cluster-based MAC protocols, Space Division Multiple Access-based protocols (SDMA), Directional Antenna-based MAC protocols and Token ring-based MAC protocols. However it is important to mention that there is a wide range of MAC protocols designed for different applications and environments, for example: MAC protocol for spatial capacity [50], MAC protocol for urban environments [51], MAC protocols to solve the problem of anti-fading of DSRC systems [52], MAC protocols to eliminate collision and to improve QoS [53] and [54]

2.4.1 Time Schedule-Based MAC Protocols

The ADHOC MAC protocol has been proposed in [55]. It is a MAC protocol developed with the European project CarTALK2000. It operates in a slotted frame structure. It is based on dynamic TDMA mechanism that can be easily adapted to the UMTS Terrestrial Radio Access Time Division Duplex (UTRA-TDD) which was chosen as physical target in the carTALK2000 project. In this case the slotting information can be provided by the Global Positioning System (GPS). ADHOC-MAC protocol can also be adapted to operate with asynchronous physical layers such as the IEEE 802.11. ADHOC-MAC is based on the Reliable R ALOHA (RR-ALOHA) which is a completely distributed access technique that establishes in a dynamic way a reliable single hop broadcast channel on a slotted/framed structure for each active terminal on the network. The terminal in ADHOC-MAC transmits periodically a packet in any frame, the synchronization is provided by the first functioning terminal. The remaining nodes synchronize by setting counters on transmission on the fly. Each active node should be assigned a Basic Channel (BCH) which corresponds to a slot in VF. The BCH assignment is done in a distributed way by RR-ALOHA

protocol.

In [56], the authors have proposed a Self-Organizing TDMA-based (STDMA) MAC protocol. Their aim has been to guarantee the timely delivery of safety critical messages. STDMA provides decentralized coordination and nearly contention-free communication. A frame in STDMA is composed of fixed number of slots and every node synchronizes its slots to GPS, however the frames are not synchronized among the nodes. Initially, each node selects a range of slots. Then at random intervals, each node chooses a different and unoccupied slot from this range. Each node may transmit multiple time in a frame and the number of transmission time depends on the speed of the vehicle. STDMA has not been originally designed for vehicular networks, it has been developed in aviation and naval surveillance as a part of the Automatic Identification System (AIS). It has very low data rates, therefore it is not suited for high volumes of data such as multimedia. STDMA is based on TDMA technique which means a slot will be wasted each time a node does not need to transmit. Therefore STDMA is more effective in dense areas than rural areas.

The authors of [57] have explored various existing methods developed in the MAC layer to find out which of them achieve near real-time communication in Vehicular Ad hoc Network VANET. They have first presented different multi-user medium access approaches such as the competitive medium access protocols, the Self-Organizing Time-Division Multiple Access (S-TDMA) and the Code Division Multiple Access (CDMA) algorithms. Then they have devised a scenario and conducted a simulation study using JiST/SWANS network simulator [58], to discover if S-TDMA outperforms CSMA/CA (used in the IEEE 802.11p protocol) in regard of the real-time performance. They have shown that S-TDMA behaves better than CSMA-CA with high number of vehicles involved in the simulation; however the latter offered better performance for low of density vehicles. Although this study was based on realistic scenario, it is only limited to the comparison of two protocols CSMA/CA and S-TDMA.

Another self-organizing TDMA-based protocol has been developed in [59] called Vehicular Self-Organizing TDMA (VeSOMAC) protocol. The objective has been to achieve a contention free

MAC technique with distributed control, which provide high data transfer between platooning vehicles in highway scenarios. The nodes in VeSOMAC are synchronized with GPS time or they can be self-adjusting asynchronously. In the asynchronous mode, the time is divided into frames and each frame is divided into equal transmission slots.The frame is a period of time in every node; it is not a structured superset of all slots for all nodes. All the frames of all nodes have the same duration but they are not synchronized with each others. Each node uses a bitmap vector to allocate a transmission slot. The bitmap vector announces which slots are used by all neighbors distant by one-hop. A new node can avoid collisions with all its two-hop neighbors by choosing a slot that is unoccupied according to the combination of all one-hop neighbor time slots. The main disadvantage of this system is that it is mainly designed for highways environment; therefore it poorly performs in urban conditions with numerous vehicles travelling in varying directions. And that is primarily because the clocks in each vehicle are not drifting relative to each other, although the operation is asynchronous. Another disadvantage is that some slots are wasted because vehicles reserve them and did not have data to transmit.

In [60] a Dedicated Multi-Channel MAC (DMMAC) protocol with adaptive broadcasting has been proposed. Its objective has been to provide collision-free and delay-bounded deliver of safety messages with an adaptive broadcasting mechanism. This protocol is built based on WAVE structure by segmenting the 100ms synchronized interval into a CCH interval and an SCH interval of 50ms each. The CCH is then divided into a equally-sized contention-free TDMA slots uses as variable length Adaptive Broadcast Frame (ABF), and to Contention-based Reservation Period (CRP). The allocation of the slots is done by using a distributive control approach. The SCH us usually used for non critical transmission called the Non-Safety Application Frame (NSAF) while the ABF is used for safety and critical transmission. The CRP is used to coordinate the allocation of channel time slots. This approach allows the negotiations for multiple channels allocation by the nodes in a geographically unstructured way. This may lead to collisions because only the ABF allocation of the two-hop neighbors is known, the NSAF allocation is not.

The authors of [61] have developed a V2I resource allocation scheme implemented at the RSU. It intends to schedule all the resources of the RSUs and share some of the load with the moving buses which are considered as relays between the vehicles and the RSUs. Their main goal has been to optimize the V2I communications by integrating new parameters such as the traffic types and the available resources. This model has failed to tackle the time synchronization issue among the vehicles.

A new TDMA-based schedule algorithm for real-time communications in VANET (CTMAC) has proposed in [62]. The RSU plays a centralized role in scheduling, maintaining and coordinating channel access for the vehicles within its coverage area. CTMAC has been designed to avoid collisions among timeslots that may occur because of the interference problem in the overlapping regions. The main drawback of this approach is being centralized. It is more vulnerable against security attacks, and there could be a scalability problem.

The authors in [63] have presented a new coordinated multichannel MAC (C-MAC) for VANET. The aim of C-MAC is to reduce the collision probability and the transmission delay of safety messages. It relies on the RSU to ensure a contention-free broadcasting for safety messages. The RSU takes care of scheduling the transmission order for safety messages coming from different vehicles.

Liu *et al.* in [64] have studied the first scheduling mechanism for cooperative data dissemination in a hybrid I2V and V2V communication systems. While broadcasting the information to vehicles engaged in a V2I communication, the RSU simultaneously connects vehicles with common interests and establish V2V communications among them. An in-depth analysis on the requirements on data dissemination in such environment has been conducted, and have resulted in formulation of a NP-hard problem, which has been solved using a greedy method.

In [65], a novel TDMA-based scheduling protocol controlled by a centralized RSU has been proposed. It has been developed based on a new scheduler scheme that calculates the weight factor of each communication link. The allocation of the timeslots to each vehicles is decided according to the each link weight factor, which in fact dependent on three factors: the channel quality, the speed

and the AC. Moreover, a novel resource-reusing mode for different V2V communication links has been employed, it allows the re-use of the same timeslots between different vehicles if the distance between them is larger than a certain threshold.

A small analysis on the characteristics of timing synchronization in IEEE 802.11p protocol has been conducted in [66].

A hybrid TDMA/CSMA multichannel MAC protocol for VANET (HTC-MAC) has been proposed in [67]. It is an improvement of the HER-MAC protocol proposed in [68]. HTC-MAC allows each vehicle to select a random time slot to access the reservation period. Meanwhile each vehicle receives an announcement packet to learn the the neighbouring vehicles every one time slot. Once a full neighbor list is determined, the vehicle will be able to make a decision about which time slots it can access on the reservation period. The simulation results have shown that HTC-MAC had a superior performance in comparison with HER-MAC.

Jiang *et al.* in [69] have proposed A prediction-Based TDMA MAC protocol aiming to reduce the vehicle collision rate in VANET. It is based on the design of a new collision prediction mechanism. It reduces the collision rate in two-way traffic and four-way intersections. A survey study about TDMA-Based protocols has been proposed by Hadded *et al.* in [70]. The authors have studied the design issues related to VANET MAC protocols in general, and they identify the reasons for adopting collision-free approach. They have provided a new MAC protocol classification based on the network topology. Finally a detailed qualitative comparison has been presented.

2.4.2 Cluster-Based Algorithms and MAC Protocols

The authors of [71] have proposed a centralized cluster-based topology for VANET. The RSU plays the role of selecting the TSs for the vehicles in each cluster. Their objective has been to reduce the overhead related to management, channel allocation time and medium access. The vehicular network has been divided into multiple spatial partially-overlying clusters, where each cluster has its own CH. The total available bandwidth has been divided among theses clusters. In a cluster, the allocated channel has been divided into multiple TSs assigned to the VMs. This approach does

not rely on the protocol IEEE 802.11p designed for VANET, it is based on bandwidth division and time division schemes.

In [72], a clustering approach originally designed for the Mobile Ad hoc Network (MANET) has been proposed. It has been been considered as a new MAC protocol solution for VANET. This clustering method has divided the vehicular network into clusters with a diameter that extends to four hops maximum. It has also incorporated a fast randomized scheduling algorithm. The main goal of the authors has been to allow quick network establishment and maintenance without relying on the use of localization tool. They have compared their algorithm with a MANET-based algorithm which presents a drawback.

A simple cluster head selection mechanism for implementing a high priority algorithm in VANET has been described in [73]. It has been based on selecting a cooperative node to be the cluster head. The cooperative node will forward the messages to the vehicles which did not get them through broadcasting.

Shahin *et al.* in [74] have proposed an enhanced TDMA Cluster-based MAC protocol for multichannel vehicular networks. ETCM protocol has enabled a collision-free channel access and increases the transmission reliability of delay-sensitive messages. It has also re-allocated dynamically the unused slot to vehicles requesting access to the medium. The simulation results have shown a big increase in performance in comparison with TC-MAC protocol.

A study about comparing the scalability of IEEE 802.11p protocol with LTE-Advanced with device-to-device communications (LTE-D2D) [75] protocol has been proposed in [76]. The results have shown that LTE-D2D has outperformed IEEE 802.11p as less resources have been used to achieve the same beaconing periodicity.

Zhioua *et al.* in [77] have proposed an algorithm to select a gateway between a vehicle network and the LTE infrastructure. The proposed algorithm has been designed within the scope of V2I communication architecture. The selection of the gateway has taken into account also the QoS class of the data transmitted. This algorithm can be applied in a cluster-based architecture, in which

the selection of the gateway is similar to operation of selection a cluster head. The algorithm has been based on fuzzy logic, it has studied two clustering and CH selection algorithms: the cluster formation in the first algorithm has been based on the direction of the vehicles, the second algorithm has assumed that the cluster head is at the center of the cluster. The simulation results have outperformed the conventional protocol in terms throughput and packet loss.

Ren *et al.* in [78] have proposed a new Mobility-Based Clustering Algorithm for VANETS (MSCA). Their approach has assumed an urban city scenario, where the direction of the mobile vehicle as well as its relative position can be estimated. They have aimed to achieve a stable communication system for information dissemination purposes in VANET. The cluster formation has been based on the usage of mobility metrics such as the vehicle's position (identified by the use of a GPS), the moving direction and velocity of the vehicle. Their simulation results have shown that the average number of clusters increases with the speed and decreases with the traffic flow.

Kwon *et al.* in [79] have proposed also a mobility-based clustering scheme (NMCS). The selection of a cluster head has been done based a metric value that indicates the level of stability of the vehicle. Each vehicle calculates this metric value, which is function of the number of neighbours that left its coverage area and the number of vehicles that entered in a the period of a processing round.

Dror *et al.* in [80] have proposed a distributed randomized hierarchical clustering and scheduling algorithm (HCA). Their aim has been to enable fast network setup. The authors have assumed that 4-hops maximum cluster is the optimal choice to form cluster, therefore the cluster head should not be away from any vehicle in the cluster more than 2 hops. The cluster head does not require the knowledge of the exact position of the vehicle, which makes HCA more efficient. The authors have not assumed a multilayer architecture, sharing the medium and scheduling the access among vehicles occur only within the cluster which reduce the collision rate.

Chen *et al.* in [81] have proposed a distributed multi-hop clustering algorithm for VANETs based on neighbourhood follow (DMCNF). The goal has been to achieve a quick and stable network

setup. The network has been assumed to be large. Each vehicle of the network collects information from the one-hop neighbour, and based on that information it will be able to determine which one is stable or similar, and thus joins it with the same cluster. The selection of the cluster head has followed the same procedure. The cluster formation process, has taken into account the gain based on the number of followers, the relative mobility, and the gain based on the historical cluster belonging information.

A multi-hop VANET architecture based on clustering the vehicular network has been studied in [82]. It has been based on combining IEEE 802.11p protocol with LTE technology. A stable clustering algorithm that uses relative mobility and the average speed as metrics to form a cluster and select the cluster head, has been implemented in [83]. The authors have aimed to attain high data packet delivery and a minimum delay. This architecture does not use the RSU as the sink node to be reached by all vehicles, instead they route the data transmitted by the vehicular network to an LTE node. It is not a multi-layer architecture since a CH communicates directly with an LTE node, not with another CH at higher layer. Therefore this architecture is not suitable for high density scenarios.

2.4.3 Space Division Multiple Access-Based MAC Protocols

In [84] a Space Division Multiple Access (SDMA) MAC protocol for vehicular networks has been proposed. The location of the vehicle at any particular time regulates the access to the channel. With this approach, the area of coverage is divided into smaller space divisions so that every division holds at most one vehicle. On the other hand, the channel bandwidth is also partitioned to time slots and frequency channels and each channel is uniquely associated to a space division. The location, the time slot and the frequency of each space division are assumed known. This protocol has provided a robust network organization and a contention free access; however it has suffered from poor bandwidth efficiency. That is because the bandwidth for each vehicle will be reduced with a growing number of vehicles involved in the communication.

An Adaptive Space Division Multiplexing (ASDM) has been proposed in [85]. This protocol has

extended the previous SDMA protocol, and it has been designed to overcome its shortcomings. With this protocol, each vehicle should know the location of its preceding one to determine the unused slots. It is based on a mapping function that allows the vehicles to use the unused time slots. It mainly suffers from the limitations of the position accuracy and the time synchronization between the vehicles.

The authors of [86] have proposed enhancements in the SDMA protocol. Its main idea is based on spatially pre-distribute TDMA slots by splitting the road into spatial slots. The size of each slot is the sum of the physical size and the safety distance which is the vehicle headways. The proposed protocol has given the RSU the responsibility of allocating the channel slot for the vehicle using the channel mapping and the physical interference modelling. This protocol has taken advantage of the channel slot reuse concept by separating the channels with large enough distance. The allocation of the time slots is done as the following: once the RSU has the location information of the vehicle, it allocates the time slots based on its respective division taking into account the speed of the vehicle. In addition to that, the vehicles can transmit to unoccupied divisions between itself and the lead vehicle. This has increased the bandwidth utilization because it has allowed the use of time slots assigned to empty divisions. Another advantage is that this protocol has eliminated the interference problem and allowed a contention free medium access. The main problem here is the centralized topology approach adopted. If for some reasons the RSU is out of service, the whole communication goes down.

2.4.4 Directional Antenna-Based MAC Protocols

The major advantage of the using directional antennas in vehicular wireless communication is that it enhances the performance by allowing multiple simultaneous transmissions to different destinations. A set of directional antennas can be installed in the vehicle to cover 360 degrees around it without any overlapping coverage area, which results in increasing the throughput of the system and the spatial reuse. An omni directional antenna can be used in some cases, or it can be used at the same time with directional antennas to send control messages. Moreover, using Multi-Input

Multi-Output (MIMO) antennas in a wireless vehicular environment can be very useful. It can be used in combination with IEEE 802.11p protocol to improve the data rate and efficiency of the network [87] [88].

In [89] a new multi-channel medium access control, called VANET Multi-Channel MAC (VM-MAC), has been proposed. It has been designed for dense vehicular network using directional antennas. This protocol is based on Multichannel MAC (McMAC) protocol originally designed for ad hoc wireless network. The key point of this protocol has been the usage of directional antennas in multi-channel network to achieve the spatial reuse. A high density network is assumed where one vehicle can communicate with numerous neighbors at the same time. Each vehicle is equipped with a single half-duplex transceiver, which means that a vehicle can do one the two operations at a certain time (but not both simultaneously): data transmission or medium sensing. It is also assumed that each vehicle switches between the CCH and one of the SCHs in a continuous way. And finally, beacons have been used for synchronization purposes. Each transmitted packet carries a beacon which includes a timestamp of the local sender's time. The design and implementation of this protocol is done in four steps. First, the communication channel should be selected before even sending the RTS/CTS messages. This protocol uses a reservation strategy based on the Ad hoc Traffic Indication Message (ATIM). At the end of this phase, a beam table for each node will be created. The beam table indicates the status of the channels with each neighbor nodes (blocked or unblocked). The second stage is about establishing the connection based on the RTS/CTS handshake scheme transmitted consecutively by the directional antennas. Third stage is about informing the receivers the durations of the transmission, the directions of the transmitters, the transmitter's ID and the unblocked SCH ID. This mode of information is based on the well-know Network Allocation Vector (NAV) technique used in various MAC protocols. The performance of this protocol has shown a great performance in terms of throughput and network reliability. However it has taken a long period to pass the initial phase where the beacon tables have to be created.

In [90] a suitable Directional MAC protocol (DMAC) for VANET has been proposed. It has been evaluated to solve the interference problem that occurs during the contention for transmissions between the vehicles. This protocols has been called DMAC using NAV Table (DMAC/NT). The authors have intended to solve the problem without using additional channels or extra frames. Each node stores a multi NAV table which includes the node ID and the NAV of each node. The multi-NAV table is updated by transmitting and receiving ORTS and OCTS (OmniRTS and Omni CTS). In this case the deafness problem is solved and the spatial reuse is improved. This protocol has been evaluated for two different scenarios. In both scenarios, this protocol has showed better results in terms of total throughput and average jitter than Omni-MAC and DMAC.

In [91], a Location and Mobility-aware (LMA) MAC protocol has been proposed for VANETs using directional antennas. The design of this protocol has taken into account the fact that the location and the mobility of the vehicles are mostly predictable. It has been assumed that the location of each vehicle as well as its velocity and its moving angle were known. The vehicles are moving at constant speed and fixed angles within a given short period of time. Four types of directional antennas have been considered: the Continuous switching with Ideal Antenna pattern (CI), the Continuous Switching with Realistic antenna pattern (CR), the Discrete switching with Ideal antenna pattern (DI), and the Discrete switching with Realistic antenna pattern (DR). According to this protocol, the mobile vehicles can effectively adjust their antenna beams in the direction of the intended receivers based on the predictive location and mobility information they have. Using the DRTS and DCTS (Directional RTS and Directional CTS) has reduced the problem of deafness. The Direction Beam (DB) mechanism used in LMA MAC protocol has improved the location prediction even if the mobility of the vehicle changes during the transmission. LMA MAC protocol has proven a better performance in terms of control packet overhead, throughput and delay comparing to DMAC protocol.

2.4.5 Token-Ring Based MAC Protocols

In [92] a Multi-Channel Token-Ring Protocol (MCTRP) for VANET has been developed. The goal has been to achieve a low-latency and high-throughput protocol for safety and non-safety applications. The design of MCTRP is based on the development of a contention-free MAC protocol that autonomously organize nodes into token rings architectures. Various vehicles running with similar speeds are grouped to form a ring. The medium access for the intra-ring data communication is controlled by a token passing TDMA scheme; however the medium access for the inter-ring data communication is controlled by CSMA/CA. With this protocol, each node is equipped with two radios, one is tuned always to WAVE channel 178 for inter-ring communications, and the other one is tuned to one of the remaining WAVE channels for intra-ring communications. The main shortcomings of this protocol are: the ring depends on one ring founder or leader, if this leader goes out of range for any reason the whole ring collapses and a new ring network should be established. This protocol is more suitable for platooning vehicles where the direction and the speed of the vehicles are well-known.

Shen *et al.* in [93] have surveyed a set of congestion control mechanisms for IEEE 802.11p-based protocols. They have also proposed a new distributed multi-priority congestion control to overcome the loss of system throughput caused by the congestion of the shared radio channel. The authors have started their study by presenting a detailed survey about the existing congestion control approaches for IEEE 802.11p. They have categorized them into four main classes: the modified CSMA/CA protocol-based class, the power adaptation-based class, the hybrid approach class and the rate adaptation-based class. Their proposed approach has been based on a distributed multi-priority congestion control system. It is an improved adapted CSMA/CA protocol that changes the contention window size dynamically according to congestion conditions. The contention window size is adjusted based on the local congestion measurements and the value of the congestion levels compared to the thresholds. Different classes with different priorities have been given different congestion thresholds, so that the higher priority classes are able to access the channel with higher

probability. And finally the proposed design aims to keep the collision probability of the overall network to the lowest possible value; they have adjusted the congestion thresholds according to the network density.

The Overlay Token Ring Protocol (OTRP) for V2I networks has been discussed in [94]. The authors have proposed to organize the vehicles of the network in various overlapped virtual rings. To be able to transmit, a vehicle must possess a unique token associated to each virtual ring. Taking into account the nature of the vehicular network, the ring size is dynamically changing and adjusting when vehicle(s) join or leave the ring area of transmission range. The authors have defined two modes of operation to meet the requirements of QoS-based and emergency messages transmission. The simulation results have shown that reliability of the network has increased and that it has achieved low latency.

A hybrid MAC protocol that incorporate the conventional random access mechanism with a taken-based mechanism has been proposed in [95] and [96] (called DTB-MAC). The objective of the new protocol has been to enhance the reliability of the network and to reduce the usage of channel contention mechanism to the minimum. In DTB-MAC, the random access mechanism is overlayed by the token passing mechanism. Basically the vehicle form multiple rings with specific token each. If a vehicle fails to access the channel by possessing the token, however if it is not possible to get the token due to the mobility of vehicles, the random access mechanism is used instead. Their simulations have shown that the delivery ratio of the beacon has increased by 60% in networks with high density.

In [97], a study has been conducted on controlling the access to the medium by vehicles running delay sensitive platooning applications. A token-based solution has been proposed to avoid the synchronization overhead that takes place in TDMA-based mechanism. It is a distributed mechanism that uses a token to exclusively access the channel. The selection of the next token holder is done based on the data age and the previous received beacons. A vehicle, member of the platoon, can access the channel and transmit the beacon only when it receives the token and the medium is

sensed free. The token is transmitted at the same time, piggybacked on the beacon, to the vehicle next in turn to be the token holder. The simulation results have shown that this protocol's performance has exceeded the one of IEEE 802.11p. It has reduced the beacon inter-reception time compared to the conventional IEEE 802.11p standard.

2.5 Survey Studies about VANET

Many survey studies about different subjects related of vehicular networks have been proposed in the literature. We present briefly some of the most recent ones.

A general brief study about the architectures, research issues, routing protocols and the applications in VANET have been presented in [98]. The security issues related to VANET have been discussed in [99] and in [100]. The authors of both papers have listed the associated security challenges, the different types of malicious attacks, the preventive measures. And they have concluded with a summary of existing solutions. Anita *et al.* in [101] have presented a survey study about the authentication schemes in VANET. This paper have summarized the different schemes and provided a comparison study based on their security features. They have also classified them according to communication environment (V2V and V2I). Kerrache *et al.* in [102] have proposed an overview about the trust management of vehicular networks. They have presented a detailed explanation about the main features, differences, advantages, and drawbacks of both trust and cryptography. They have talked about some specific malicious techniques to bypass the the cryptography solutions.

A detailed survey study about the media access control in VANET has been proposed in [103]. The study has started with a list of the recent research areas and challenges in VANET at the different protocol layers. It has discussed the main MAC design elements that should be taken into account. The authors have also summarized the future MAC challenges, the Non-IEEE 802.11p protocols and the different standards that support VANET.

A brief clustering algorithms survey has been proposed in [104]. It has described the existing al-

gorithms and the applications used in cluster-based network. On the other hand, an in-depth and big comparative survey study about the clustering techniques has been proposed by Cooper *et al.* in [105]. It has included several important aspects of the subject such as: Development of clustering in VANET, anatomy of clustering algorithm, applications of clustering, cluster head selection strategies, taxonomy of VANET clustering techniques, and other related topics.

Chen *et al.* in [106] have proposed a survey study about the existing techniques and solutions for cooperative intersections. They have discussed in details the cooperative methods that include time slots, space reservation, trajectory planning and virtual traffic lights. They have concluded their research by introducing the major cooperative intersections management projects.

We present a final survey study proposed by Jia *et al.* in [107]. They have proposed an overview about platoon-based vehicular cyber-physical system. They have studied the associated network architectures, standards and the traffic dynamics.

2.6 Conclusion

In this chapter, we have provided an overview of the available research proposals that target improving MAC protocols in VANET. This survey of the research contributions reveal the central role of the IEEE 802.11p protocol in the context of vehicular communications. It shows the importance of enhancing this protocol to enable applications that provide various services. In light of this study, we can clearly see that new adaptive-based approaches can be developed to increase the performance of IEEE 802.11p protocol in a star topology architecture. We can also clearly conclude that new QoS-based mechanisms combined with a new distributed time synchronization system can be realized in a large-scale network.

Chapter 3

Performance Analysis of IEEE 802.11p Protocol With Finite Buffers

3.1 Introduction

The Dedicate Short Range Communication (DSRC) system is considered as one of the main communication standards used in wireless inter-vehicular and Vehicles to Infrastructure (V2I) communication applications. DSRC is primarily designed to suite the requirements of highly dynamic environments such as the Vehicular Ad hoc Networks (VANETs). Various Intelligent Transportation System (ITS) applications such as road safety, transportation management and Vehicle-to-Grid (V2G) applications explicitly rely on the reliable and timely operation of VANETs.

The IEEE 802.11p defines the specifications for the physical and the Medium Access Control (MAC) layers of DSRC. The physical layer of the IEEE 802.11p is similar to the physical layer of the IEEE 802.11a [108]. However, the signal bandwidth is scaled down to 10 MHz (instead of 20 MHz in IEEE 802.11a protocol), this is done to cope with the high mobility in vehicular environments. On other hand, the MAC layer of the IEEE 802.11p follows the MAC layer of the IEEE 802.11e [109]. There is a major difference between the two MAC layers, the IEEE 802.11p supports only four Access Categories (ACs) instead of eight ACs in the IEEE 802.11e, and this is also done to support high mobility.

In general, analytical models of wireless communication protocols are considered as excellent benchmarking and testing tool to investigate the performance of these systems under different traffic and network conditions.

In addition to benchmarking and testing, analytical models can also be used to derive various optimization problems to optimize the performance of the network before being deployed. In the past,

there has been many publications that consider developing analytical models for the legacy IEEE 802.11 protocols [10, 110–112]. Furthermore, in past few years, there has been some attempts to model the IEEE 802.11p protocol [28, 31, 32, 113]. However, some of these models were too general and in some cases can be considered as incomplete because they overlook very important facts about the operation of the protocol.

In this chapter, we propose a Markov-based analytical model for the IEEE 802.11p protocol. In this model, we consider critical aspects that represent accurate operation of the protocol, these aspects are; the unsaturated traffic condition, the internal collision and the backoff blocking probability. In addition to that, we develop an analytical model to investigate the effects of finite buffers at the head of the MAC layer queue. We validate our analytical results by performing comprehensive simulations for different traffic and network conditions using Network Simulator 2 (NS2).

The main contributions of this chapter can be outlined bellow:

- We model unsaturated traffic conditions, we do this by considering probabilistic traffic arrival patterns and by considering periods where certain nodes can be idle.
- We model the backoff blocking probability at the backoff stage. We consider the case where the counter can not be decremented unless the medium is detected free for one period of time.
- We model the internal competition. We do this by considering four ACs with different levels of priorities at the MAC layer. We consider the competition of these ACs among each other to gain a transmission opportunity.
- We model the effects of finite buffer at the MAC layer. We model the impact of a finite size buffer at the head of each AC queue at the MAC layer. We investigate the impact of these buffers on the performance of the entire network.

The remainder of this chapter is organized as follows. In Section 3.2 we present a comprehensive review of the related work. Section 3.3 derives the analytical model. It consists of three

parts: an overview of the IEEE 802.11p standard, a realistic analytical model of IEEE 802.11p, and an analytical model of the IEEE 802.11p with the buffer. In Section 3.4 we discuss of backoff blocking probability and the internal collision probability. In Section 3.5 we identify and describe thoroughly the performance metrics that we use in our study. In Section 3.6 we show our results and conduct the analysis, and finally in Section 3.7 we conclude this chapter.

3.2 Related Work

In the literature, we find multiple modelling methods that were adopted to describe different proposed schemes and services [114], such as the finite multi-state model in [115], the fuzzy logic based algorithm in [116], and the probabilistic approach in [117]. Many developed analytical models for the IEEE 802.11 MAC protocol family have been based on the well-known Markov chain model proposed by G. Bianchi [10] in 2000. These Bianchi-based models have studied a wide range of mechanisms such as the simple IEEE 802.11 Distributed Coordination Function (DCF), the IEEE 802.11a and IEEE 802.11e Enhanced Distributed Channel Access (EDCA) for Quality of Service (QoS)-based networks, and finally the IEEE 802.11p EDCA for vehicular networks.

The authors of [118] have studied the performance of IEEE 802.11 in terms of reliability in a VANET. They have evaluated the packet reception rate, the packet delivery ratio and the packet deliver probability of the 1-D one-hop VANET assuming practical conditions such as interference range and non-identical transmission range. However this paper failed to take the unsaturated traffic condition and the inter-AC competition into account.

Many research papers have tackled the modelling of the IEEE 802.11e protocol using Markov chain. Most of them have taken into account some realistic conditions however they have missed some important factors such as the freezing probability and the unsaturated traffic pattern. A three-dimensional Markov chain of the IEEE 802.11e EDCA protocol have been introduced in [119] and in [120]. The Aim of both studies is to analyse the impact of different AIFS values, contention

window size, and transmission retries limits. Both have considered the internal blocking probability, however the difference is that the former has considered a saturated traffic condition while the latter an un-saturated traffic condition. [121] and [122] have presented two-dimensional Markov chain model for saturated and unsaturated IEEE 802.11e protocol respectively. Similar to [119] and [120], they have described differentiation based on different EDCA parameter values, and they have evaluated their modes by studying its throughput and its delay.

Several studies have implemented Markov chain-based analytical system to model the EDCA behavior in the IEEE 802.11p protocol. The work done in [22, 23, 123–125] propose a two-dimensional Markov chain model for a saturated traffic condition and it assumes that the channel is available every time it is checked in the backoff stage. In [33], a two-dimensional Markov model that takes into account the backoff blocking probability, the unsaturated traffic condition and the internal collision probability has been considered, however the study was limited to two ACs only. Sun *et al.* in [31] have proposed an analytical model based on two-dimensional Markov chain model that includes the backoff blocking probability and the internal competition among the classes, however assumed a saturated scenario. In [29], a new comprehensive analytical system that depicts the operation of IEEE 802.11p protocol has been established. It is based on a three-dimensional Markov chain model that takes into account the QoS features of the EDCA and also the vehicle mobility in terms of velocity and direction. To evaluate the performance of the proposed model, the authors have devised a scenario where many moving vehicles are running multiple applications with different QoS requirements, competing among each other to communicate with the infrastructure. Their findings show that the vehicles moving with high speed have experienced severe variations of service quality. The proposed model did not consider the case of unsaturated traffic.

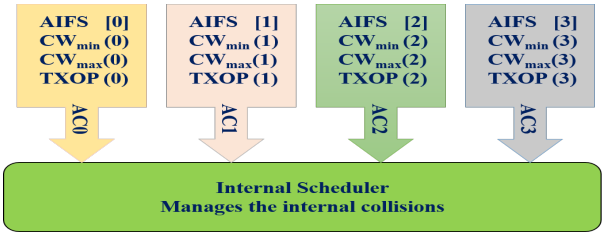

Figure 3.1: EDCA Operation

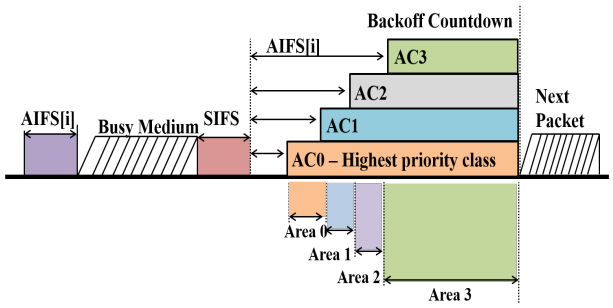

Figure 3.2: Backoff Phase

Table 3.1: Default EDCA Parameters

AC	$CW_{min}[i]$	$CW_{max}[i]$	AIFSN[i]
AC0	$\frac{CW_{min}+1}{4}-1$	$\frac{CW_{min}+1}{2}-1$	2
AC1	$\frac{CW_{min}+1}{4}-1$	CW_{min}	3
AC2	$\frac{CW_{min}+1}{2}-1$	CW_{max}	6
AC3	CW_{min}	CW_{max}	9

3.3 Analytical Model

3.3.1 IEEE 802.11p Standard Overview

The IEEE 802.11p MAC [8] implements the same EDCA mechanism adopted by IEEE 802.11e [109]. The EDCA is an extension of the 802.11 DCF, it is designed to enable QoS support for contention-based wireless communications. The MAC protocol maps each frame coming from the application layer to an AC queue. In fact, multiple applications with different requirements could be running simultaneously in a node. Each application requires different level of service and thus different ranks of priority. Unlike IEEE 802.11e, only four queues to specific ACi are defined, which provide prioritized data traffic according to the characteristics of each traffic such as video, voice, best effort and etc. Each AC queue is defined by its own set of EDCA parameters: the minimum and maximum Contention Window (CW) size, *CWmin*, *CWmax*, the Arbitration Inter-frame Space (AIFS), and Transmission Opportunity (TXOP). Internally, there is a scheduler that manages the internal collision among the ACi. The role of the scheduler is to decide which AC earns the transmission opportunity over the medium. Figure 3.1 describes the internal scheduler process used in the IEEE 802.11p MAC. Each AC queue contends for the transmission indepen-

dently. Each ACi is permitted to contend for the medium access after an AIFS period specified to it as shown in Figure 3.2 AIFS[i] is set as given below:

$$AIFS[i] = T_{SIFS} + AIFSN[i] \times T_{Timeslot} \tag{3.1}$$

Where, AIFSN[i] is a parameter associated with the queue AC_i, it presents the AIFS slot count for priority class i. It is defined, along with the CW parameters, in Table 3.1. $T_{Timeslot}$ and T_{SIFS} are the duration of the timeslot and SIFS respectively.

Low AIFSN values are assigned to high-priority classes to grant them access to the medium before classes with lower priority. In addition, the CW parameters of the high-priority classes have smaller sizes than those associated with low-priority classes as it is clear in Table 3.1. TXOP also differentiates the QoS of each AC_i. With a larger $TXOP$, more packets are exchanged between the vehicle and the Road Side Unit (RSU) during each transmission. After waiting for AIFS[i] since the channel became idle, each ACi is proceeded with a backoff procedure before transmitting its packets. The backoff counter is set to a random integer number drawn from the range *(0,CWi)*. CW_i is the maximum window size at stage i. It is defined as:

$$CW_i = \begin{cases} CW_{min} & \text{if } i = 0, \\ 2^i \times CW_{i-1} + 1 & \text{if } 1 \leq i \leq M-1, \\ CW_{max} & \text{if } M \leq i \leq M+f. \end{cases} \tag{3.2}$$

And thus the window size W_i

$$W_i = \begin{cases} CW_{min} + 1 & \text{if } i = 0, \\ 2^i \times W_0 + 1 & \text{if } 1 \leq i \leq M-1, \\ CW_{max} + 1 & \text{if } M \leq i \leq M+f. \end{cases} \tag{3.3}$$

The value of CW_{min} and CW_{max} are defined as 15 and 1023 according to [8]. For every time slot sensed idle, the backoff counter is decremented by one unit, otherwise it keeps the same value until the channel becomes idle again for a period of *AIFS[i]*. When the counter reaches zero, the packet

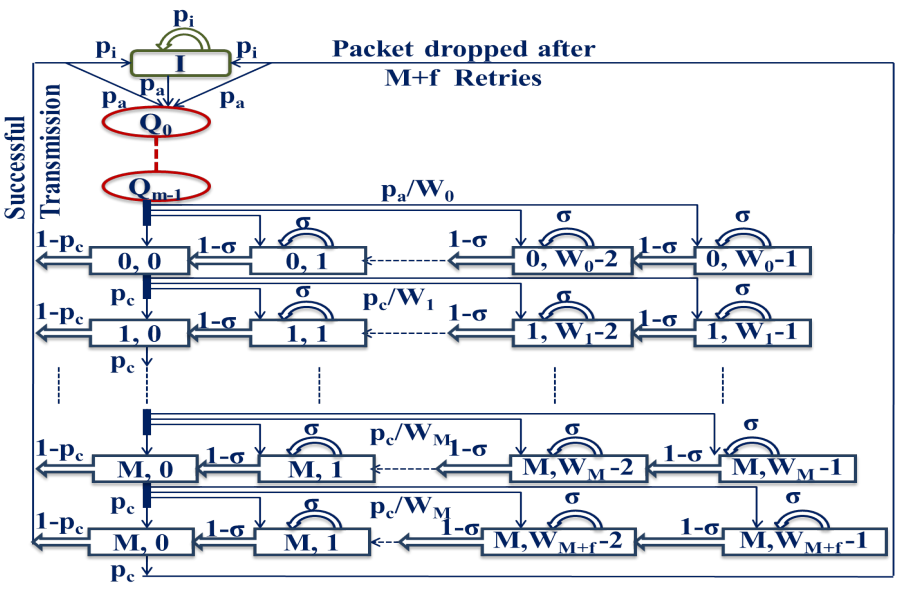

Figure 3.3: Markov Chain representation of EDCA with buffer for one AC

in the AC_i queue is transmitted. In case of a collision, the backoff window size doubles, and the backoff procedure is re-initiated. After a maximum number of retries *(M+f)*, the packet is dropped and the system returns back to the idle state waiting for packets from the upper layers. One of the most suitable and realistic tools to model a wireless MAC protocol is the discrete event Markov chain model. We adopt this method to present the slotted CSMA/CA protocol in the IEEE 802.11p. In contrast to the majority of the proposed models in the literature, our analytical representation reflects a realistic operation of the protocol. It incorporates three important factors: the unsaturated traffic condition, the internal *ACi* competition for a transmission chance, and the backoff blocking probability. An application running over an IEEE 802.11p protocol does not generate continuous data especially in the absence of any event that trigger it, and thus the assumption of the unsaturated traffic. As described in the previous section, there are four competing *ACi* at the MAC layer that reflect four priority levels for the packets sent by different applications , therefore this competition should be calculated. The backoff blocking probability is associated with the state of the channel sensed when the AC is in the backoff stage. As per the standard, there is a probability of having the channel busy or idle and as a result the backoff counter freezes or decreases.

The two-dimensional Markov chain is illustrated in Figure 3.3 (without the buffer Q_0 to Q_{m-1}).

This model shows the three main states that the protocol may be in: the idle state, the backoff state and the transmission state. The performance of the network can be evaluated by studying and analysing the analytical model in Figure 3.3 (without the buffer Q_0 to Q_{m-1}). We need first to define each state with the basic stochastic processes that distinctively identifies it. Two stochastic processes are required:

- The first one characterizes the value of the backoff counter at a given time t. Its value does not exceed W_{i-1} in the stage i, and it is always greater than or equal to zero. We denote this process as *b(t)*.

- The second one characterizes the backoff stage at a given time t. Its value does not exceed $M+f$ and it is always greater than or equal to zero. We denote this process as *s(t)*.

The couplet *(s(t), b(t))* identifies uniquely each state in the model. The initial state of the model is the idle state presented by I. In this position, the MAC sub-layer awaits the arrival of a packet from the application layer. As long as no packet has been sent from the upper layer, the node remains in the idle state with a probability p_i. The node leaves this state at the moment of a packet arrival with a probability $p_a = 1 - p_i$. Then the AC picks a random number between 0 and W_0 and continues to the correspondent state in the first backoff stage with a probability equal to $1/W_0$. At this phase, the AC examines the availability of the channel every AIFS period of time. If the channel is found unused, the AC advances to the next state in the backoff stage and the backoff counter decrements by one with a probability σ. Otherwise, it does not leave the current state and the backoff counter freezes with a probability $1 - \sigma$. Eventually, it reaches the state *(0,0)* and the packet is then transmitted. Given that the wireless medium is shared among all nodes, there is a chance that the packet collides with another packet sent by another node, as a result the packet is either transmitted successfully with probability p_t or unsuccessfully due to a collision ($p_c = 1 - p_t$). In case of a successful transmission, the node returns back to the initial state or to the first backoff stage depending on the absence or the presence of a new packet arrival. However,

following a packet collision, the *AC* picks a new random number between *0* and W_1 and selects consequently a random state in the next backoff stage. The *AC* repeats the same process that took place in the first backoff stage, given that the size of the contention window has doubled. In the event of recurrent collisions, the node switches to a new random state in the next backoff stage for a maximum number of times equal to *M+f*. After *M+f* times, the AC goes back to its initial whether the packet is successfully sent or it is dropped due to a collision.

The transition probability from the state *(m,n)* at time *t* to the state *(i,j)* at time *t+1* is given as $p(i, j|m, n)$. The transition probabilities that we need to define are the following:

- The probability of staying in the idle state from time *t* to time *t+1* because no packet has been sent from the upper layer. We denote it as $P(I|I)$.
- The probability of switching to a random state in the first backoff stage from the idle state after receiving a packet. We denote it as $P(0,k|I)$. *(0,k)* is a random state selected in the first backoff stage.
- The probability of sensing the channel idle for AIFS period of time in the backoff stage. It is in fact the probability to decrement the backoff counter by one unit and the AC passes to the next state in the same backoff stage. We denote it as $P(i,k|i,k+1)$.
- The probability of sensing the channel busy in the backoff stage. It is the probability of freezing the backoff counter from a period of AIFS. We denote it as $P(i,k|i,k)$
- The probability of transiting to new random state in the next backoff stage *i+1* in case of an un-successful transmission at the backoff stage *i*. we denote it as $P(i+1,k|i,0)$.
- The probability of transiting to the first backoff stage (in case of the presence of a new packet) after a successful transmission at a backoff stage *i*. we denote as: $P(0,k|i,0)$.

- The probability of returning to the idle state after M+f retries to transmit the packet.

The above-defined probabilities are expressed in the following system of equations (at this stage we are not considering the buffer shown in the model):

$$\begin{cases} P(I|I) = 1 - p_a & \\ P(0,k|I) = \frac{p_a}{W_0} & \text{for } 0 \le k \le W_0 - 1, \\ P(i,k|i,k+1) = 1 - \sigma & \text{for } 0 \le k \le W_i - 1, \\ & 0 \le i \le M + f \\ P(i,k|i,k) = \sigma & \text{for } 0 \le k \le W_i - 1, \\ & 0 \le i \le M + f \\ P(i+1,k|i,0) = \frac{p_c}{W_{i+1}} & \text{for } 0 \le k \le W_i - 1, \\ & 0 \le i \le M + f - 1 \\ P(0,k|i,0) = \frac{(1-p_c)\times p_a}{W_0} & \text{for } 0 \le k \le W_i - 1, \\ & 0 \le i \le M + f - 1 \\ P(I|M+f,0) = 1 - p_a & \end{cases} \tag{3.4}$$

We define the stationary probability (b_{ij}) of the state *(i,j)* as:

$$\lim_{t\to\infty} P(s(t) = i, b(t) = j),$$

$$0 \le i \le M + f, 0 \le j \le \max(W_{i-1}) \tag{3.5}$$

The stationary probability of the idle state is given as b_I. Our main goal is to calculate the probability of transmission τ_i of each AC_i. We conclude the relation between the stationary probabilities of two consecutive states at the backoff stage *0*:

$$b_{0,i} = b_{0,i+1} + \frac{1}{W_0} \times \left(\left(1 - p_c\right) \times \Big(\sum_{i=0}^{i=M+f-1} b_{i,0} \Big) + b_{M+f,0} \right) \tag{3.6}$$

The stationary probability of the last state in the first backoff stage is :

$$b_{0,W_0-1} = \frac{1}{W_0} \times \left(\left(1-p_c\right) \times \left(\sum_{i=0}^{i=M+f-1} b_{i,0} \right) + b_{M+f,0} \right) \tag{3.7}$$

From Eq.(3.6) and Eq.(3.7) we can calculate the stationary probability of any state at stage *0* as:

$$b_{0,k} = \frac{W_0 - k}{W_0} \times b_{0,0} \tag{3.8}$$

The relation between the stationary probabilities of two consecutive states at a stage i (i is not equal to 0) is given by :

$$b_{i,j} = b_{i,j+1} + b_{i-1,0} \times \frac{p_c}{W_i} \tag{3.9}$$

The stationary probability of the last state in any backoff stage is given as :

$$b_{i,W_{i-1}} = b_{i,j+1} + b_{i-1,0} \times \frac{p_c}{W_i} \tag{3.10}$$

From Eq.(3.9) and Eq.(3.10) we can calculate the stationary probability of the last state in any backoff stage:

$$b_{i,W_{i-1}} = b_{i-1,0} \times \frac{p_c}{W_i} \tag{3.11}$$

We conclude that:

$$\begin{cases} b_{i,0} = b_{0,0} \times p_c^i & \text{for } 0 \leq i \leq M+f, \\ b_{i,k} = \frac{W_i - k}{W_i} & \text{for } 0 \leq k \leq W_i - 1, \\ & 1 \leq i \leq M+f \end{cases} \tag{3.12}$$

The stationary probability of the idle state is:

$$b_I = (1-p_a) \times b_I + (1-p_a) \times \sum_{i=0}^{i=M+f-1} (1-p_c) \times b_{i,0} + (1-p_a) \times b_{M+f,0} \tag{3.13}$$

The derivation of the Eq. (3.13) (taking into account Eq. (3.8), (3.11), and (3.12)) leads to:

$$b_I = \frac{1-p_a}{p_a} \times b_{0,0} \tag{3.14}$$

Our objective is to calculate the transmission probability of each class τ_i. To achieve this objective, we need first to form a system of a nonlinear equation that describe the Markov-chain model.

And then, we need to solve this system mathematically. To avoid the repetition, we restrict our calculation to one AC in this chapter. The sum of all the stationary probabilities of all the model's state is normally equal to one:

$$\sum_{i=0}^{M+f}\sum_{k=0}^{W_i-1} b_{i,k} + b_I = 1 \tag{3.15}$$

With some derivation and based on the equations Eq.(3.8), (3.12), and (3.14), we can easily determine the stationary probability of the state *(0,0)* i.e. $b_{0,0}$ (see Appendix A for detailed derivation of the equation):

$$\begin{aligned} b_{0,0} = 2 \times \Bigg[\frac{1-p_c^{M+f+1}}{1-p_c} + W_0 \times \left(\frac{1-2\times p_c^{M+1}}{1-2\times p_c} \right) \\ + W_M \times \left(\frac{p_c^{M+1} - p_c^{M+f+1}}{1-p_c} \right) + 2 \times \frac{1-p_a}{p_a} \Bigg]^{-1} \end{aligned} \tag{3.16}$$

The transmission probability of a node is the sum of the probability of transmissions at all the backoff stages. Therefore it is given as:

$$\tau = \sum_{i=0}^{M+f} b_{i,0} = b_{0,0} \times \frac{1-p_c^{M+f}}{1-p_c} \tag{3.17}$$

The system of non-linear equation is formed by joining the four equations which are the transmission probabilities of each AC.

3.3.2 Analytical Model of IEEE 802.11p with Buffer

The previous Markov chain models the real operation of the CSMA/CA mechanism used in the IEEE 802.11p protocol. In this section we append the model with a buffer at the entrance of the MAC sub-layer. Figure 3.3 shows our proposed two-dimensional Markov chain. The states Q_o to Q_{m-1} presents the buffer with a size m. The packets sent by the application layer, reach the MAC and enter into the buffer. The packets inserted in the buffer follows the First-In First-Out (FIFO) method. Every AIFS period of time, the packet in the buffer moves one state till it reaches the state Q_{m-1}.

The new system of equation of the transition probabilities is the following:

$$\begin{cases} P(I|I) = 1 - p_a & \\ P(B_0|I) = p_a & \\ P(0,k|B_{m-1}) = \frac{p_a}{W_0} & \text{for } 0 \leq k \leq W_0 - 1, \\ P(i,k|i,k+1) = 1 - \sigma & \text{for } 0 \leq k \leq W_i - 1, \\ & 0 \leq i \leq M + f \\ P(i,k|i,k) = \sigma & \text{for } 0 \leq k \leq W_i - 1, \\ & 0 \leq i \leq M + f \\ P(i+1,k|i,0) = \frac{p_c}{W_{i+1}} & \text{for } 0 \leq k \leq W_i - 1, \\ & 0 \leq i \leq M + f - 1 \\ P(B_0,k|i,0) = \frac{(1-p_c)\times p_a}{W_0} & \text{for } 0 \leq i \leq M + f - 1 \\ P(I|M+f,0) = 1 - p_a & \end{cases} \tag{3.18}$$

The steady states probabilities in first and the succeeding backoff stages are given as:

$$\begin{cases} b_{0,j} = \frac{W_0 - j}{W_0} \times \frac{1}{1-\sigma} \times b_{0,0} & \text{for } 0 \leq j \leq W_0 - 1, \\ b_{i,0} = b_{0,0} \times p_c^i & \text{for } 0 \leq i \leq M + f, \\ b_{i,j} == \frac{W_i - j}{W_i} \times \frac{1}{1-\sigma} \times b_{i,0} & \text{for } 1 \leq j \leq W_i - 1, \\ & 0 \leq i \leq M + f \end{cases} \tag{3.19}$$

The steady state probability of the idle state is similar to the one calculated in the previous model (Eq. (3.14))

The steady state probability of the first buffer state b_{B0} is determined in the same way:

$$b_{Q0} = (1 - p_a) \times b_I + p_a \times b_{M+f,0} + p_a \times \Big(\sum_{i=0}^{i=M+f-1} p_c \times b_{i,0} \Big) \iff b_{Q0} = b_{0,0} \tag{3.20}$$

Therefore the sum of all the steady state probabilities at the buffer is:

$$\sum_{i=0}^{m-1} b_{Qi} = m \times b_{Q0} = m \times b_{0,0} \tag{3.21}$$

From Eq. (3.14), (3.19), (3.20) and (3.21) we can find $b_{0,0}$. It is given by:

$$b_{0,0} = 2 \times \left[2 \times \frac{1 - p_c^{M+f+1}}{1 - p_c} + W_0 \times \left(\frac{1 - 2 \times p_c^{M+1}}{1 - 2 \times p_c} \right) + W_M \times \left(\frac{p_c^{M+1} - p_c^{M+f+1}}{1 - p_c} \right) + 2 \times \frac{1 - p_a}{p_a} + 2 \times m \right]^{-1} \tag{3.22}$$

The transmission probability of a node is the sum of the probability of transmissions at all the backoff stages:

$$\tau = \sum_{i=0}^{M+f} b_{i,0} = b_{0,0} \times \frac{1 - p_c^{M+f}}{1 - p_c} \tag{3.23}$$

The system of non-linear equation is formed of four equations which are the transmission probabilities of each AC.

3.4 Internal Collision Probability and Backoff Blocking Probability

In this section we present a detailed description of the internal collision and the backoff blocking mechanisms.

3.4.1 Internal Collision Probability

The internal scheduler handles the internal contention among the *ACs*, its main aim is to resolve which *AC* has the priority to access the medium. As we stated previously, each *AC* acts like an independent DCF station, therefore the four *ACi* tend to compete internally as four different self-governing stations. The operation of the internal scheduler is illustrated in Figure 3.4. After the backoff stage, an *AC* either wins a transmission opportunity or collides with another *AC* which has already started transmitting at earlier time. To thoroughly understand the virtual competition among *ACi*, we refer you to Figure 3.5. In this figure we divide the backoff stage into four contention areas: *Area0*, *Area1*, *Area2* and *Area3*. Each area presents the contention zone of its corresponding *AC*. These areas are defined based on the values of the EDCA parameters allocated

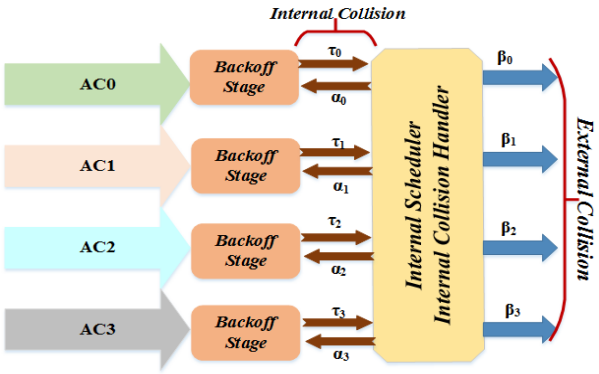

Figure 3.4: Internal Collision

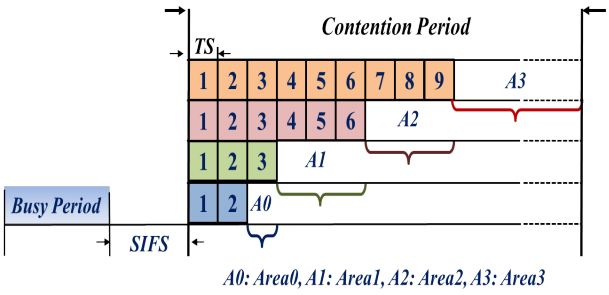

Figure 3.5: Size of Collision Areas

to each *AC* (is shown in Table 3.1). We denote n_i the size of $Area_i$, it is calculated as the following:

$$n_i = AIFSN[i+1] - AIFSN[i] \tag{3.24}$$

as a result:

$$\begin{cases} n_0 = 1 \\ n_1 = 3 \\ n_2 = 3 \\ n_3 = 8 \end{cases} \tag{3.25}$$

An internal collision occurs if at least two *ACi* have packets to transmit, and they start backing off at the same time. As per the standard, *AC0* waits only two timeslots before setting on the backoff counter, however *AC1*, *AC2* and *AC3* pauses three, six and nine timeslots respectively prior the backoff phase (see AIFSN values in Table 3.1, refer to Figure 3.5). Thus, *AC0* is the only class that begins the backoff segment at the third timeslot (*Area0*), therefore in *Area0* there is no competition with *AC0*. On the other hand, *AC1* starts the backoff period at the fourth timeslot, just one timeslot after *AC0* and three timeslots before *AC2* (*Area1*). In this area, *AC1* may only collide with *AC0*, it never collides with *AC2* and *AC3*. By analogy, we prove that *AC2* competes only with *AC0* and *AC1* in *Area2* and it is never affected by *AC3*. Finally *AC3* cannot transmit in *Area3* unless all other *ACi* are not engaged in a communication process. We assume α_i is the internal collision probability,

τ_i is the internal transmission probability, and β_i is the external transmission probability of ACi (As illustrated in Figure3.4). β_i is only noticed externally by other nodes. The internal collision probabilities are then given as:

$$\begin{cases} \alpha_0 = 0 \\ \alpha_1 = \tau_0 \\ \alpha_2 = 1-(1-\tau_0)\times(1-\tau_1) \\ \alpha_3 = 1-(1-\tau_0)\times(1-\tau_1)\times(1-\tau_2) \end{cases} \tag{3.26}$$

The first term in Eq.(3.26) proves that *AC0* is the class with the highest priority, therefore any packet coming from this class should not suffer any competition with those arriving from other classes. The second equation shows that *AC1* is ranked second in terms of priority, its packets may compete only with packets generated from *AC0*, the collision in this area depends only on whether *AC0* is transmitting or not. The third equation shows that *AC2* packets experience internal collision only if *AC0* or *AC1* are ready to transmit. The fourth equation shows that *AC3* has the lowest priority, it collides internally when any of the above classes is transmitting.

A specific *AC* is able to transmit externally if and only if it has packet ready for transmission and it does not experience an internal collision. The external transmission probability is calculated as the following:

$$\begin{cases} \beta_0 = \tau_0 \times (1-\alpha_0) = \tau_0 \\ \beta_1 = \tau_1 \times (1-\alpha_1) = \tau_1 \times (1-\tau_0) \\ \beta_2 = \tau_2 \times (1-\alpha_2) = \tau_2 \times (1-\tau_0)\times(1-\tau_1) \\ \beta_3 = \tau_3 \times (1-\alpha_3) = \tau_3 \times (1-\tau_0)\times(1-\tau_1)\times(1-\tau_2) \end{cases} \tag{3.27}$$

The first term in Eq. (3.27) shows that *AC0* transmits externally directly without any complication once it receives frames from the upper layer. The second equation shows that AC1 transmits externally if it is ready to transmit and at the same time AC0 is not trying to communicate. The third equation proves that AC2 cannot be connected externally if AC0 or AC1 are active. Same logic

applies on AC3 in the fourth equation.

The total transmission probability of a vehicle is the sum of all the external transmission probability:

$$\beta = \beta_0 + \beta_1 + \beta_2 + \beta_3 \tag{3.28}$$

The total external collision probability is the probability of having at least one node transmitting while the current node decides to transmit. It is given by:

$$P_c = 1 - (1 - \beta)^{N-1} \tag{3.29}$$

The collision probability of the class AC_i is calculated as:

$$p_{ci} = \alpha_i + (1 - \alpha_i) \times P_c \tag{3.30}$$

p_{ci} is the probability of having an internal collision or an external collision if no internal collision has occurred.

3.4.2 Backoff Blocking Probability

Our next step is to calculate the backoff blocking probability. In the backoff phase, each AC senses periodically the channel to verify its availability. This leads to either decreasing the backoff counter and proceed to the next state if the channel is detected free for an *AIFS* period of time, or otherwise to freeze the backoff counter and stay in the actual state for another *AIFS* period of time.

The probability of finding the medium busy by *ACi* in the backoff stage is in fact the same as the backoff blocking probability. To calculate it we have to take into account the following probabilities:

- The transmission probability of another AC in the same node
- The transmission probability of another node in the network

Table 3.2: Simulation Parameters

Parameter	**Value**
Transmission power	20 dbm
bandwidth	10 MHz
Floor noise	-99 dbm
CWM_{in}	15
CWM_{ax}	1023
Slot Time	13 μs
SIFS period	32 μs
Propagation delay	1 μs
Link Layer queue size	50 Packets
Data rate	6 Mbps
Packet size	1024 bits

So the backoff blocking probability is given as:

$$\begin{cases} \sigma_0 = 1 - \Big((1-\beta)^{N-1} \times (1-\tau_1) \times (1-\tau_2) \times (1-\tau_3)\Big) \\ \sigma_1 = 1 - \Big((1-\beta)^{N-1} \times (1-\tau_0) \times (1-\tau_2) \times (1-\tau_3)\Big) \\ \sigma_2 = 1 - \Big((1-\beta)^{N-1} \times (1-\tau_0) \times (1-\tau_1) \times (1-\tau_3)\Big) \\ \sigma_3 = 1 - \Big((1-\beta)^{N-1} \times (1-\tau_0) \times (1-\tau_1) \times (1-\tau_2)\Big) \end{cases} \tag{3.31}$$

Each equation in Eq. 3.31 shows that the backoff blocking happens if at least one of the other nodes in the network or one of the AC_i in the same node is involved in a communication process.

3.5 Performance Metrics

We evaluate the performance of our proposed model by assessing the following metrics: The transmission probability, the collision probability, the average network throughput and the average end-to-end delay. We define a successful transmission cycle as the total period needed for a packet to be transmitted successfully from the moment it reaches the MAC layer till the moment of the Acknowledgement (ACK) packet is received from the destination.

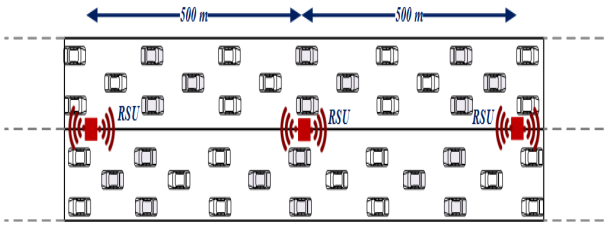

Figure 3.6: Simulation scenario

3.5.1 Average Throughput

The average throughput of a vehicle (Th) is equal to the sum of the average throughput of its four AC_i. The throughput (Th_i) of a particular AC is defined as the quotient of the average successful transmission time over the average overall time spent during a transmission cycle.

$$Th_i = \frac{E_i[T_{suc}]}{E[T_I] + E[T_{suc}] + E_i[T_{col}]} \tag{3.32}$$

$E_i[T_{suc}]$ is the average time of a successful packet transmission done by a class AC_i. $E[T_I]$ is the average idle time of the channel. $E[T_{suc}]$ is the average successful transmission time. $E_i[T_{col}]$ is the average failed transmission time due to a collision by AC_i.

$$E_i[T_{suc}] = P_i[suc] \times E[L/R] \qquad E[T_I] = P[I] \times TS \tag{3.33}$$

$$E[T_{suc}] = \sum_{j=0}^{3} P_j[suc] \times T_{sj} \qquad E_i[T_{col}] = P[fail] \times T_{ci} \tag{3.34}$$

Where,

- $P_i[succ]$ is the AC_i probability of successful transmission.
  $P_i[succ] = N \times \beta_i \times (1-\beta)^{N-1}$
- $P[I]$ is the probability of the channel being idle.
  $P[I] = (1-\beta)^{N-1}$
- $P[fail]$ is the probability of packet transmission failure due to a collision.
  $P[fail] = 1 - P[I] - N \times \beta \times (1-\beta)^{N-1}$

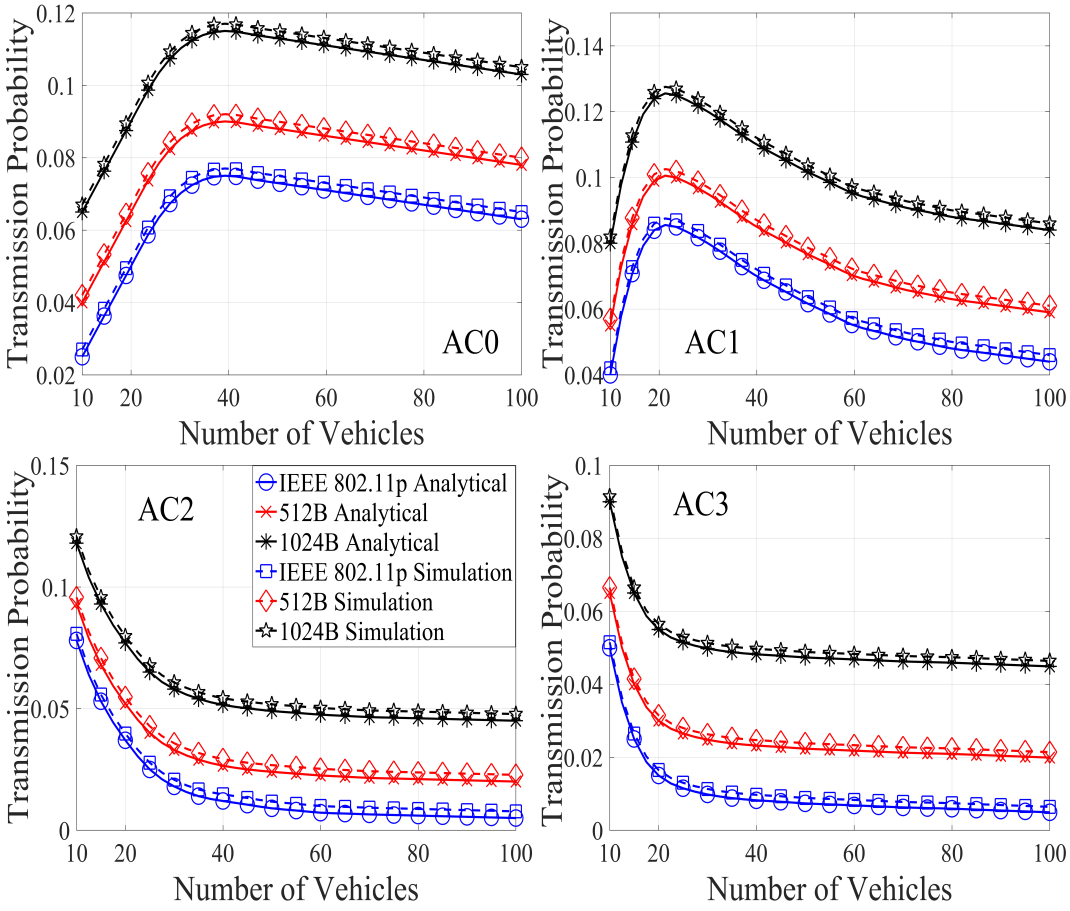

Figure 3.7: Transmission probability as function of the number of vehicles

- L is the packet length (in bits).
- R is the data transmission rate (in Mbps).
- TS is the duration of a timeslot.
- T_{si} is the duration of successful packet transmission.

  $T_{si} = T_{AIFS[i]} + T_{Header} + T_{Load} + \delta + T_{SIFS} + T_{ACK} + \delta$

- T_{ci} is the duration of the unsuccessful packet transmission.

  $T_{ci} = T_{AIFS[i]} + T_{Header} + T_{Load} + \delta$.

  δ is the propagation delay.

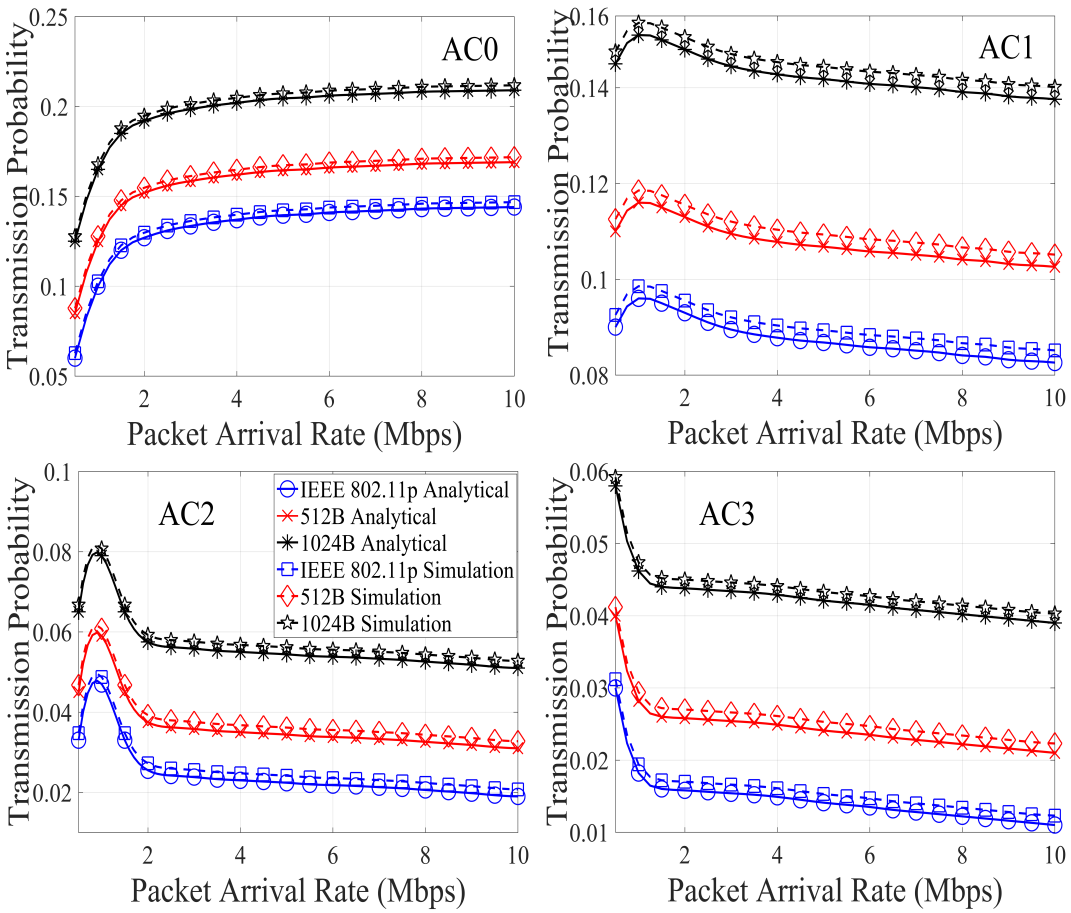

Figure 3.8: Transmission probability as function of the packet arrival rate

3.5.2 Average End-to-End Delay

The average end-to-end delay $E[D_i]$ is defined as the time elapsed between the arrival of the packet at the head of the MAC buffer till an ACK packet is received from the destination. One packet can be be successfully transmitted after one attempt, or after experiencing several collisions. However if the number of collisions exceed the $M+f$ threshold the packet is dropped. The average end-to-end delay can be expressed as the sum of two values that reflect two possible cases:

- Case 1: Successful transmission after only one attempt. We denote it as $E[D_{suc}]$
- Case 2: Successful transmission after few number of attempts due to several collisions. We denote it as $E[D_{col}]$.

$$E[D_i] = E[D_{suc}] + E[D_{col}]$$

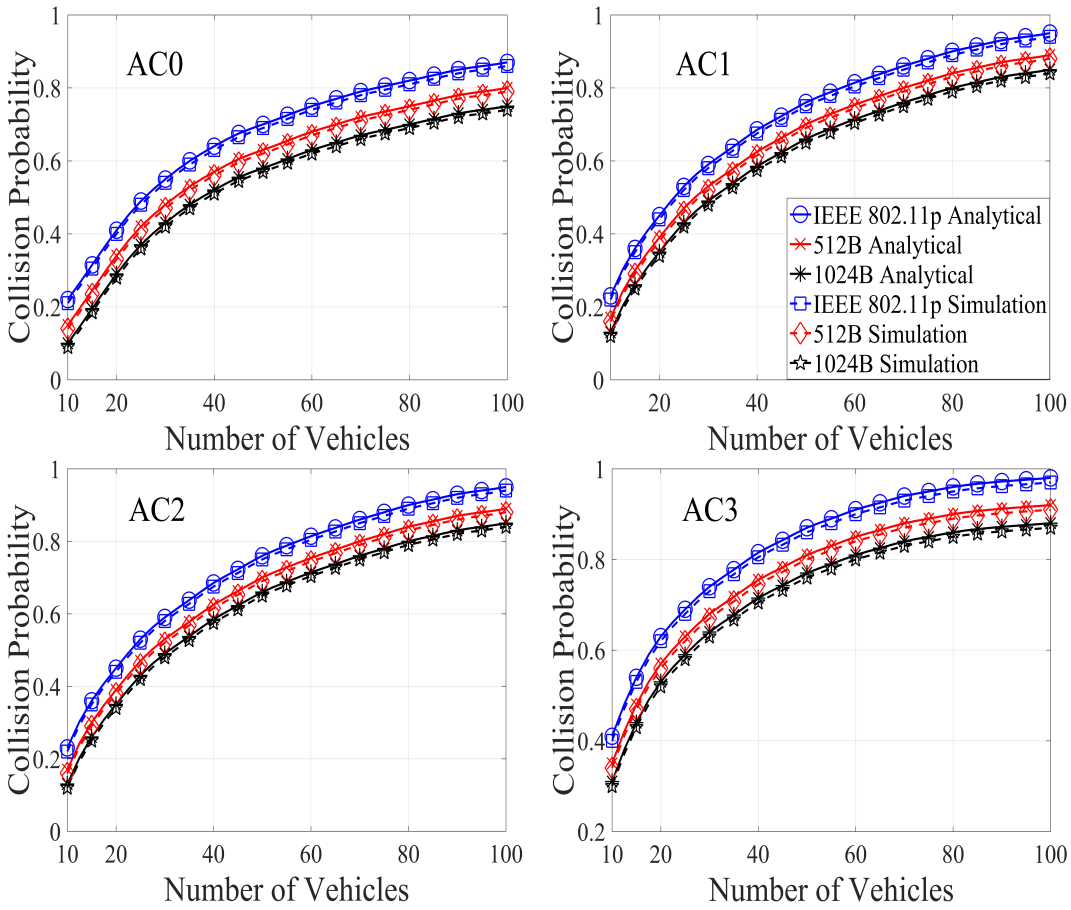

Figure 3.9: Collision probability as function of the number of vehicles

In Case 1, the delay depends on the average time spent in the backoff stage $E_i[boff]$ and on the time taken to successfully transmit the packet T_{si}.

$E[D_{suc}] = E_i[boff] + T_{si}$.

In Case 2, the delay depends on the number of retransmission attempts $E_i[Retr]$, the average delay in the backoff stage $E_i[boff]$, the transmission time lost due to the collision T_{ci} and finally the time elapsed before sensing the channel after a collision T_{sens}.

$$E[D_{col}] = E_i[Retr] \times \Big(E_i[boff] + T_{ci} + T_{sens} \Big) \tag{3.35}$$

The average time spent by a packet in the backoff stage is affected by two main variables: the average time spent in each state $E_i[State]$ and the average time spent due to the blocking mechanism

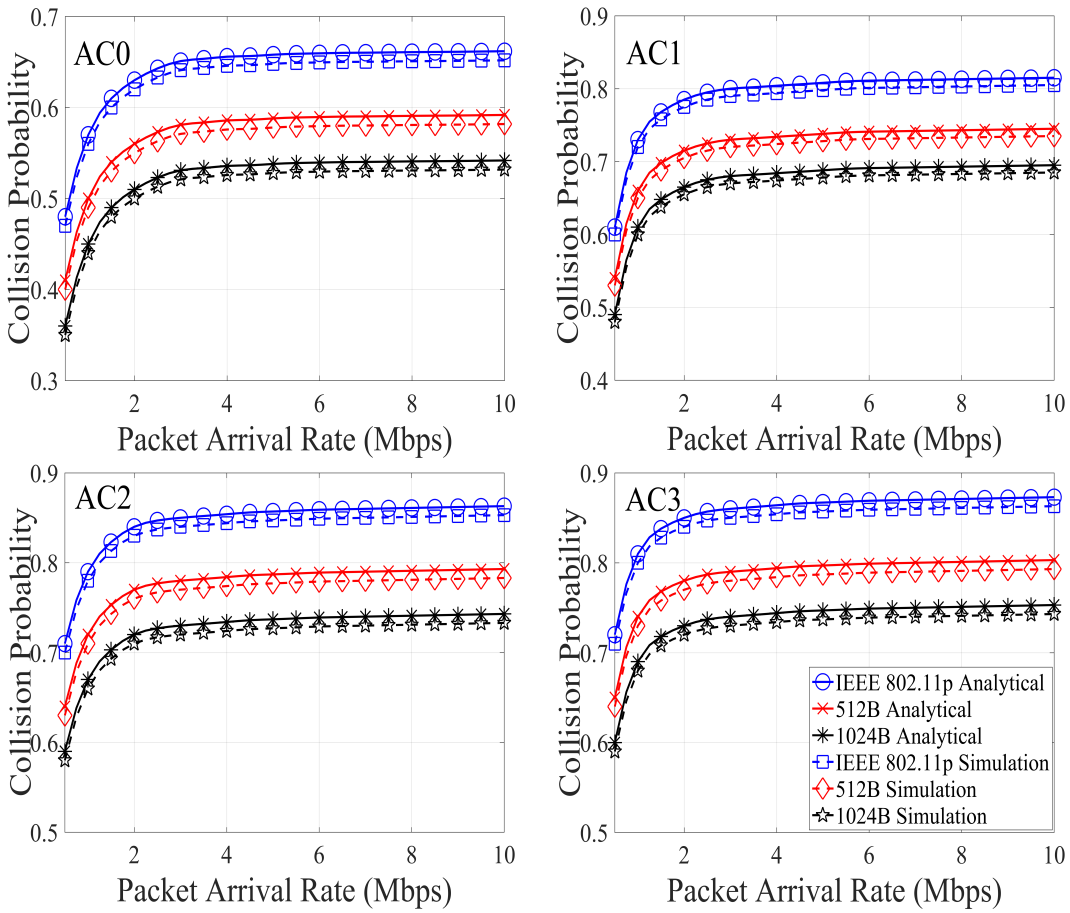

Figure 3.10: Collision probability as function of the packet arrival rate

respectively $E_i[Bloc]$. Therefore:

$$E_i[boff] = E_i[State] + E_i[Bloc] \tag{3.36}$$

At the backoff stage k, the maximum size of the window is $W_k - 1$. However, since picking the window size is a random process, the backoff size may vary between 1 and $W_k - 1$. The average time of a the backoff in this case is calculated as: $\sum_{s=1}^{W_k-1} s \times b_{ks}$.

On the other hand, the number of possible backoff stages ranges between 1 and $M+f$, which we need to consider in our calculation. Therefore the variable $E_i[State]$ is calculated as the following:

$$E_i[State] = \sum_{n=1}^{M+f} \sum_{s=1}^{W_k-1} s \times b_{si} \tag{3.37}$$

The average period spent in the backoff stage due to the blocking mechanism depends on the average number of times a state got frozen $E_i[N_{block}]$

$$E_i[N_{block}] = E_i[State] \times \frac{\sigma_i}{1-\sigma_i} \tag{3.38}$$

As a result:

$$E_i[Bloc] = E_i[N_{block}] \times \Big(E[T_{suc}] + E_i[T_{col}]\Big) \tag{3.39}$$

What remains is to determine $E_i[Retr]$ and T_{sens} in order to calculate $E[D_{col}]$. T_{sens} can be simply expressed as:

$$T_{sens} = T_{SIFS} + T_{ACK-timeout} \tag{3.40}$$

The probability of successfully transmitting a packet after exactly n collision is: $p_c^n \times (1-p_c)$. The maximum number of transmission retrial is *M+f*, therefore the average number of packet retransmission is:

$$E_i[Retr] = \sum_{n=1}^{M+f} n \times p_{ci}^n \times (1-p_{ci}) \tag{3.41}$$

3.6 Simulation Results and Analysis

3.6.1 Simulation Scenario

To evaluate the performance of our proposed model, and to validate the accuracy of the analytical model, we use the network simulation tool NS-2 [126]. The standard IEEE 802.11p is already employed in the version NS 2.34, we modify it by applying the required changes in the MAC file to achieve our design. We devise a simulation scenario that reflects the same conditions assumed in our analytical model. We assume a star topology that consists of one RSU connected to a number of vehicles. We assume that the RSU is located at in the middle of highway separating two road with different directions(see Figure 3.6) . The vehicles are passing with a fixed velocity, and the distance separating between each pair is identical. The distance between each vehicle and the RSU, as well as the communication channel conditions for each vehicle, are the same. All the vehicles and the RSU are assumed to be equipped with a communication system in which our

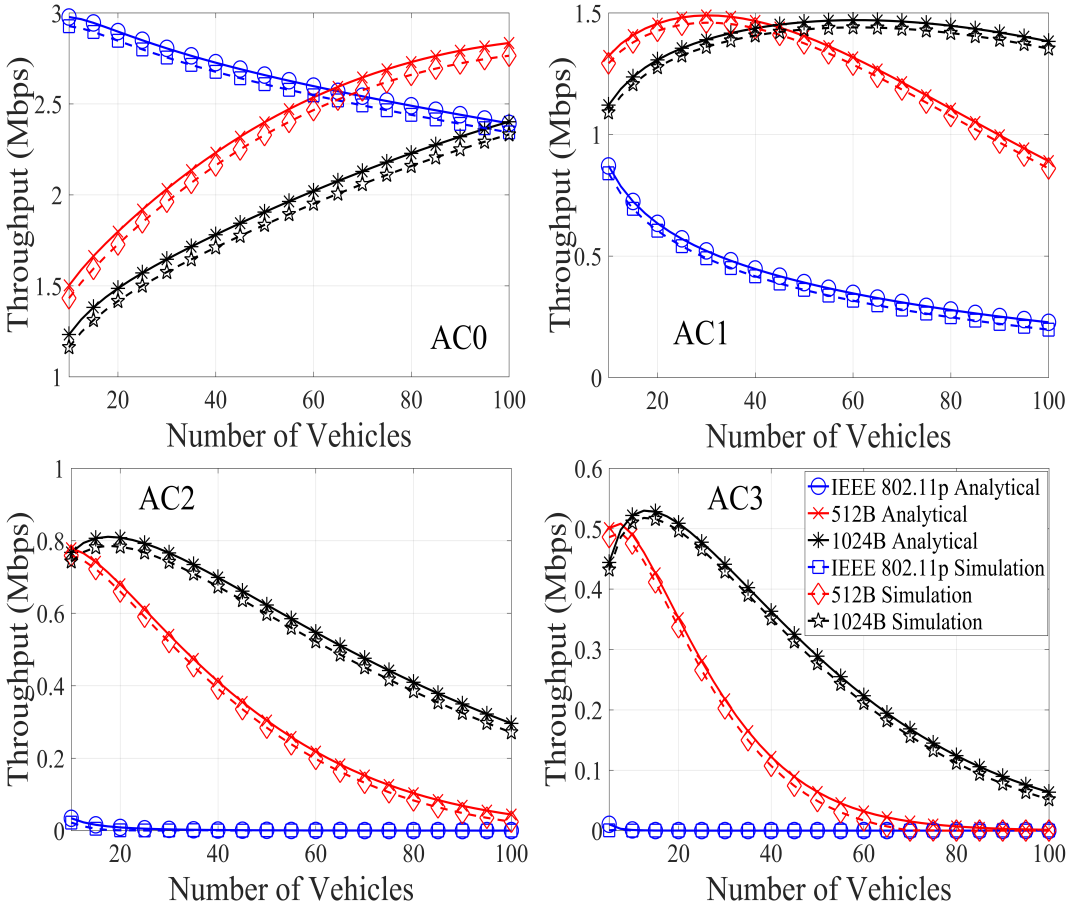

Figure 3.11: Average Throughput as function of the number of vehicles

protocol is implemented. Each vehicle falls within the transmission range of all other vehicles. When a vehicle enters the RSU coverage area, it initiates the communication with a constant-bit-rate data transmission, while competing with all other vehicles in the network for channel access. Each transmitted packet is acknowledged by an ACK packet sent by the RSU. All the simulation parameters used are summarized in the Table 3.2. In the remaining of the chapter, we use the terms 512B model and 1024B model to refer to the model that introduces a buffer of size 512B and 1024B at the entry of the MAC layer respectively. In all simulation scenarios we assume, unless stated otherwise, that the packet arrival probability is $\alpha = 0,5$, the data rate is $R = 6Mbps$, the packet size is $L = 512$.

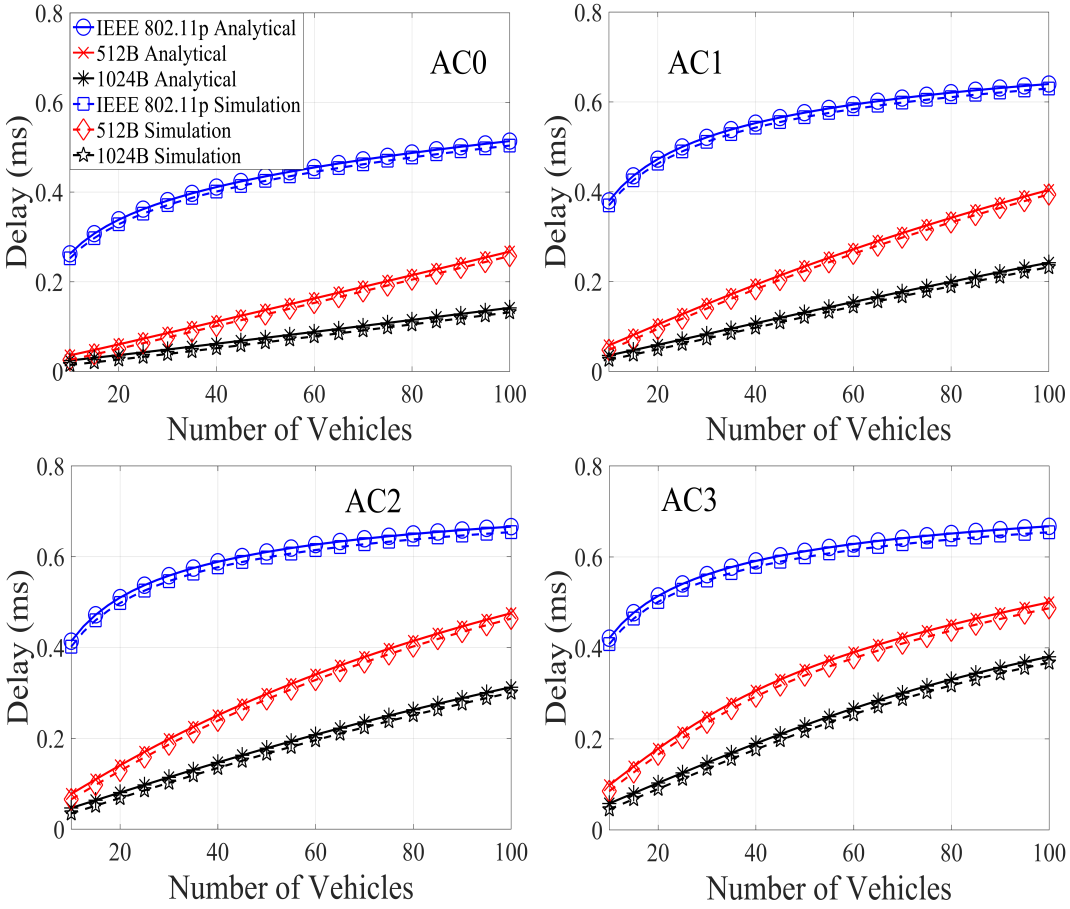

Figure 3.12: Average delay as function of the number of vehicles

3.6.2 Analysis

Figure 3.7 and Figure 3.8 shows the transmission probability of each AC versus the number of vehicles and the packet arrival rate respectively. We notice that with small number of vehicles in the network, the transmission probability reaches its higher value across all ACs. Then it decreases as the network size increases, because more vehicles are trying to transmit at the same time. We notice also that the transmission probability behaves in the same way against the number of packet arrival in Figure 3.8.

Figure 3.9 and Figure 3.10 shows the collision probability of each AC versus the number of vehicles and the packet arrival rate respectively. This metric behaves exactly the opposite of the previous, as the collision probability across all ACs tend to increase as the number of vehicles in the network and as the packet arrival rate increases. It is due to the fact that extra vehicles in

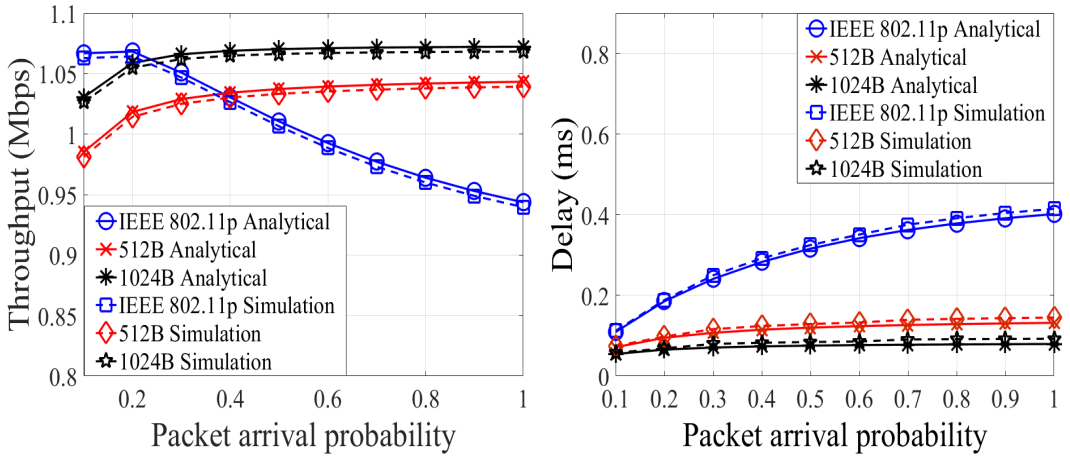

Figure 3.13: Throughput and average end-to-end delay as function of the packet arrival rate

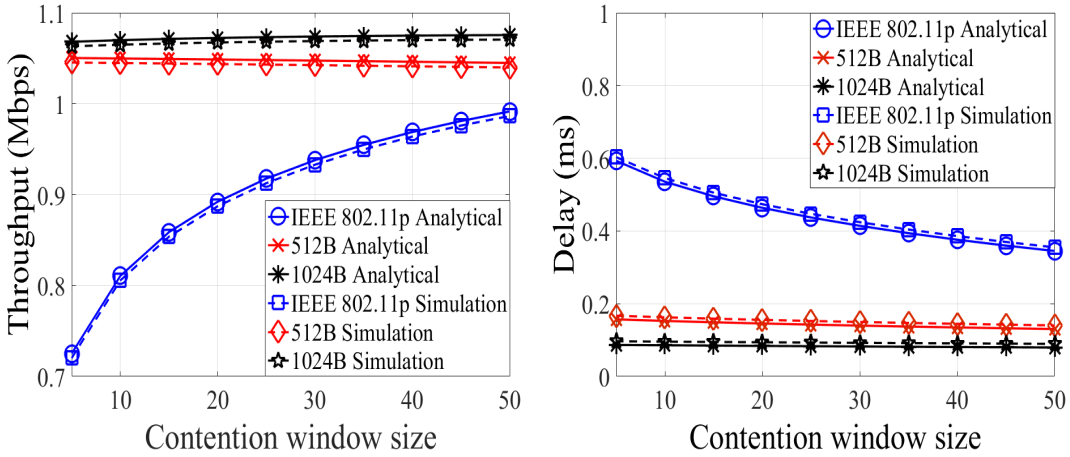

Figure 3.14: Throughput and average end-to-end delay as function of the contention window size

the network or higher number of packet arrival lead to additional collisions among the transmitted packets.

We notice that in both probabilities the simulation results are very close to the analytical model results which prove the accuracy of our model, and they show also that increasing the buffer size enhances the performance of the protocol.

Figure 3.11 shows the simulation and analytical results of the average network throughput for all ACs. We notice that the throughput of the IEEE 802.11p tends to increase at the beginning and then starts to decrease as the number of vehicles in the network increases. When the number of vehicle is small, there is a high possibility that the majority of the transmitted packets reach

their destination successfully, which increases the average throughput of the network. On the other hand, when more vehicles enter the network and participate in the communication, the number of packet exchanged increases leading to a higher probability of collisions among them, and hence the drop of the average throughput values. This figure shows also the effect of buffer (512B and 1024B). Introducing a buffer at the entry of the MAC enhances highly the performance especially in low-priority ACs. In AC0, on the contrary to the IEEE 802.11p, the throughput of 512B and 1024B increases as the number of vehicles increases, and they outperform the IEEE 802.11p at the points of 50 and 100 vehicles respectively. In AC1, AC2 and AC3, we notice that higher buffer size aligns with enhanced and better performance.

The reason behind the performance improvement when adding buffer, is that delaying the packet at the MAC layer has reduced the traffic flow to the network, so instead of overflowing the medium with packets in a very short period of time, the packets wait for a finite duration at the MAC layer which decreases the level of contention in the medium, and thus decreases the collisions rate and increases the throughput.

The average end-to-end delay of the network for different number of vehicles across all ACs is illustrated in Figure3.12. We can see that the average end-to-end delay increases with the number of vehicles. The contention of the channel access tends to augment when greater amount of vehicles is engaging in the communication process. Intense contention among vehicles is equivalent to growing percentage of packet collisions and to rising number of packet dropped. This leads to more frequent packet retransmission which cost a lot in terms of delay. Another reason is that the backoff blocking probability increases with dense network. Figure3.12 proves also that adding a buffer at the MAC layer enhances performance related to the delay. In all ACs, the value of the 1024B delay is less than the 512B which is also less than the IEEE 802.11p delay. We notice also that the delay of the highest priority AC (AC0) is less than all other ACs.

Due to the limited space, we show in Figure 3.13 the average throughput and end-to-end delay per vehicle (instead of per AC) against the packet arrival probabilities. We set the number of

vehicles to 50. We notice that the average throughput of the IEEE 802.11p protocol decreases when the packet arrival rate from the upper layer increases. The reason behind this observation is that with fixed network size, generating further data for transmission at each vehicle will flood the medium with supplementary packets that create numerous collisions, and reduce the successful transmission rate. Figure 3.13 illustrates also that adding the buffers to the MAC layers enhances the performance by improving the throughput when the packet arrival is accelerating.
Figure 3.13 demonstrates that the IEEE 802.11p protocol suffers from an excessive delay as the packet arrival probability increases. It shows also that the end-to-end delay of the 512B and 1024B models are much shorter then the IEEE 802.11p protocol. It is true that adding a buffer at the entrance of the MAC layer introduces additional delay, however this delay is very small compared to the delay caused by a collision in the medium and a packet retransmission.

In Figure 3.14, we study the influence of different contention window sizes on the performance of the protocols in terms of average throughput and average end-to-end delay. we set the network size to 50 vehicles, the packet arrival probability to 0.5, and we vary CWmin from 0 to 50.
Both figure show that increasing the contention window size enhances the performance of the IEEE 802.11p protocol, as the throughput tends to increase and the end-to-end delay tends to decrease with increasing the value of CW. Both figures show also that 512B and 1024B have higher throughput and lower delay than the IEEE 802.11p protocol.

3.7 Conclusion

In this chapter, we developed a Markov-based analytical model for the EDCA mechanism in the IEEE 802.11p. Then we extended our model by inserting a buffer at the entry point of each AC in the MAC layer. We took into account all the factors that depicts the real behaviour of IEEE 802.11p. We relied on the IEEE 802.11p standard to specify the different parameters values and we assumed an unsaturated traffic conditions, where packets are not continuously sent from the upper layers. We considered the internal competition among ACs and we included the backoff

blocking mechanism. Using the model, we determined the mathematical expressions of the average throughput and the average end-to-end delay. Our results show that our proposed model outperforms the convention IEEE 802.11p protocol. It also demonstrates that doubling the buffer size have a positive impact on the overall performance, it has increased the throughput and reduced the latency. All the figures show that our simulator results strongly agree with our mathematical model, which proves proves its accuracy.

In the next chapter, we plan to extend our work and develop new adaptive schemes at the backoff phase to adaptively select the value of the contention window size, and at the AIFS stage to dynamically set the value of the AIFS.

Chapter 4

Adaptive Algorithms for EDCA in the IEEE 802.11p protocol

4.1 Introduction

Real-time and reliable communications among vehicles and between vehicles and the surrounding infrastructure is very important in many safety related applications [13, 113, 118]. The Enhanced Distributed Channel Access (EDCA) is the main component of the IEEE 802.11p standards that enables efficient and safe communication in vehicular environment. The complete operation of EDCA have been discussed thoroughly in the previous chapter. One essential process of EDCA is the Carrier Sense Multiple Access with Collision Avoidance (CSMA/CA) algorithms. CSMA/CA manages the access of packets to the medium and its main role is to avoid collisions among them. The first key element of CSMA/CA algorithm is the backoff period in which the packets has to wait for a random number of Time Slots (TS) before attempting to access the medium. The second key element of the operation of CSMA/CA is the value of the Arbitration Inter-Frame Space (AIFS) parameter. Once a packet arrives to the head of the queue, it waits for a period of AIFS expressed in TSs. The value of the AIFS parameter differs from one AC to another in order to enforce priority differentiation among the Access Categories (AC)s. Low AIFS value is assigned to high priority AC and vice versa.

Both processes, the backoff operation and assigning values to AIFSs, are deterministic and they are not adaptive. The CSMA/CA operates by doubling the size of the backoff stage every time a packet experiences a collision in the channel: it employs the conventional Binary Exponential Backoff (BEB) scheme to achieve that. This scheme is based on deterministic approach, it uses static parameters that do not take into account the status of the medium. On the other hand, AIFS parameter of each AC is also assigned a fixed value. This value combined with the size of the contention window, may lead to an unexpected result: a higher priority AC is pre-empted by a

lower priority AC ta use the medium, as we prove later in this chapter. In addition to this problem, AIFS values are not adaptive, they do not depend on any factor affecting the medium, which impact negatively the overall performance of EDCA.

In this chapter we propose a new adaptive backoff algorithm for the EDCA operation that takes into account the current status of the communication medium. More precisely, it evaluates the congestion level in the medium and uses this information to estimate the size of the backoff stage in the next transmission attempt. We also propose a new approach to assign new values to AIFS parameters in order to ensure that high priority ACs have always the preference in utilizing the channel resources before the low priority AC. The main contributions in this chapter are:

- We propose two new Adaptive Backoff Algorithms (ABA1 and ABA2) that, instead of doubling the backoff stage, increase it while considering the status of the medium.
- We propose two new AIFS algorithms, the first one is deterministic however it assures a strict priority provisions among the ACs. The second one is adaptive that enables each AC to calculate its own AIFS value based on the congestion level in the medium.
- Analytical models are presented, and the results are evaluated using Matlab and Network Simulator 2 (NS2).

The remaining of this chapter is divided into two main sections: Adaptive backoff algorithms and Adaptive AIFS algorithms. In both sections, we present a model description, we explain in details the proposed algorithms and we present the analytical model. Then we show our simulation results and analysis, and finally we conclude this chapter.

4.2 Related Work

Performance analysis of the EDCA mechanism in the IEEE 802.11p based on discrete Markov chain model has been explored in the research community [22, 124, 125, 127]. Most of these studies are based on the well known Bianchi Model [10] for IEEE 802.11 protocol.

[22] has proposed a Markov-based model to study the performance of EDCA protocol. This model has considered the specific conditions of the Control Channel (CCH) in a vehicular network. This model took into account all the important factors defined in the standard, such as the internal collision probability and the non-saturation condition. However, this model is still based on a deterministic approach in determining the size of the backoff phase.

In [128], the authors have evaluated the performance of the EDCA mechanism in the IEEE 802.11p protocol. They have presented 2 Markov chain models: a two dimensional model to explain the backoff procedure of an AC, and one dimensional model to estimate the internal collision probabilities among the ACs. As a result of these models, the authors have calculated the relation between the transmission probability and the collision probability of a vehicle for every AC. This study. This model adopted the standard parameters and conditions without any modifications.

An analytical model for the IEEE 802.11p behaviour in the control channel has been proposed in [129].This model has considered the conditions related to the safety applications in a vehicular network and it has taken into account some physical conditions such modulation and coding robustness. To evaluate its performance, two scenarios have been created by varying the channel load and the distance between the communicating vehicles. This model did not include the non-saturation condition which is an important factor in the vehicular communications, and the study did not show the performance of each AC.

4.3 Adaptive Backoff Algorithms

4.3.1 Model Description

In this section we explain our adaptive backoff mechanism for CSMA/CA in the IEEE 802.11p protocol. As it is defined in the standard, the backoff stage in the CSMA/CA mechanism changes its size every time a packet has failed during the transmission. The contention window size doubles and a random number is chosen to specify the number of TS which presents the length of the backoff phase. This operation is very simple, it takes into account only one parameter: number of packet transmission failure. It does not consider any other variables that may greatly affect the communication such as the variables that define the current medium status: is it congested or not?; is the number of successful transmission increasing, is it stable or is it decreasing?.

We propose a backoff model that takes into account an important factor of the system: The current collision rate in the medium, more precisely the probability of packet collision in the medium. The proposed model is an adaptive model that reacts based on the situation of communication channel. Opposite to the conventional backoff operation where the window size always increases following the same pattern independently of what happening in the medium, our adaptive model adjusts the length of the backoff period according to the collision rate in the medium.

In our proposed model, the initial backoff period W_0 is set to CW_{min}. Once a packet is dropped due to a collision in the medium, the next (and possible subsequent) backoff stage size is calculated as the following:

$$W_j = \Psi_i^j \times W_{max} \iff W_j = \Psi_i^j \times (2^{BE_{max}} - 1) \tag{4.1}$$

where W_{max} is the maximum window size the backoff can reach according to the IEEE 802.11p standard, and Ψ_i^j is factor calculated as a function of the packet collision probability in the medium for the class AC i at j^{th} phase, and BE_{max} is the maximum value of the backoff exponent. Ψ_i^j is a dynamic multiplicative factor which assures the adaptability of the backoff phase according to the channel status at the current time.

4.3.2 Probability of Collision

The probability of collision is defined as the probability of having at least two packets transmitted, by two different nodes or two different ACs, at the same period of time and experience a collision in the medium. It depends on three variables:

- The total number of packets transmitted in a period of time.
- The number of packets experiencing a collision in that period of time.
- The number of packets successfully received at the destination in the same period of time.

The probability of collision varies depending on the AC. Given that different ACs have different rate of transmission and different schedules, their packets transmission successful rates are different.

We assume $P_{c,i}^{j}$ is the probability of collision of AC i at the j^{th} attempt after j transmission failure. We estimate the value of $P_{c,i}^{j}$ as the following:

$$P_{c,i}^{j} = \frac{n_{c,i}^{j}}{n_{c,i}^{j} + n_{s,i}^{j}} = \frac{n_{c,i}^{j}}{n_{t,i}^{j}} \tag{4.2}$$

where $n_{c,i}^{j}$, $n_{s,i}^{j}$ and $n_{t,i}^{j}$ are the number of collisions experienced, the number of successful transmissions, and the total number of packet transmitted at a fixed period of time respectively. As it can be concluded from the Eq. 4.2, the value of $P_{c,i}^{j}$ varies in the range $[0..1]$.

4.3.3 Linear Adaptive Backoff Algorithm

In the first adaptive backoff algorithm (ABA1), we assume that the contention window size is directly proportional to the probability of collision in the medium. The value of Ψ_{i}^{j} and W_j of the the AC i at the j^{th} attempt are given as:

$$\Psi_{i}^{j} = P_{c,i}^{j} \iff W_j = P_{c,i}^{j} \times (2^{BE_{max}} - 1) \tag{4.3}$$

In ABA1, if the probability of collision increases(decreases), the backoff window size of the next phase increases (decreases) accordingly, which allow the AC in the node to wait longer before transmitting its packet in case of a high contention medium, or encourages the AC to send more packets (if available) in case of free medium.

4.3.4 Exponential Adaptive Backoff Algorithm

In the second adaptive backoff algorithm (ABA2), we assume that the relation between the contention window size and the collision probability is exponential. The corresponding values of Ψ_i^j and W_j are calculated as the following:

$$\Psi_i^j = 2^{P_{c,i}^j} \iff W_j = 2^{P_{c,i}^j} \times (2^{BE_{max}} - 1) \tag{4.4}$$

The general behaviour of ABA2 is similar to the one of ABA1, however the main difference is that the size of the backoff phase increments slower in ABA2 than in ABA1 in case of collision in the medium. Remember that $¶_i^j$ is in the range of $[0,1]$, which means that $2^{¶_i^j}$ increases with lower slope compared to $¶_i^j$.

4.3.5 Algorithms of ABA1 And ABA2

The main goal of our proposed model is reduce the flux of packets to the medium at the time when the medium is suffering from high congestion situation. At the end of every backoff stage, each vehicle measures locally the number of successful packets it transmits and the number of packets that encounter collisions, then it calculates its probability of collision. Once calculated, the next backoff stage adjusts its period length accordingly. If the collision probability is high, the backoff window size increases, leading the packet to a wait longer internally, and that relieves the pressure in the medium. In the opposite case, if the collision rate is low, there is no need to waste time in the backoff stage, it is better to send the packet as soon as possible to guaranty its deliverance. The flowchart in Figure 4.3 shows the complete ABA algorithm. The Total average delay estimation algorithm is presented in Algorithm. 4.1. We note that we assume that the collision probability is

Algorithm 1 Total Average Delay Estimation in ABA

// Initialization phase

read (N); // Number of vehicles in the network
read (CW_j); // Contention window size of AC_j
read $(TxOP_j)$; // Transmission opportunity of AC_j
read $(AIFS_j)$; // $AIFS_j$ of AC_j

// Calculation Of The Collision Probability

calculate $(n^j_{t,i})$; // Total number of packets transmitted
calculate $(n^j_{c,i})$; // Total number of packets collided in the medium
calculate $(n^j_{s,i})$; // Total number of packets successfully transmitted
calculate $(P^j_{c,i})$; // The collision probability
check medium status;

// Backoff window calculation

calculate $(\Psi^j_i \times W_{max})$; // Window size
if Channel is busy **then**
  Return to step 5
else
  $CW_j \longleftarrow CW_j - 1$
decrease window size by one
  if $CW_j \neq 0$ **then**
    Return to step 10
  else
    Transmit the packet
    if Transmission is successful **then**
      Return to step 1
    else
      if $i \longleftarrow m + f$ **then**
        Transmission is a failure
      else
        Return to step 5
End of Algorithm

the same at every backoff phase, therefore we can drop the j parameter from $P^j_{c,i}$.

4.3.6 Analytical Model

Figure 4.1 illustrates the discrete Markov chain analytical model of our ABA scheme for one AC. Once a packet arrives to the AC queue at the Medium Access Control (MAC) sub-layer, it selects one of the state at the first backoff period with a probability $\frac{(1-p_i)}{\Psi^0_i \times W_{max}}$. Then the packet passes through the backoff stage by moving one state at the time when the channel is detected idle for one TS. Once the backoff counter reaches zero, the packet is transmitted immediately. In the medium, a collision may occur to the packet with probability P_c, so the packet returns to one of the states

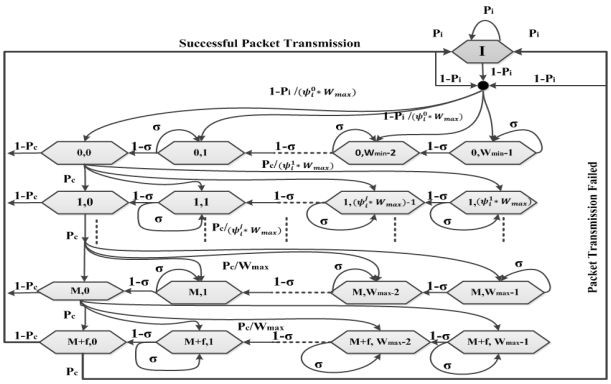

Figure 4.1: Markov Chain representation of ABA scheme

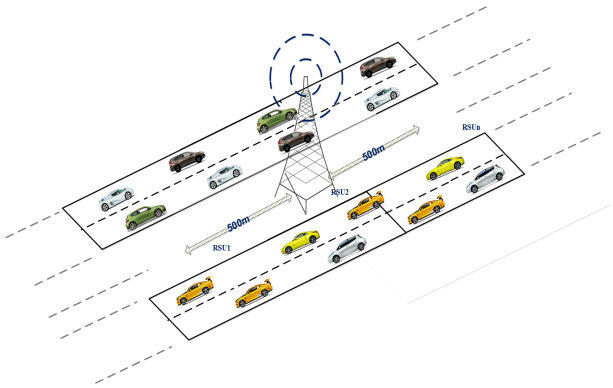

Figure 4.2: Simulation Scenario

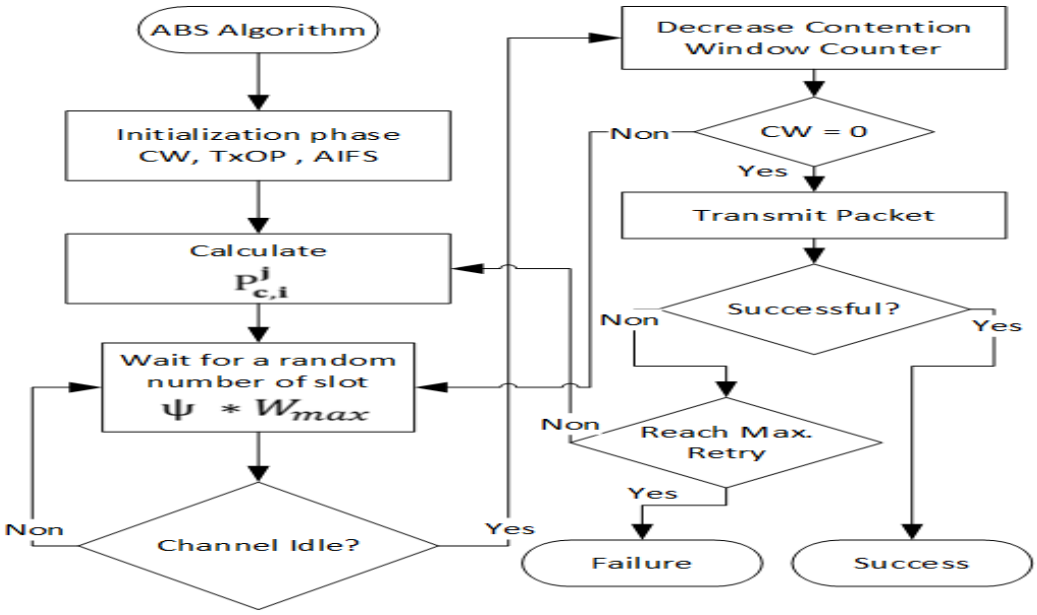

Figure 4.3: Flow Chart of ABA algorithm

of the next backoff stage with the probability $\frac{(1-p_i)}{\Psi_i^1 \times W_{max}}$. After M failures, the size of the backoff periods remains W_{max} till the number of retransmissions reaches its maximum value $M+f$. The model goes back to its idle stage in two possible cases: successful packet transmission and $M+f$ failed attempts.

The remaining of the model is similar to what presented in the previous chapter. The transition

probabilities is presented in Eq. 4.5.

$$\begin{cases} P(I|I) = p_i & \\ P(0,k|I) = \frac{(1-p_i)}{\Psi_i^0 \times W_{max}}, & 0 \leq k \leq W_0 - 1. \\ P(i,k|i,k+1) = 1-\sigma, & 0 \leq k \leq W_i - 1, \\ & 0 \leq i \leq M+f. \\ P(i,k|i,k) = \sigma, & 0 \leq k \leq W_i - 1, \\ & 0 \leq i \leq M+f. \\ P(i+1,k|i,0) = \frac{P_c}{\Psi_i^j \times W_{max}}, & 0 \leq k \leq W_i - 1, \\ & 0 \leq i \leq M+f-1. \\ P(0,k|i,0) = \frac{(1-P_c)\times(1-p_i)}{\Psi_i^0 \times W_{max}}, & 0 \leq k \leq W_i - 1, \\ & 0 \leq i \leq M+f-1. \\ P(I|M+f,0) = p_i. & \end{cases} \tag{4.5}$$

The stationary probabilities and the total transmission probability are calculated the same way as in Chapter 3. The only variable that needs to be presented is the stationary probability at state (0,0) ($b_{0,0}$).

In ABA1, $b_{0,0}$ is given as:

$$\begin{aligned} b_{0,0} = 2 \times \Bigg[& (\frac{1}{1-\sigma}) \times (\frac{1-P_c^{M+f+1}}{1-P_c}) + (W_0+1) \\ & + W_0 \times P_c \times \left(\frac{1-P_c^{M+1}}{1-P_c}\right) \\ & + W_{max} \times \left(\frac{P_c^{M+1} - P_c^{M+f+1}}{1-P_c}\right) + 2 \times \frac{p_i}{(1-p_i)} \Bigg]^{-1} \end{aligned} \tag{4.6}$$

In ABA2, $b_{0,0}$ is given as:

$$b_{0,0} = 2 \times \left[\left(\frac{1}{1-\sigma}\right) \times \left(\frac{1-P_c^{M+f+1}}{1-P_c}\right) + (W_0+1) \right.$$
$$+ ((2^{P_c} \times W_0) - W_0 + 1) \times \left(\frac{1-P_c^{M+1}}{1-P_c}\right) \tag{4.7}$$
$$\left. + W_{max} \times \left(\frac{P_c^{M+1} - P_c^{M+f+1}}{1-P_c}\right) + 2 \times \frac{p_i}{(1-p_i)} \right]^{-1}$$

4.4 Adaptive AIFS Algorithms

4.4.1 Model Description

As explained before, the parameters that affect the packet transmission (especially in term of delay) in the MAC layer are the Contention Window (CW), AIFS and the Transmission Opportunity (TxOP). In the previous section, we proposed two algorithms that adaptively calculate the size of the contention window depending on the competition status in the medium. In this section we propose a new adaptive algorithm that optimizes the value of the second parameter, the AIFS, in order to maintain the priority sequence among the ACs.

Each AC is assigned a specific value of AIFS (Table3.1). Upon receiving a packet from the upper layers, the AC must sense the medium idle for AIFS period of time before calculating the CW size and enters the backoff phase. To ensure the priority arrangement among the ACs, AC0 is assigned a smaller AIFS value than the AC1, which has smaller AIFS value than AC2, which has smaller AIFS value than AC3. However this does not really guarantee that AC0 will have access to the medium before AC1 in some situations, if both have packets to transmit at the same time. This is because the backoff size is picked randomly, although the values of AIFS0 and AIFS1 are fixed and constant.

Assume at $t = 0$ two applications associated to AC[i] and AC[i+1] have packets to send simultaneously. Assume AC[i] has a higher level of priority than AC[i+1]. After waiting for AIFS[i] and AIFS[i+1] period of time, assume the contention window size randomly picked by AC[i] and

AC[i+1] are CW[i] and CW[i+1], such as CW[i] has a greater value than CW[i+1]. This scenario results in AC[i+1] transmitting its packet before AC[i].

For example, in the worst case scenario, AC0 may randomly select $CW0_{max} = 7 \times T_{Timeslots}$ while AC1 chooses randomly $CW1_{min} = 3 \times T_{Timeslots}$ (Table 3.1). The total Wait Time (WT) before sending a message is given as:

$$WT[i] = AIFS[i] + CW[i] = T_{SIFS} + AIFSN[i] \times T_{Timeslots} + CW[i] \tag{4.8}$$

So in our case WT of AC0 and AC1 are:

$$WT[0] = T_{SIFS} + 2 \times T_{Timeslots} + 7 \times T_{Timeslots} = T_{SIFS} + 9 \times T_{Timeslots} \tag{4.9}$$

$$WT[1] = T_{SIFS} + 3 \times T_{Timeslots} + 3 \times T_{Timeslots} = T_{SIFS} + 6 \times T_{Timeslots} \tag{4.10}$$

As we can see in Eq. 4.9 and Eq. 4.10,

- AC1 will wait less time than AC0.
- AC1 will send its packet before AC0.
- AC0 will find the medium busy because of AC1 packet transmission, and it is forced to repeat again the same backoff process

As a result of that, AC0 loses its priority against AC1 if the standard values are used. A new approach should be taken in order to establish firm priority levels among the ACs.

In what follows, we propose two algorithms:

- Strict Priority Algorithm.
- Adaptive AIFS Algorithm

Table 4.2: SPA EDCA parameters

AC	$CW_{min}[i]$	$CW_{max}[i]$	$AIFSN\prime[i]$
AC0	3	7	2
AC1	3	15	7
AC2	7	1023	16
AC3	15	1023	23

4.4.2 Strict Priority Algorithm

The Strict Priority Algorithm (SPA) provides strict priorities to the ACs in the IEEE 802.11p protocol. SPA ensures that AC0 has the absolute priority over AC1 whatever the random value of CW0 and CW1 are chosen. Figure 4.4 shows the total wait time of different ACs operating under the IEEE 802.11p protocol. Figure 4.5 shows the total wait time of different ACs implemented in our proposed algorithm SPA.

To ensure strict priority arrangement among ACs, we propose that the relationship between the different AIFS parameters is as the following:

$$\begin{aligned} &\Big(AIFS[i]+CW_{max}[i]) < (AIFS[i+1]+CW_{min}[i+1]\Big) \\ \Longleftrightarrow\ &AIFS[i+1] > \Big(AIFS[i]+CW_{max}[i]\Big) - CW_{min}[i+1]. \end{aligned} \tag{4.11}$$

The value of AIFS[0] remains the same as the one in IEEE 802.11p. Since there are no safety messages transmitted on the least priority AC (AC[3]), and since the inequality presented in Equation 4.11 leads to a very big value of AIFS[3] (greater than 1023), we assume that the new value of AIFS[3] is the sum of the previous AIFS and CW_{min} values.

The new proposed AIFS values are define in the following equation and in Table 4.2

$$\begin{cases} AIFS\prime[0] = 2 \\ AIFS\prime[1] > AIFS[0]+CW_{max}[0]-CW_{min}[1] \\ AIFS\prime[2] > AIFS\prime[1]+CW_{max}[1]-CW_{min}[2] \\ AIFS\prime[3] = AIFS\prime[2]+CW_{min}[2] \end{cases} \tag{4.12}$$

Figure 4.4 and Figure 4.5 illustrate the difference between the default AIFS values for EDCA in IEEE 802.11p and in SPA. They show clearly, that AIFS[i] has an absolute priority over AIFS[i+1]

in SPA, because in this case AIFS[i+1] does not start the backoff phase before AIFS[i] sends his packets. The detailed algorithm of SPA is presented in Algorithm 4.3.

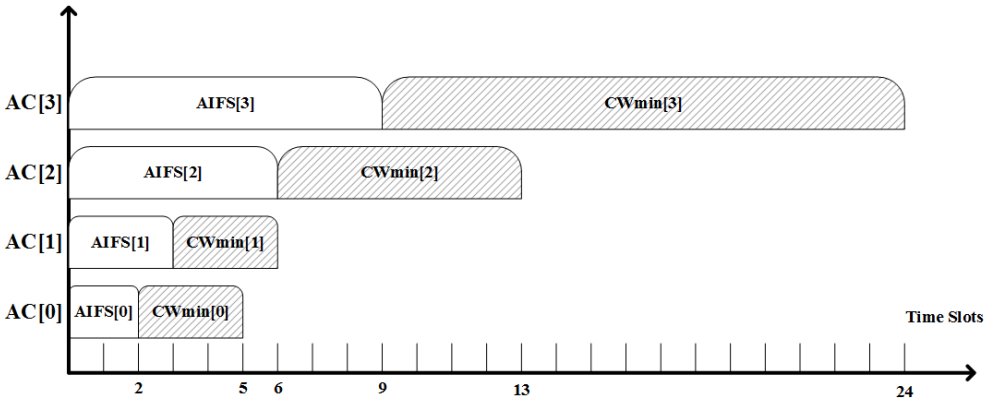

Figure 4.4: Default AIFS values for EDCA in IEEE 802.11p

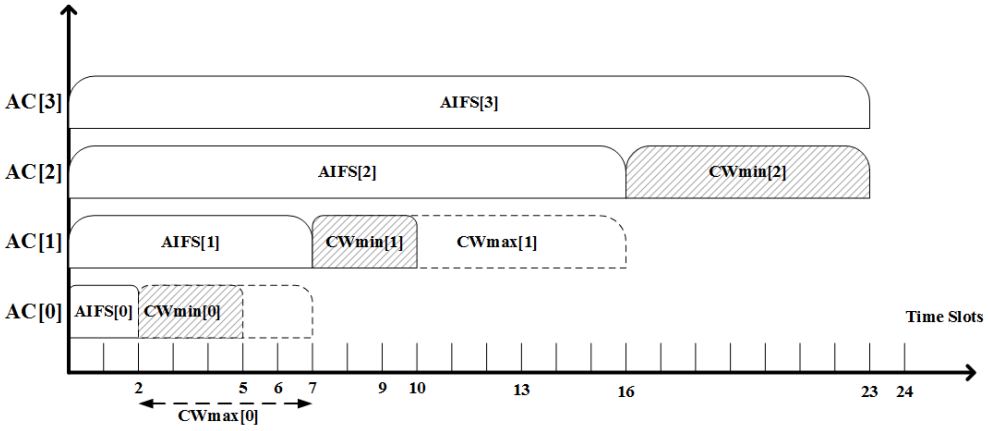

Figure 4.5: AIFS value proposed for EDCA in SPA

4.4.3 Adaptive AIFS Algorithm

In SPA, the value of the AIFS were fixed in a way to provide a strict priority for different ACs. In the current proposed algorithm, the Adaptive AIFS Algorithm (AAA), the values of the AIFS varies, to a certain limit, depending on the state of the medium at the time of collision. With AAA, the AIFS[i+1] value of a lower priority AC[i+1] increases in case a packet of a higher priority AC[i] encounters a collision in the medium. AIFS[i+1] increases to increase the probability of successful transmission of an AC[i] packet, however AAA does not guarantee strict priority mechanism among ACs.

Algorithm 2. SPA Algorithm

// Initialization phase

1 read (N);
// Nb. of veh. in the net.
2 read (CW_j);
// Cont. wind. size of AC_j
3 read ($TxOP_j$);
// Trans. Opp. of AC_j
4 read ($AIFS_j$); // $AIFS_j$ of AC_j

// Setting up AIFS[i] values

5 set $AIFS[0] \longleftarrow 2$; // Value of AIFS[0]
6 set $AIFS[1] \longleftarrow 7$; // Value of AIFS[1]
7 set $AIFS[2] \longleftarrow 16$; // Value of AIFS[2]
8 set $AIFS[3] \longleftarrow 23$; // Value of AIFS[3]
9 check medium status;

// Backoff window calculation

10 calculate window size
if channel is busy **then**
Return to step 5
else
11 $CW_j \longleftarrow CW_j - 1$
decrease window size by one
if $CW_j \neq 0$ **then**
12 Return to step 10
else
13 Transmit the packet
if Transmission is successful **then**
Return to step 1
else
if $i \longleftarrow m + f$ **then**
Transmission is a failure
else
Return to step 5
End of Algorithm

Algorithm 3. AAA Algorithm

// Initialization phase

1 read (N); // N. of veh. in the net.
2 read (CW_j); // Cont. wind. size of AC_j
3 read ($TxOP_j$); // Trans. Opp. of AC_j
4 read ($AIFS_j$); // $AIFS_j$ of AC_j

// Calculation Of The Collision Probability

5 calculate ($n^j_{t,i}$); // Tot. nb. of pckts. trans.
6 calculate ($n^j_{c,i}$); // Tot. nb. of col. pckts.
7 calculate ($n^j_{s,i}$); // Tot. nb. of suc. pckts.
8 calculate ($P^j_{c,i}$); // The col. prob.

// Calculation Of IF and PF Factors

10 $IF_j[i] \longleftarrow AIFS_j[i-1] + CW_{min}[i-1] - CW_{min}[i]$;
// IF parameter
11 $PF_j[i] \longleftarrow P^j_{c,i} \times IF_j[i]$;
// PF parameter

// Calculation Of AIFS

9 set $AIFS[0] \longleftarrow 2$; // Value of AIFS[0]
if $P^j_{c,i} < 0.5$ **then**
for k = 1,2,3 **do**
10 set $AIFS[k] \longleftarrow AIFS[k-1] + \lfloor PF[k-1] \rceil$
endfor
else // if $P^j_{c,i} > 0.5$
11 set $AIFS[1] \longleftarrow 7$; // Value of AIFS[1]
12 set $AIFS[2] \longleftarrow 16$; // Value of AIFS[2]
13 set $AIFS[3] \longleftarrow 23$; // Value of AIFS[3]
endif
14 Check medium status;

// Backoff window calculation

if channel is busy **then**
Return to step 5
else
15 $CW_j \longleftarrow CW_j - 1$
decrease window size by one
if $CW_j \neq 0$ **then**
16 Return to step 10
else
17 Transmit the packet
if Transmission is successful **then**
Return to step 1
else
if $i \longleftarrow m + f$ **then**
Transmission is a failure
else
Return to step 5
End of Algorithm

To express AAA in terms of equation, we define two variables,

- The Increment Factor (IF_i^j) of AC i at j^{th} backoff phase.
- The Priority Factor (PF_i^j) of AC i at j^{th} backoff phase.

$$IF_i^j = AIFS[i-1] + CW_{max}[i-1] - CW_{min}[i]. \tag{4.13}$$

$$PF_i^j = P_{c,i}^j \times IF_i^j. \tag{4.14}$$

Since the range $[CW_{min}, CW_{max}]$ for all the backoff stages is the same, we can drop the j parameter. The AAA algorithm is defined based on the following points:

- AIFS[0] keeps the same value defined by the standard.
- AIFS[1] and AIFS[2] are recalculated according to the congestion level in the channel. They are incremented by a certain percentage to preserve a higher chance of transmission for higher priority ACs.
- AIFS[3] is defined similarly to SPA algorithm.

The new values of AIFS as defined in the AAA algorithm are as follows

$$\begin{cases} AIFS\prime[0] = 2 \\ AIFS\prime[1] = AIFS[1] + \lfloor PF_1 \rceil \\ AIFS\prime[2] = AIFS[2] + \lfloor PF_2\prime \rceil \\ AIFS\prime[3] = AIFS\prime[2] + CW_{min}[2] \end{cases} \tag{4.15}$$

where $PF_i\prime$ is

$$PF_i\prime = P_{c,i} \times IF_i\prime = P_{c,i} \times \Big(AIFS[i-1]\prime + CW_{max}[i-1] - CW_{min}[i] \Big) \tag{4.16}$$

Table 4.5: AAA EDCA parameters

AC	$\mathbf{CW_{min}[i]}$	$\mathbf{CW_{max}[i]}$	**AIFSN** $P^j_{c,i} = 0.2$	**AIFSN** $P^j_{c,i} = 0.5$
AC0	3	7	2	2
AC1	3	15	4	6
AC2	7	1023	8	13
AC3	15	1023	23	23

Note that $\lfloor \frac{a}{b} \rceil$ is equal to the nearest integer of $\frac{a}{b}$. We can easily prove that when probability of collision increase beyond 50%, AAA becomes SPA. In fact,

if $P_{c,i} > 50\% \Longleftrightarrow AFSI[i] + CW_{min}[i] < AFSI[i-1] + CW_{min}[i-1]$

The new AIFS value as define in AAA assuming that $P^j_{c,i} = 0.2$ and $P^j_{c,i} = 0.5$ are shown in Table 4.5. The detailed algorithm of AAA is presented in Algorithm 4.4.

We note that the analytical model of the adaptive AIFS algorithms is similar to the one of the adaptive backoff algorithm, however in this case we do not alter the backoff process, we only perform the required changes at the AIFS phase.

4.5 Simulation Results and Analysis

4.5.1 Simulation Scenario

We use MATLAB to compute the system of equations derived from the discrete event Markov chain model. To validate our results, we carry out a simulations using ns-2.35. We create a star-topology scenario. We generate two highways in two opposite directions centred by one RSU as shown in Figure 4.2. Each highway consists of two lanes. The RSU covers 500m in each direction. we assume that no handover between RSUs is required, the established vehicle-to-RSU communication is terminated before the vehicles looses the RSU signal. The vehicles are moving with random average speed that varies between 50 to 80 Km/h. The parameter values used in the simulation are presented in Table 4.6.

Table 4.6: Analytical Model Parameters

Parameter	Value	Parameter	Value
CW_{min0}	3	CW_{min2}	7
CW_{min1}	3	CW_{min3}	15
CW_{max0}	7	CW_{max2}	1023
CW_{max1}	15	CW_{max3}	1023
Time Slot	13 μs	SIFS period	32 μs
Propagation delay	1 μs	LL queue size	50 Packets
Data rate	6 Mbps	Packet size	1024 bits

4.5.2 Results and Analysis of ABA1 And ABA2

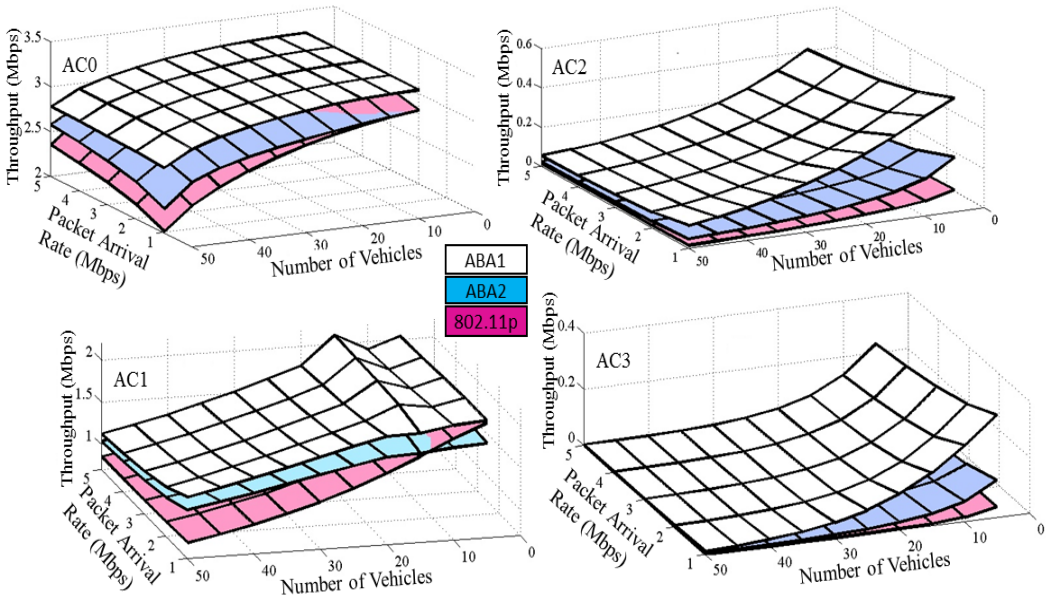

Figure 4.6: Average network throughput as function of the number of vehicles and the packets arrival rate in ABA1 and ABA2

Figure 4.6 shows the average network throughput of all the ACs as a function of two variables: The vehicular network size which varies from 5 to 50 vehicles and the average packet arrival rate which varies in the range 1 to 5. Figure 4.6 shows that the average throughput decreases when the number of vehicles involved in the communication increases and when the packet arrival rate from the application layer increments. In both cases, the throughput drops due to the rising number of packets transmitted in the medium leading to intense competition and higher number of collisions among the packets. In all ACs, we notice that the performance of the ABA1 and ABA2 surpass

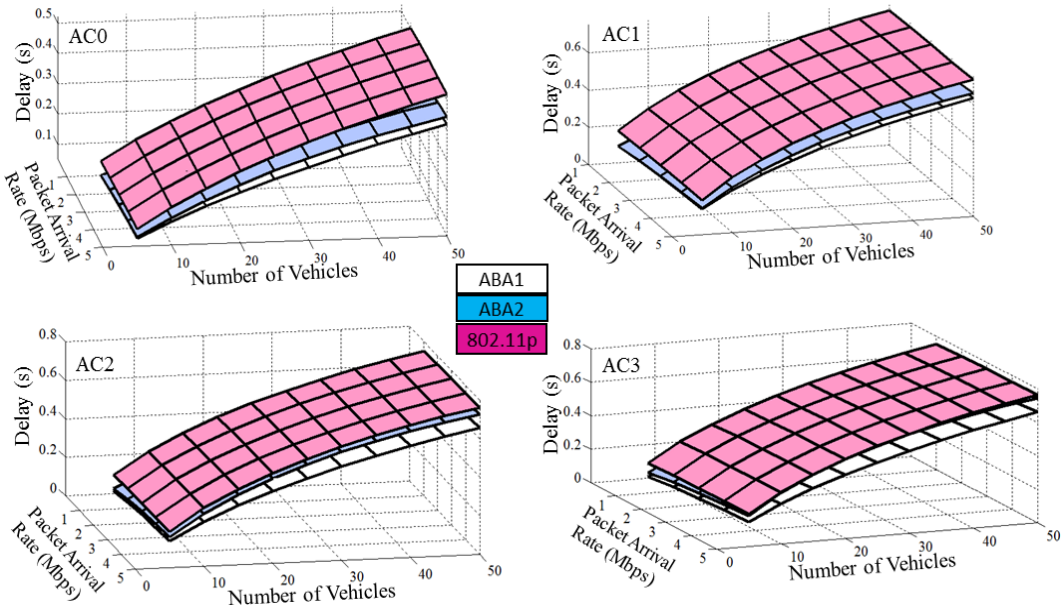

Figure 4.7: Average end-to-end delay as function of the number of vehicles and the packets arrival rate in ABA1 and ABA2

the conventional IEEE 802.11p protocol. This proves that an adaptive backoff stage that takes into account the current status of the medium reacts better and provides more efficient results. Moreover we show that the ABA1 outperforms the other algorithms in four ACs, and it is more effective in AC1 and AC2. This is because AC1 and AC2 are prone more than AC0 and AC1, to higher collision rate in the medium because they reside last in the priority scale compared to AC0 and AC1. Therefore, the adaptive scheme is more advantageous for them than the other ACs.

Figure 4.7 shows the average end-to-end delay of all the ACs as a function of the number of vehicles in the network and the packet arrival rate. Figure 4.7 shows that across all the ACs, the delay increases with increasing number of vehicles and with increasing number of packet arrivals from the higher layer. This is due to the fact that additional vehicles involved in the network and additional packets transmitted result in excessive contention in the channel and results in big amount of packet loss, these packets have to be re-transmitted which means they have to return back to the beginning of the cycle: internal competition phase, backoff phase, and re-transmission phase. Figure 4.7 shows also that the adaptive approach behaves better by providing lesser delays than the IEEE 802.11p protocol. It shows also that ABA1 performance exceeds ABA2 performance. In

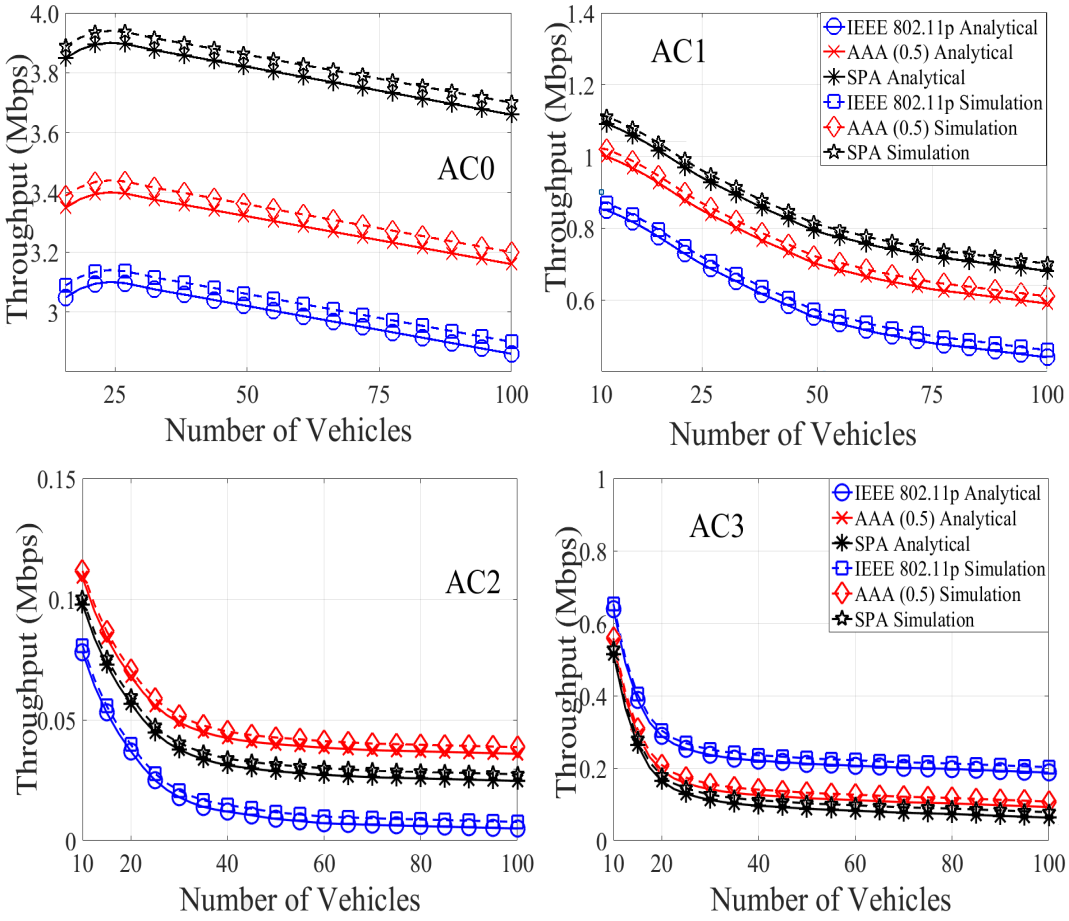

Figure 4.8: Average throughput against the number of vehicles in SPA and AAA

fact, since ABA1 adopts a linear function of the probability of collision and ABA2 adopts an exponential function, ABA1 provides smaller window size values which results in shorter waiting time in the backoff stage and thus reduces the average end-to-end delay.

4.5.3 Results and Analysis of SPA and AAA

We present the throughput results against the number of vehicles and the average end-to-end delay against the packet arrival rate.

Figure 4.8 shows the simulation and analytical results of the average network throughput for all ACs. We notice that the throughput of AC0 tends to increase at the beginning and then starts to decrease as the number of vehicles in the network increases. When the number of vehicle is small, there is a high possibility that the majority of the transmitted packets reach their destination

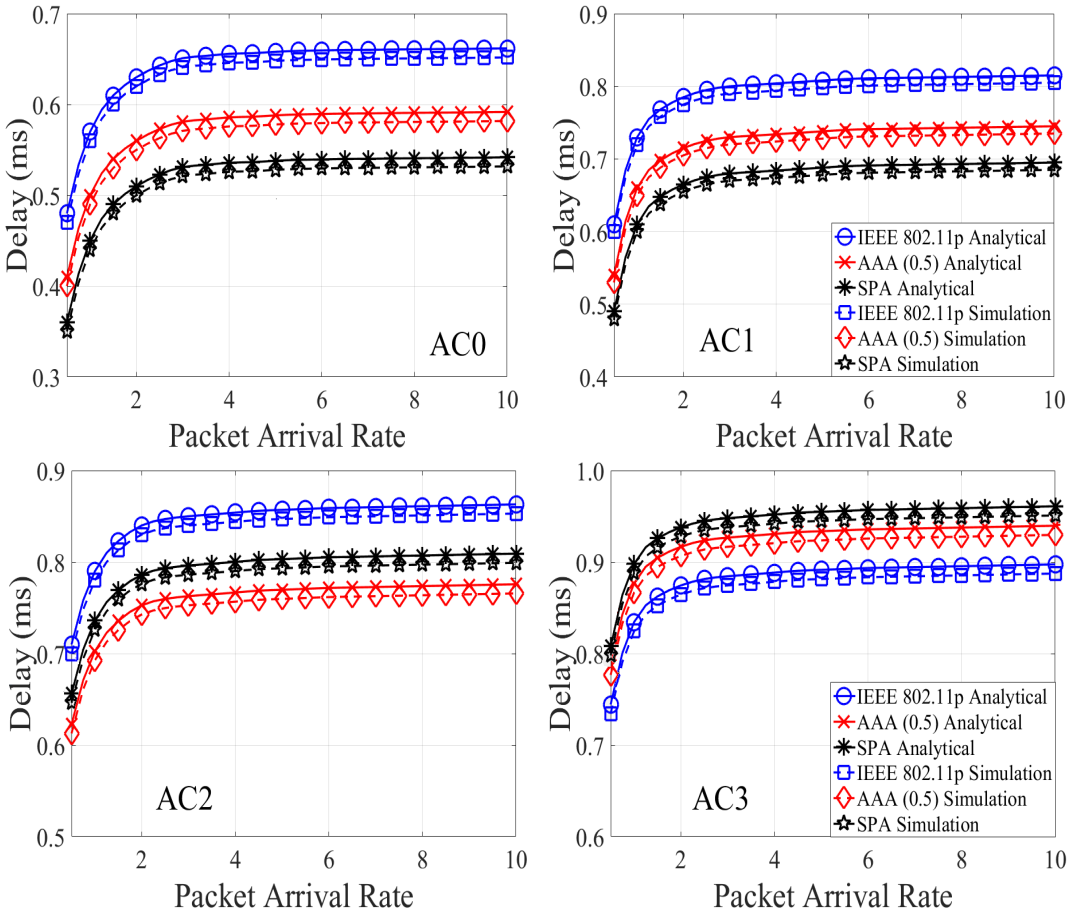

Figure 4.9: Average end-to-end delay against the package arrival rate in SPA and AAA

successfully, which increases the average throughput of the network. On the other hand, when more vehicles enter the network and participate in the communication, the number of packet exchanged increases leading to a higher probability of collisions among them, and hence the drop of the average throughput values. This figure shows also the effect of changing the values of the AIFS. Introducing SPA and AAA enhances highly the performance especially in hight-priority ACs. We notice that the SPA throughput of AC0 is the highest in comparison with AAA and IEEE 802.11p, and that is because SPA provides AC0 with the absolute highest priority level. Although the AIFSN value of AC1 provided by SPA is less than that provided by AAA, the SPA throughput still slightly outperforms the one of AAA because the AIFS value of AC2 in SPA is a bit higher than the one of AAA. That results in AC1 waiting in the backoff stage in SPA less time than in AAA. Figure 4.8 shows also that the throughput of AC2 in AAA outperforms the one in SPA and in the IEEE

802.11p standard. The AIFSN value of IEEE 802.11p standard is relatively small compared to SPA and AAA, however the difference of the combined variables (AIFS+CW) between AC3 and AC2 in IEEE 802.11p standard, SPA and AAA are 11, 15 and 18. Which means that the probability of AC3 pre-empting AC2 in accessing the medium is the highest in IEEE 802.11p and the lowest in AAA, and thus the throughput of AAA is the best.

The average end-to-end delay of the network (N=100) for different packet arrival rates across all ACs is illustrated in Figure4.9. We can see that the average end-to-end delay increases with the number of packets arriving from the application layer, however it tends to converge toward a fixed value after a certain threshold. The contention of the channel access tends to augment when greater amount of packets is engaging in the communication process. Intense contention among vehicles is equivalent to growing percentage of packet collisions and to rising number of packet dropped. This leads to more frequent packet retransmission which cost a lot in terms of delay. This figure shows clearly that enhancing the IEEE 802.11p protocol by changing the values of the AIFS leads to a better performance in terms of delay. SPA shows the lowest delay in AC0 and AC1 because it provides strict priority for these classes. However its performance falls behind AAA in AC2 and AC3 because AAA has lower AIFS+CW value than SPA in those classes. We notice finally that the IEEE 802.11p standard outperforms both protocols in AC4, because with SPA and AAA the class AC4 has lower chance to access the medium compared to AC4 in IEEE 802.11p.

4.6 Conclusion

In this chapter, we have provided an alternative solution to the backoff operation in the conventional CSMA/CA algorithm employed by the EDCA of IEEE 802.11p. Instead of being deterministic, we have proposed a new adaptive probabilistic approach for the backoff stage and for assigning new values to the AIFSs. This approach integrates the probability of collision experienced in the medium, into the backoff stage process and into the calculation of the AIFS parameters. We have proposed two algorithms for each scheme. All algorithms have proved better performance in terms

of delay and throughput than the algorithm adopted in the IEEE 802.11p.

In the next chapter we conduct a delay analysis study and we present a new adaptive scheme between the vehicles and the RSU. We analyse the effect of vehicle's speed on the MAC protocol in V2I environment. We develop a new adaptive service time scheme that optimizes the end-to-end delay value after considering the RSU's queue effect on the communication.

Chapter 5

Mobility Impact And Adaptive Time Control studies in Wireless Access for Vehicular Environment

5.1 Introduction

In Chapter 3 and Chapter, 4 we have focused on improving the performance of the IEEE 802.11p protocol. We have succeeded through incorporating a buffer at the entry of each Access Category (AC), and by adopting an adaptive-based approach in the backoff phase and in the Arbitration Interframe Space (AIFS) calculations. In this Chapter, we present studies at a higher level than the Medium Access Control (MAC) protocol. Our first study, the mobility impact study, is in the context of Electric Vehicle (EV)-Smart grid communications or Vehicle to Grid (V2G) communications. We present a comprehensive analysis of the impact of speed on the end-to-end delay and throughput in communications between a Plug-in Electric Vehicles (PEV) and smart grid servers in situations where authentication is performed. In V2G communications, authentication is applied when essential information, such as payment information, is exchanged. In the second study, we propose an Adaptive Service Time Control (ASTC) scheme in Vehicle to Infrastructure (V2I) network. ASTC aims to adaptively compensate the additional delay introduced in the Road Side Unit (RSU) queue, by changing the size of the buffer at the vehicle MAC layer.

In the mobility impact study, we present a realistic delay analysis that includes the delay due to security processing and data transmission with the presence of mobility. The security processing latency takes place in the vehicle during the certificate generation and the message signature. It also takes place in the RSU when it verifies the signature. At the end of the study, we establish recommendations based on our test scenarios and simulations results.

In the ASTC study, we recognize that the communication latency is a pivotal performance factor in

Vehicular Ad hoc Networks (VANET), especially for safety-related applications. In reality, delay sensitive services such as broadcasting collision prevention information or transmitting essential updating data about the current status of a highway, cannot tolerate any extra delay because it jeopardizes the safety of the drivers and pedestrians. Therefore, reducing the end-to-end delay is essential to achieve cooperative system that maximizes the safety on the roads. In the ASTC scheme, we take into account all the factors that contribute in the delay measurements: processing overhead, in-vehicle latency due to the backoff mechanism, the communication delay and the queuing delay at the RSU. The main contributions in this chapter are:

- Analysis of the effect of the speed on the end-to-end delay in V2G environment.
- Proposing a new Adaptive service time control scheme that helps to mitigate the effect of the RSU's queue, on the overall performance.

The remainder of this chapter is divided to two main parts: Mobility impact analysis and the ASTC scheme. In the first part 5.3, we describe our scenario in Section 5.3.1, then we present the total delay analysis in Section 5.4. In the second part 5.5, we start with a description of the scenario in Section 5.5.1, then we present our model in Section 5.6, in which we study the end-to-end delay and describe the ASTC algorithm. We show the simulation results and the analysis in Section 5.7. Section 5.8 concludes this chapter.

5.2 Related Work

There have been several studies that consider the effect of vehicles mobility on the performance of the communication protocol [130]. A study on the impact of the vehicles mobility on the performance of IEEE 802.11p protocol has been proposed in [131]. The authors have assumed that the communicating vehicles form clusters and they exchange the location and the speed information of each other. Based on the local data, each vehicle is able to calculate its speed as well as the speed of the one-hop neighbour vehicles. The authors have shown that the level of contention is

affected deeply by the average speed of the vehicles. They have proven that the behaviour of the IEEE 802.11p may be affected in Vehicle-to-Vehicle (V2V) communication, however they did not evaluate the impact on the V2I communications, and they have not considered the authentication and processing overhead that change mainly the average end-to-end delay of the network. Our work consider these factors and include them in the performance evaluation.

Many research papers studying the IEEE 802.11p protocol in V2V and V2I environment have been published in the literature [128] [11]. In [36], the authors have proposed a study to identify the differences between saturation and non-saturation schemes in terms of end-to-end delay. The authors have developed an analytical model to assess the end-to-end delay as a function of the transmission range and the packet arrival rate in a saturated and unsaturated mode. Although this study took into account several factors that affect the communication delay in the network, it did not consider the delay related to security overhead, and it did not show the delay due the internal collisions by the ACs. Our work considers these factors and it is based on a protocol that outperforms IEEE 802.11p protocol.

Several papers have tackled the security perspective of the communication in VANET [132], [133]. In [134], the author has introduced security processing overhead in a VANET environment. He has studied its impact on the performance in terms of average end-to-end delay, and analysed its effect on the braking distance of the vehicle. He has described that the time processing related to security is due to issuing the certificate and signing the data at the source, and verifying the received data at the destination. This study proved that the braking distance of a vehicle may decrease below the safety threshold due to this additional overhead.

The same author has extended his work in [135] by introducing the communication overhead in his model. In fact, the end-to-end communication delay has increased because of the extra load presented by the certificate and the signature. His results has shown that the delay imposed by the processing overhead is longer than the communication delay, and that the distance covered during the emergency braking has relatively increased. This work has targeted V2V communication

system and it relied on the conventional IEEE 802.11p protocol without any enhancement. In our work, we take into account the security-related overhead and our communication protocol is more efficient in terms of the end-to-end delay and the throughput.

5.3 Mobility Impact on Vehicle to Grid Communications

The availability of charging stations and the power required to charge multiple PEVs at the same time are major concerns for electrical utility operators and PEV owners. The smart grid continually adapt the cost of charging PEVs to the time of the day, the instantaneous load on the grid and to instantaneous availability of charging infrastructure. This can be done by allowing the smart grid to manage the load between PEVs and the power grid on a micro-level. This two-way management is achieved by enabling reliable, timely and secure communication between PEVs and electricity suppliers to manage, schedule and distribute the load and generation efficiently [136].

In general, communication systems are considered as the backbone of any smart grid system. In scenarios where a communication between PEVs and the smart grid (i.e. V2G) is required, multiple problems in communication arise due to the nature of the deployment environment. In VANETs, low communication latency and security become main challenges that face network designers and developers. These problems are magnified in dense scenarios where vehicles are travelling at high speed.

The IEEE 802.11p standard is the most popular standard for V2G communication scenarios. The IEEE 802.11p standard is an amendment to the IEEE 802.11 standard which is proposed for Vehicular Environments [8]. The standard is designed to enable communication at high speed and yet maintain high data rates. To cope with high mobility, the bandwidth of the IEEE 802.11p standard is reduced to the half of that of the IEEE 802.11a standard [108] . In addition, its MAC protocol uses similar techniques used in the IEEE 802.11e standard [109]. However, to handle the highly mobile environment, the IEEE 802.11p implements some modifications to the IEEE802.11e MAC to make it more suitable for mobility (e.g. the use of 4 ACs instead of 8).

In a highly dynamic environment, mobile PEVs may initiate the communication at a location covered by one RSU, but due to their speed, they may move to the coverage area of a second RSU before completing their session. Therefore, this may cause an extra delay due to the handover between the RSUs. One major factor that plays role in this delay, is the speed of the PEVs [137]. A PEV moving with high speed may require multiple handovers till it terminates its connection, which decrease the communication performance especially its latency. However, a stationary PEV that establishes, initiates and terminates its communication while residing in the coverage of one RSU, will not suffer additional delay due to handover.

In this section, we present a comprehensive analysis of the impact of speed on the end-to-end delay in communication between PEVs and the smart grid in situations where authentication is performed when essential information such as payment information is exchanged between PEVs and their charging infrastructure. In addition to that, we present realistic delay analysis that includes the delay due to security processing and data transmission with the presence of mobility. The security processing latency takes place in the vehicle during the certificate generation and the message signature, and in the RSU when it verifies the signature. Our simulation results show the impact of traffic density and speed on both the end-to-end delay and the throughput. We establish recommendations based on our test scenarios and simulation results.

5.3.1 Scenario Description

In our proposed scenario we assume a two lane road where vehicles can travel in opposite directions. The road is covered by multiple RSUs which transmit and receive information using the IEEE 802.11p protocol. We assume that RSUs can exist at distances of 500 m or less as shown in Figure 5.1. The transmission range of each RSU reaches maximum 500 m in each direction based on the standard. We assume that the vehicles passing by the RSUs are provided with communication capabilities, they are equipped with an On-Board Unit (OBU) that enables the communication with the RSUs, as well as with the other vehicles, by employing the IEEE 802.11p standard. The

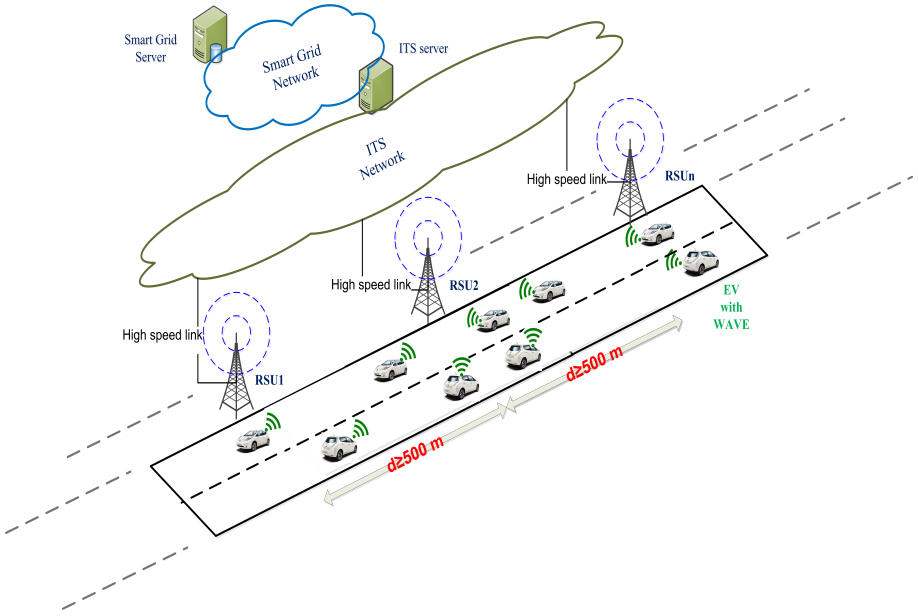

Figure 5.1: Proposed simulation scenario

communication between a vehicle and an RSU starts at the moment when the vehicle enters in the coverage area of that RSU and terminates at the second the vehicle leaves it. We do not consider the handover between the RSUs, for the sake of delay.

We assume that there are a number of vehicles are exchanging information with one RSU, approximately half of them are moving in one direction and the other half is travelling in the opposite direction with the same average speed. The vehicles initially are outside the coverage area of the RSU, they enter the coverage area where the actual communication takes place and finally they move out the communication area. We assume the RSU is connected, via a high speed link, with an Intelligent Transportation System (ITS) network, which in its turn is connected with a smart grid network via a Wide Area Network (WAN).

In our scenario, all the vehicles are powered by batteries, and they require to exchange their battery level information, availability of charging stations, and any other requirements from the smart grid. All of the information related to the charging station is available and updated in the smart grid network which can be only accessed by an ITS network. The RSU accepts all the requests from the vehicles and send them to the ITS server. The ITS server then passes the requests to the

smart grid server. After processing all the requests, the smart grid server replies to the ITS server which passes the information to the RSU which transmits them to the vehicles.
The round trip communication from the PEV to the smart grid server back to the vehicles undergoes several delay. We can summarize these delays as follows:

- The delay of the certificate generation and the digital signature of the message at the vehicle (D_{cer}).
- The medium access delay between the vehicles and the RSU (E[D]).
- The delay between the RSU and the ITS server ($D_{RSU-ITS}$).
- The communication delay between the ITS server and the smart grid server ($D_{ITS-sgs}$).

The major contributors in the latency are the medium access delay between the vehicles and the RSU and the security-related delays in the vehicle. We focus on the effect of the PEVs speed on the communication end-to-end delay.

5.4 Delay Analysis

To study the impact of the vehicles speed on the end-to-end latency in our proposed network, we need first to identify all the factors that contribute in the overall delay, and then to determine their numerical values.

5.4.1 Processing and Authentication Delay

In the WAVE protocol, The security services for applications and management messages are handled by the IEEE 1609.2 standard [138]. The WAVE standard adopts the usage of the Public-Key Infrastructure (PKI) techniques when sending secure messages. Each secure message should be encrypted and digitally signed. The IEEE 1609.2 selects the Elliptic Curve Digital Signature Algorithm (ECDSA) to support the digital signature in V2V and V2I communication systems. Its

main advantage over the the other algorithms such as the Digital Signature Algorithm (DSA) and RSA algorithm is its capability to ensure high lever of security with smaller size of public keys.
Encrypting a message is not enough, we need to specify the entity that issued the message. In other words, we need to guarantee that a specific message with a specific public key is coming form the anticipated vehicle. Thus a certificate is required. The main objective of the certificate is to prevent the situation where an unauthorized user, who uses a fake public key. The certified message is supposed to be digitally signed after being issued over to the medium access, although each certificate is by itself signed.
The average length of a certificate in bytes as given by [134] is:

$$L_{cer} = L_{pk}/8 + 1 + L_{sig}/4 \tag{5.1}$$

where, L_{pk} is the point size (in bits) of the elliptic curve G depending on the public key algorithm associated with the key, and L_{sig} is the size of the signature used to sign the certificate.
One final stage in the security process is the authentication. Each certified message should be signed digitally. This signature is performed by the ECDSA. In fact, each message must include the location and the time information in order to prevent some attacks such as replay attack.
After being determined and issued, the digital signature is added to the certified message (see Figure 5.2)which introduces the authentication delay. The size of the signature attached to the packet is given as [135]:

$$L_{sig} = L_{Smsg}/4 \tag{5.2}$$

L_{Smsg} is the elliptic curve used in ECDSA, and it is in bits.
The total delay of the certificate and its signature is given as: D_{cer}.

The digital signature issued in the vehicle need to be verified at the RSU. The time taken to verify the signature should be added to the processing overhead. We denote this delay as: D_{ver}.
The numerical values that we use are taken from [135]:

- Key size = 224 bits.

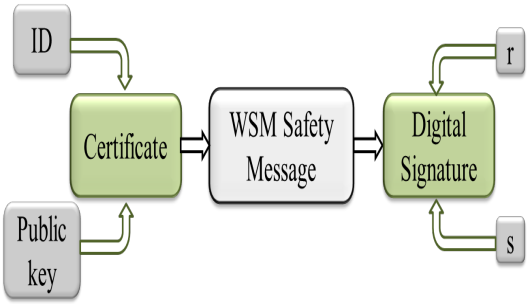

Figure 5.2: Message digitally signed appended with a certificate

- Signature generation delay = 2.5 ms.
- Signature verification delay = 4.97 ms.

5.4.2 Medium Access Delay

All PEVs that are located within the transmission range of the RSU are assumed active, i.e they all have requests to send to the RSU. These vehicles share the medium using the Carrier Sense Multiple Access with Collision Avoidance(CSMA/CA) technique. They employ Enhanced Distributed Channel Access (EDCA) to support applications with four different priorities. The priority of each application is mapped to an AC at the MAC layer. Each AC is defined by its own proper variables such as the Contention Window (CW) size, the AIFS, and the Transmission Opportunity (TXOP). During the communication process, the vehicles contend for the channel access, meanwhile the four ACs compete for a TXOP internally. Once a packet of a specific AC succeeds to pass the internal filtering process, it waits for random number of timeslots in the backoff stage. Every AIFS period of time, the vehicle checks the availability of the medium, if the medium is free, the backoff counters decreases by one unit, otherwise it waits for a new AIFS to check again. When the backoff counter reaches zero, the vehicle send the packet to the RSU. The packet then is either successfully received by the RSU or it encounters a collision, in this case the vehicle returns to the backoff process with a new random size.

Detailed description of this process is explained in [124] and [125]. The average end-to-end delay

between the Vehicles and the RSU is also calculated in [124] [125] by modelling the IEEE 802.11p protocol with 2-D discrete Markov chain:

$$E[D] = E[backoff] \times T_{suc} + (E[Retr] + E[backoff]) \times T_{col} \tag{5.3}$$

Where:

- E[backoff]: The average delay in the backoff stage.
- E[Retr]: The average number of retransmission, when the packet experiences one or multiple collisions.
- T_{suc}: The time duration of a successful transmission.
- T_{col}: The time duration of an unsuccessful transmission.

Ts and Tc are given as the following:

$$T_{suc} = T_{AIFS} + T_{Header} + T_{Load} + T_{SIFS} + \delta + T_{ACK} + \delta \tag{5.4}$$

$$T_{col} = T_{AIFS} + T_{Header} + T_{Load} + \delta \tag{5.5}$$

where

- T_{AIFS} and T_{SIFS} are the periods of AIFS and SIFS respectively.
- $(T_{Header} + T_{Load})$ and T_{ACK} are the transmission time of a packet and of an acknowledgement.
- δ is the propagation delay.

5.4.3 RSU to ITS Server Delay

An ITS server is a network component that plays the role of mediator between the users (RSU in this case) and the smart grid server. It serves as gateway between the RSU and the server. The RSU-ITS server connection is of type many-to-one. In fact, one ITS server serves multiple RSU connections at the same time. It collects the requests coming from various RSUs, aggregates them and send them to the smart grid server. These requests are actually the inquiries about the location, the availability and other exchanged information of the charging station issued by the vehicles.
In our proposed scenario, we are only concerned with the connection of one RSU, and we assume that the link is a high speed link (e.g. fiber optic). Therefore, the average RSU-ITS server delay is assumed to be in the range of microseconds.

$$D_{RSU-ITS} = L/R \tag{5.6}$$

Where L is the packet size in bits, and R is the data rate of the fibre in bits per seconds.

5.4.4 ITS Server to Smart Grid Server

The ITS server is connected with the smart grid server via a WAN, which is an IP-based backbone network. All the demands that the ITS server acquires, are forwarded to the smart grid server. Once received, the smart grid server processes the requests, and sends back the required charging station information, such as their locations, their availability and their costs.
For the sake of simplicity, we assume that the backbone network is the network used in [139], the Sprint's backbone. As per the study conducted in [139] each packet experiences a 20 μs if it is sent and received on the same linecard, and it experiences 40 μs if it is transmitted over the switch fabric.
We assume that it is more probable to have the packet transmitted and received on different linecard, therefore we consider the packet delay between the ITS server and the smart grid server is

$$D_{ITS-sgs} = 40\ \mu s \tag{5.7}$$

5.4.5 Total Delay

To summarize this section, we present here the total end-to-end delay of a packet sent from a vehicle to a smart grid server.

$$D_{tot} = D_{cer} + E[D] + D_{ver} + D_{RSU-ITS} + D_{ITS-sgs} \tag{5.8}$$

5.5 Adaptive Service Time Control

In this section, we present our ASTC model. We start with a scenario description, then we describe in details the model.

5.5.1 Scenario Description and Model Assumptions

In our scenario (shown in Figure 5.3), we assume a V2I communication network in the context of a safety-related application. The network consists of one RSU serving a number of vehicles travelling on the nearby road. It is a star topology centralized by the RSU which provides the vehicles with updated warning messages regarding the condition of the roads to prevent accidents. We use the Wave Short Message (WSM) provided by the IEEE 1609.4 protocol [7] because it is the one used when transmitting safety messages.

Each vehicle is equipped with an OBU that supports a Dedicated Short Range Communication (DSRC)-based communication system. The MAC protocol in the communication system is the enhanced IEEE 802.11p protocol we proposed in [124], in which we introduced a buffer at the beginning of each AC at the MAC layer. The additional buffer helps to improve the performance by increasing the average vehicle throughput and decreasing the average end-to-end delay. It was proven that incrementing the size of the buffer at the entry point of each AC, leads to further improvement in the performance, it boosts more the throughput and lessen more the delay. In the current ASTC model, we take advantage of this fact to minimize the end-to-end delay as we demonstrate later in this chapter.

In our adaptive scenario, we assume that the communication is secured. Therefore, before sending

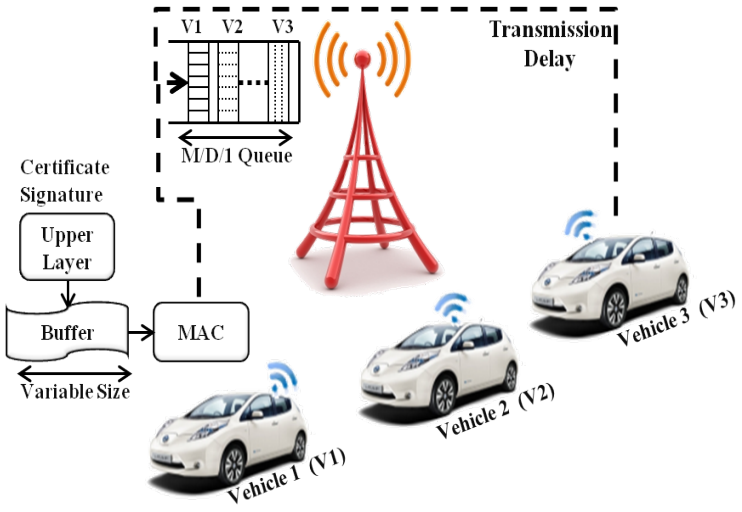

Figure 5.3: Proposed simulation scenario

a message, it needs to be signed using the ECDSA [140]. Furthermore each message should be authenticated, hence a signed certificate is produced and appended to the WSM message. This security-related process (issuing a certificate and signing the WSM message) adds a computational overhead that raises the end-to-end delay. Moreover, appending the message with additional load (the certificate and the signature) increases the communication delay because extra bits need to be transferred over the medium. At the RSU, each message needs to be verified before being processed which presents an additional processing delay.

In our proposed adaptive model, we assume that the RSU employs a queue at its entry point. The RSU uses this queue to store the messages upon receiving them from the vehicles. We assume that the message arrival rate follows Poisson process, and that the processing time of each message in the RSU is constant. Consequently, we consider the RSU having an M/D/1 queue. The following are other important assumptions considered in our model:

- We consider an unsaturated mode of traffic conditions, which means that the flow of packets from the upper layers to the MAC layer is not continuous. We consider the packet arrival rate from the application layer is set to 50% of the time.

- The packet losses over the medium occur only due to collisions during transmission.

- Each vehicle has a variable buffer size at the MAC layer to adapt with the communication conditions.
- The communication between the RSU and the vehicle is completed before the vehicle goes out of the RSU coverage. No handover is assumed.
- The distance of each vehicle to the RSU is assumed identical, and they all fall within the range of the RSU coverage area.
- The vehicle waits for an Acknowledgement (ACK) packet from the RSU for every message sent.

5.6 ASTC Model

Here we describe the problem introduced in the RSU when the queue service time increases in case of a small network. We start by identifying all the elements that contribute in the calculation of the end-to-end delay, then we illustrate the queue delay problem at the RSU, and finally we present the ASTC algorithm.

5.6.1 End-to-End Delay Analysis

Based on the scenario description, from the moment the message reaches the MAC layer till the instance the vehicle receives an ACK from the RSU, each message undergoes the following delays:

- Processing delay in the vehicle due to the certificate generation and the ECDSA signature of the message. We denote it: D_{Proc}.
- Communication delay. It includes the latency in the backoff phase of the MAC layer, the delay caused by a collided message during the transmission, and the delay of a successful message transmission. We denote it: D_{Tx}

- Queuing delay in the RSU. As described previously, each received message is stored in a queue in the RSU waiting for its turn to be served. We denote it: D_Q

The details of the certificate generation mechanism and the ECDSA signature process is out of the scope of this chapter. However taking their effect into account is important to reflect a realistic operation of the communication protocol. Therefore, we take the case where the size of the key used equal to 224 bits. D_{Proc} is given as:

$$D_{Proc} = 2.5\,ms \tag{5.9}$$

As per our proposed algorithm in [124], the communication delay is the sum of the following elements:

- Delay in the backoff stage which is given as:

$$D_{Boff} = \frac{W-1}{2}\Big[E[boff] \times T_{Timeslot}\Big] \tag{5.10}$$

- Delay due to successful transmission of the data:

$$D_{Suc} = \frac{W-1}{2}\Big[P_{Suc}[Payload] \times T_{suc}\Big] \tag{5.11}$$

- Delay due to repetitive collisions in the channel, which is the major contributor factor at this stage. It results in multiple retransmission due to numerous collisions in the medium which is shown below:

$$D_{Col} = \frac{W-1}{2}\Big[P_{Col}[Payload] \times T_{col}\Big] \tag{5.12}$$

- Delay due to the transmission of the overhead (successful and unsuccessful)

$$D_{Ov} = \frac{W-1}{2}\Big[(P_{Suc}[Ov] \times T_{suc}) + (P_{Col}[Ov] \times T_{col})\Big] \tag{5.13}$$

P_{Suc} and P_{Col} are the probability of successful and unsuccessful transmission respectively. $T_{Timeslot}$, T_{suc}, and T_{col} are the time slot duration, the duration of a successful and unsuccessful transmission respectively. W is the backoff window size. We conclude the total transmission delay is

$$D_{Tx} = D_{Boff} + D_{Suc} + D_{Col} + D_{Ov}. \tag{5.14}$$

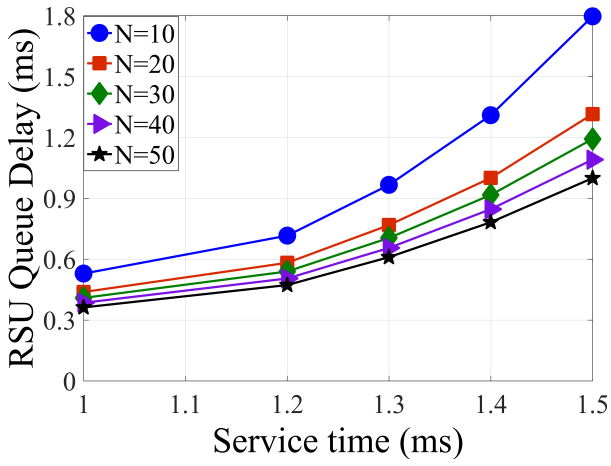

Figure 5.4: RSU queue delay of IEEE 802.11p as function the service time

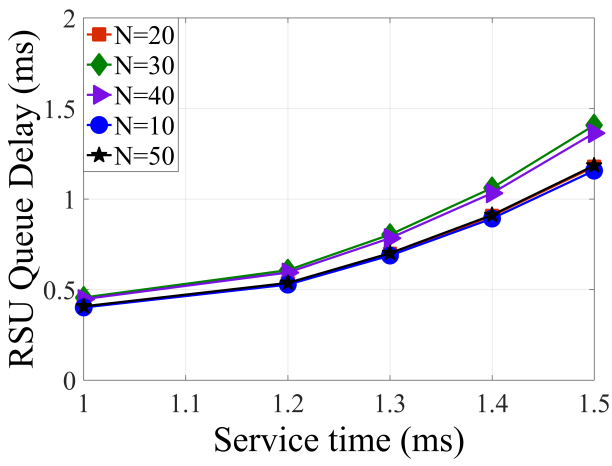

Figure 5.5: RSU Queue delay of the ASTC protocol as function of the service time

All the messages sent by the vehicles have the same format, they carry the same certificate and are signed with the same key size. Therefore, the RSU takes the same amount of time to verify and process all the received messages, that is why the RSU service time is considered deterministic. On the other hand, to depict a realistic scenario, the messages arrival to the RSU are treated as a Poisson process. This queueing behaviour matches the stochastic process of the queue M/D/1.

The message arrival rate (λ) is dictated by the throughput of the communication protocol. In fact, the values of the throughput refer to the number of packets received successfully by the RSU. It is measured in bits per seconds. To convert its value to number of messages (WSM) per second, we need first to determine the size of the WSM. As per the standard [7], the size of the WSM message payload and header is 53 bytes and 19 bytes respectively. However, in our case the WSM is signed and it is joined with a certificate. The size of the certificate is 126 bytes (including 1 byte to identify the type of the certificate). The signature is composed of two parts: r and s [140], each has a size of 28 bytes. So the total size of a signed certified WSM message is:

$$\begin{aligned} L_{WSM} &= L_{payload} + L_{Header} + L_{cer} + L_{sig} \\ &= 53 + 19 + 126 + 56 = 254\,Bytes. \end{aligned} \tag{5.15}$$

The service rate of the RSU (μ) is defined as the number of messages it can verify and process in a second. The service time is the inverse ($\frac{1}{\mu}$), it is the time needed to server one message. In

order to prevent an overflow, the message service rate (service time) should be bigger (smaller) than the message arrival rate (the time elapsed between the arrival of two messages). Therefore, the following in-equation should be satisfied

$$\frac{1}{\mu} > \frac{1}{\lambda} \tag{5.16}$$

The time spent by a message in the queue at the RSU is determined as:

$$D_Q = \frac{1}{2\mu} \times \frac{\lambda}{\mu - \lambda} \tag{5.17}$$

Our objective is to study the influence of the service time on the end-to-end delay of the IEEE 802.11p protocol for different network sizes. Therefore, we vary its value in the range of [1ms, 1.5ms] and we evaluate the queueing delay for network of sizes N = 10, 20, 30, 40 and 50. The input to the queue is, as stated before, the throughput of IEEE 802.11p determined in [124].

Our simulation result is illustrated in Figure 5.4. As we can see the queue delay increases when the service time increases across all network sizes. However, the impact of the growing service time is more severe on the network with small size. For example when $N = 10$, for $\frac{1}{\mu} = 1.5ms$, the RSU queue adds a time overhead of 80% more compared to the network when $N = 50$.

Our solution to this problem is to implement the enhanced IEEE 802.11p-based protocol to mitigate the effect of the additional delay. The enhanced protocol [124] incorporate a buffer at the entry point of the MAC layer to reduce the average delay of the vehicle. Our simulation results demonstrate that the average communication delay is inversely proportional to the size of the introduced MAC buffer, i.e increasing the buffer size tend to decrease significantly the communication delay. We notice also that the declining value of the delay affects more the small size network, which is exactly what we want: to alleviate the influence of the additional queueing delay.

On the other hand, there is a side effect, the enhanced IEEE 802.11p-based protocol improves also the average throughput of the communication. That means it increases the successful message arrival rate to the RSU, which in turns increases the queueing delay at the RSU. However, this delay augmentation is still lower than the delay deduction achieved. But yet in order to mitigate this side

effect, we have to either increase the buffer size at the MAC layer because it results in reducing the communication delay, or to increase the service time at the RSU to shorten the time spent in the queue.

To summarize, we note the following points:

- Higher number of vehicles leads to higher end-to-end delay.
- Larger buffer size at the MAC layer leads to lower end-to-end delay.
- At the same time, larger buffer size at the MAC layer leads to higher throughput, which increases the queueing delay.
- Faster service rate in the RSU queue leads to lower end-to-end delay.

5.6.2 Numerical Analysis

Figure 5.6 and Figure 5.7 show the numerical results of our simulation. In each figure, the transmission delay table shows the delay dropped due to the incorporation of a (or multiple) buffer(s). The RSU Service Time table shows the difference between the delay dropped in the transmission delay table and the delay added due to the RSU queue service time. If the difference is positive, it means that the delay dropped is greater than the delay added. However, if the difference is negative, it means that the delay introduced in the RSU queue is greater than the delay dropped by the buffer at the MAC layer.

The cells highlighted in light green present the cases where the buffer at the MAC layer has compensated for the additional delay encountered by the message at the RSU queue. The cells highlighted in light blue present the cases where the buffer at the MAC layer did not have the desired impact on the system.

From the results obtained we can conclude that, in order to eliminate the effect of the delay at the RSU queue, we should do the following: (we assume that one buffer unit is equal to 512 Bytes)

Transmission delay:	One buffer unit				
N	10	20	30	40	50
Delay: No Buffer	0.27337579	0.369181663	0.422946096	0.458659907	0.484848934
Delay: One Buffer unit	0.040008099	0.067284688	0.094366228	0.120800326	0.146246286
Delay Dropped	0.233367691	0.301896974	0.328579868	0.337859581	0.338602648
RSU Service Time (ms)	1	1.1	1.2	1.3	1.4
N=10	0.361273375	0.421524092	0.511576047	0.650267637	0.873037432
N=20	0.253334426	0.22980588	0.194148675	0.13833508	0.046964818
N=30	0.19600411	0.13264205	0.037183013	-0.111327911	-0.353057652
N=40	0.165732881	0.083920526	-0.039119216	-0.230315385	-0.541576862
N=50	0.14134958	0.04888458	-0.089274518	-0.302383372	-0.646417306

Buf 512 Bytes		
Conclusion	N< 20, add 1 buf	Always
	N=30, add 1 buf	if Mu<1.3
	N=40, 50 add 1 buf	if Mu<1.2

Delay dropped
Delay added

Transmission delay:	2 buffer units				
N	10	20	30	40	50
Delay: No Buffer	0.27337579	0.369181663	0.422946096	0.458659907	0.484848934
Delay: 2 Buffer units	0.026949199	0.041096747	0.055390652	0.069694429	0.08402926
Delay Dropped	0.246426591	0.328084916	0.367555444	0.388965478	0.400819673
RSU Service Time (ms)	1	1.1	1.2	1.3	1.4
N=10	0.493983176	0.601362088	0.755850567	0.983633533	1.331569935
N=20	0.380532468	0.404230242	0.438831429	0.49054326	0.570339365
N=30	0.305772567	0.277671858	0.236496572	0.17468654	0.078761978
N=40	0.26382022	0.206270194	0.121352964	0.007347438	-0.20983169
N=50	0.229830788	0.151154108	0.034866841	-0.141945861	-0.421765033

Buf 1024 Bytes		
Conclusion	N< 30, add 2 buf	Always
	N=40, add 2 buf	if Mu<1.2
	N=50, add 2 buf	if Mu<1.3

Delay dropped
Delay added

Figure 5.6: Numerical analysis 1 of the end-to-end delay

- If the size of network is equal to 10 or 20, add one unit of buffer whatever the value of the service time $\frac{1}{\mu}$.
- If the size of the network is equal to 30, add one unit of buffer if $\frac{1}{\mu} \leq 1.3ms$, or add two units of buffer if $\frac{1}{\mu} \geq 1.3ms$.
- If the size of the network is equal to 40, Add one unit of buffer if $\frac{1}{\mu} \leq 1.2ms$, or add two units of buffer if $\frac{1}{\mu} = 1.3ms$, or add three units of buffer if $\frac{1}{\mu} \geq 1.3ms$.
- If the size of the network is equal to 50, add one unit of buffer if $\frac{1}{\mu} \leq 1.1ms$, or add two units of buffer if $\frac{1}{\mu} = 1.2ms$, or add three buffer units if $\frac{1}{\mu} = 1.3ms$, or add 4 buffer units if $\frac{1}{\mu} = 1.4ms$.

Transmission delay:	3 buffer units				
N	10	20	30	40	50
Delay: No Buffer	0.27337579	0.369181663	0.422946096	0.458659907	0.484848934
Delay: 3 Buffer units	0.0224	0.031925	0.0415	0.051125	0.06085
Delay Dropped	0.25097579	0.337256663	0.381446096	0.407534907	0.423998934
RSU Service Time (ms)	1	1.1	1.2	1.3	1.4
N=10	0.56549666	0.695611791	0.879237794	1.144413472	1.540512905
N=20	0.465461791	0.520368043	0.598504849	0.7118134	0.880493913
N=30	0.381446096	0.381446096	0.381446096	0.381446096	0.381446096
N=40	0.336467715	0.305021059	0.25958449	0.192530717	0.090651879
N=50	0.295968889	0.238839441	0.155843841	0.032435088	-0.157102233
Buf 1536B				Delay dropped	
Conclusion	N<40, add 3 buf Always			Delay added	
	N=50, add 3 buf if Mu<1.4				

Transmission delay	4 buffer units				
N	10	20	30	40	50
Delay: No Buffer	0.27337579	0.369181663	0.422946096	0.458659907	0.484848934
Delay: 4 Buffer units	0.0201	0.027225	0.034425	0.041675	0.049
Delay Dropped	0.25327579	0.341956663	0.388521096	0.416984907	0.435848934
RSU Service Time (ms)	1	1.1	1.2	1.3	1.4
N=10	0.609134864	0.752043058	0.951484295	1.236164702	1.656301146
N=20	0.522245124	0.596614874	0.700712974	0.848875556	1.064812682
N=30	0.44291115	0.465670485	0.497649799	0.543276927	0.609768596
N=40	0.392849751	0.382526045	0.367867207	0.346692229	0.315374346
N=50	0.350948202	0.314226978	0.261762515	0.185372378	0.071198815
Buf 2048B				Delay dropped	
Conclusion	All N, add 4 buf Always			Delay added	

Figure 5.7: Numerical analysis 2 of the end-to-end delay

5.6.3 ASTC Algorithm

Based on the description presented in the previous section, we present our ASTC algorithm (see Algorithm 5.1) In the association phase, and every time the RSU detects an increase in the number of vehicles in the network, it evaluates the number of nodes and measures the queue service time. Based on these two information, the RSU may send a signal to the vehicles to increase their buffer size at the MAC layer. The signal is performed by setting a flag F in the MAC packet to 1. The basic unit size (U) of the MAC buffer (Buf) is set to 512 Bytes. Each time a vehicle receive a signal, it increments its buffer size by one U. The algorithm takes into account the cases where optimal solution can be achieved with less buffer size if the service rate is high enough.

Algorithm 1. ASTC Algorithm in the RSU

// Initialization phase

$Buf \longleftarrow 0$
$U \longleftarrow 512 Bytes$
$F \longleftarrow 0$

//Association phase

RSU estimates N
RSU measures $\frac{1}{\mu}$
if $(N \leq 20) \parallel (N > 30 \ \&\& \ \frac{1}{\mu} \leq 1.2ms)$ **then**
  RSU **set** $Flag \longleftarrow 1$
  RSU signals vehicles
  RSU signals vehicles // Two times buffer increase
  $Buf \longleftarrow Buf + 2 \times U$
elseif $(N \leq 30) \parallel (N > 40 \ \&\& \ \frac{1}{\mu} \leq 1.3ms)$ **then**
  RSU **set** $Flag \longleftarrow 1$
  RSU signals vehicles
  $Buf \longleftarrow Buf + U$
else $(N \leq 40) \parallel (N = 50 \ \&\& \ \frac{1}{\mu} \leq 1.4ms)$ **then**
  RSU **set** $Flag \longleftarrow 1$
  RSU signals vehicles
  $Buf \longleftarrow Buf + U$
end if

5.7 Simulation Results and Analysis

5.7.1 Mobility Impact Study Results and Analysis

The proposed scenario (as shown in Figure 5.1) is simulated using Network Simulator 2 (NS2). We study the effect of the vehicles speed on the end-to-end delay between the vehicle and the smart grid server, taking into account several factors: the authentication and processing delays, the medium access delay, the total delay from the RSU to the smart grid server. Another important metric is the throughput which measures the rate of successfully receiving packets. We conduct two simulation scenarios, in each scenario we assume fixed number of vehicles (20 and 50 vehicles), moving with the same speed, communicating with the RSU. We vary their speed from 60 km/h to 100 km/h (and that is in accordance with the transportation regulations in Ontario Canada) and we observe the impact of the speed on the end-to-end delay as well as on the throughput.

Figure 5.8 illustrates the average throughput of the network as a function of the vehicles speed. Figure 5.8 shows the results of two network sizes: 20 and 50 vehicles. In both networks, the av-

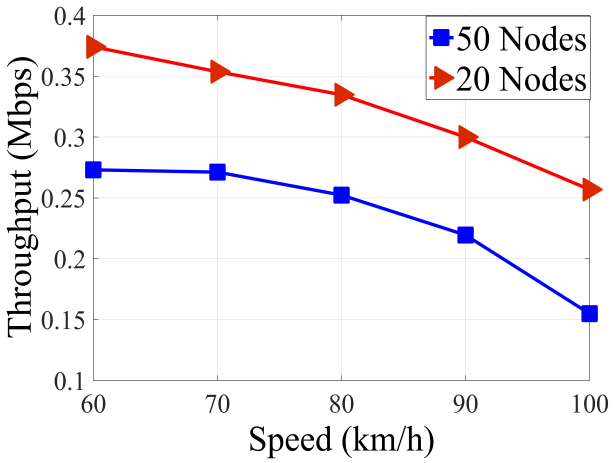

Figure 5.8: Average throughput as function of the vehicles speed

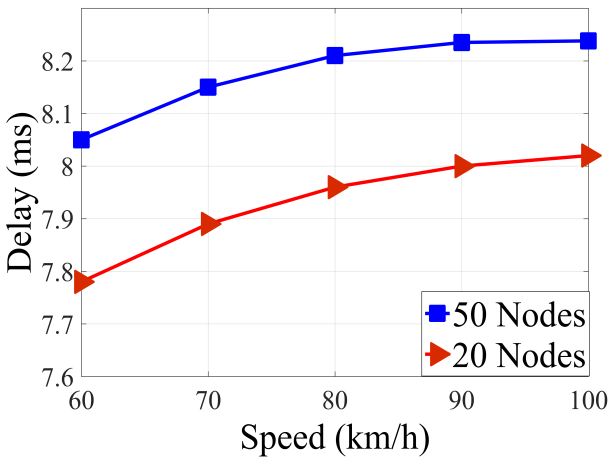

Figure 5.9: Average end-to-end delay as function of the vehicles speed

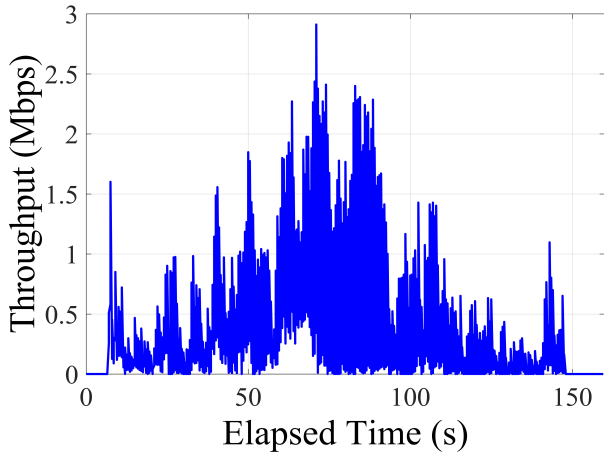

Figure 5.10: Average throughput as function of the simulation time

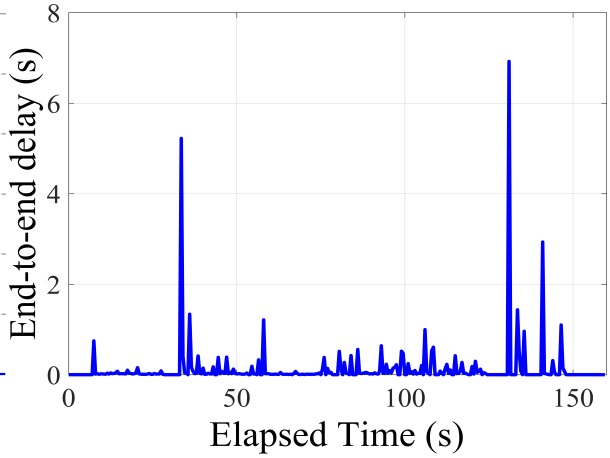

Figure 5.11: Average delay as function of the simulation time

erage throughput value decreases with higher speeds. When the vehicles move slower, they spend more time in the coverage area of the RSU than when they move faster. This allows the slower moving vehicles to exchange more data over longer period than the faster vehicles, which results in greater network throughput.

Another important observation is that the numerical values of the 20-nodes network throughput exceeds the one of the 50-nodes network throughput. The reason behind this observation is that with low density network the contention over the medium is not so intense, which allows the vehicles to gain access to the transmission channel more often, and enable them to transmit more

packets over time. Furthermore, fewer competing vehicles means fewer rate of packet collisions, which signifies greater successful packet transmission rate and therefore higher throughput. On the other hand, in a larger network such as the case of the 50-nodes network, each vehicle has smaller transmission opportunity, therefore it is unable to transmit as much packet as in smaller network. Besides, if it succeeds to transmit a packet, this packet is more probable to experience collision than in the case of a smaller network. Thus, the overall average throughput drops.

Figure 5.9 illustrates the end-to-end delay of the network with different vehicles speed . As we can see, the network with lower number of nodes encounters lower delay than the network with higher number of nodes across all speeds. This result is totally logical since the throughput results in Figure 5.8 shows the opposite operation. In both networks, the end-to-end delay rises with the increase of the speed. In fact, with higher speeds, the vehicles are less exposed to the RSU transmission range, which leads to lower number of transmitted packet compared slower vehicles and thus it increases the latency. We notice also that the end-to-end delay of the low density network is lower than the one of the high density network. This is because lower contention happens, and higher opportunities of packet transmission are available to vehicles in smaller networks.

Figure 5.10 and in Figure 5.11 show the instantaneous network throughput and the end-to-end delay in a network composed of 20 vehicles at the speed of 90 km/h. All the vehicles start moving from a region not covered by the RSU until they leave the RSU since the metric values are zeros at the beginning and at the end of the graphs. Figure 5.10 shows that the throughput behaves in an incremental way at the beginning till it reaches a peak and then it starts decrementing gradually till it reaches zero. In contrast, Figure 5.11 shows the opposite behaviour, the end-to-end delay is relatively high at the extremities and small in the middle. This performance reflects the accuracy of the scenario, at the entrance and at the exit of the RSU coverage field, the vehicles are at that furthest distance from the RSU, which causes the long delay and small throughput. However, as they approach the RSU, their delay shortens and thus their throughput increases. We have repeated the same scenario with various number of vehicles and different speeds, every time we obtain the

same behaviour.

In order to study the impact of the speed on the end-to-end delay, we have to delve into more details. The processing delay and the certificate generation and signing delay are taken from [134], we select the case where the key size is 224 bits. The delay between the RSU and the ITS server depends on the data rate of the fiber optic cable. The delay between the ITS server and the smart grid server is considered constant, and it is taken from [139]. The only delay that varies with the speed is the medium access delay, and it ranges between 0.3 ms to almost 0.4 ms. The total end-to-end delay is then sum of all the above-mentioned delays. We take the highest speed case, with a speed of 100 km/h, the time needed for a vehicle to pass one kilometre is 36 seconds, which is way greater than the time needed to transmit a successful packet. Therefore, we conclude that the speed does not really have an effect on the end-to-end delay in scenarios where PEVs exchange charging information with the smart grid.

Table. 1.1 shows the latency requirements of some delay-sensitive applications in VANET [9]. The latency values show that security-related processing overhead in addition to the transmission delay does not really affect any of these applications.

Based on the data rate values $R = 6\,Mbps$, a vehicle can transmit 6×10^6 bits per second. The packet size is approximately 10^3 bits, which means that a vehicle can send nearly

$$R_p = \frac{R}{L} = \frac{6 \times 10^6}{10^3} = 6 \times 10^3\ pkt/s. \tag{5.18}$$

R_p is the data rate in packets/second. Therefore a vehicle driving with a speed equal to 100 km/h can transmit N_p packets during the 36 seconds:

$$N_p = R_p \times 36 = 216 \times 10^3\ pkts \tag{5.19}$$

So if we want to transmit a large file, such as in the case of a multimedia communication, where the number of packet needed to be sent surpasses the limit of N_p, the service will be interrupted.

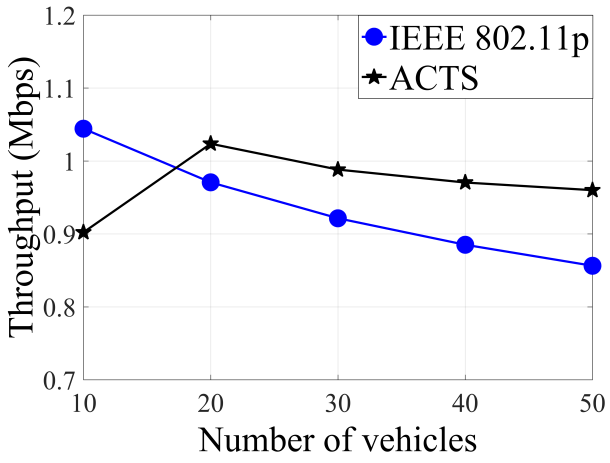

Figure 5.12: ASTC - Average throughput as function of the number of vehicles

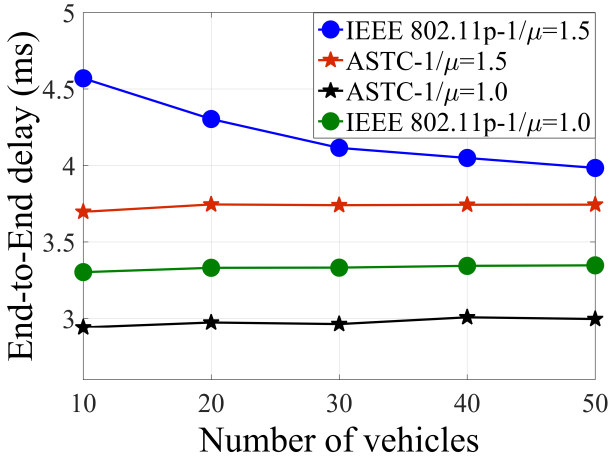

Figure 5.13: ASTC - Average end-to-end delay as function of the number of vehicles

5.7.2 ASTC Results and Analysis

We implement the scenario described previously with our adaptive communication scheme using NS2 tool. The MAC protocol parameter values are set according to the IEEE 802.11p standard. The number of vehicles varies from 10 to 50, the probability of the packet arrival rate from the application layer to the MAC layer is set to 0.5.

Figure 5.5 shows the delay experienced in the RSU queue after applying the ASTC algorithm. We notice first that average end-to-end delay across all network sizes is quasi-homogeneous. The maximum delay difference does not exceed 0.25 ms, however we see that the difference in delay values can reach 0.8 ms without implementing the adaptive algorithm (see Figure 5.4). We notice that the average queueing delay of the network with N=10 vehicles has dropped by 33% from 1.8 ms to 1.2 ms. This proves that our adaptive mechanism has accomplished its required goal, which is reducing the queueing (and consequently the end-to-end) delay of the small size network. This figure shows also that there is a slight increase in the delay values for larger networks ($N >$ 10). That is justified since the average throughput of these network escalates as a result of ASTC scheme.

We present the vehicle average throughput in Figure 5.12. This figure shows that our proposed adaptive mechanism outperforms the conventional IEEE 802.11p protocol in most cases. We notice

that the throughput for the network N=10 decreases a little bit (less than 14%), but it still has an acceptable value. This decrease in value is necessary to adjust the traffic flow reaching the RSU, which result in shorter queuing delay (as we can see in Figure 5.5). Figure 5.12 shows also that the throughput behaviour is incremental then decremental when the network size enlarges. In fact, with small number of vehicles there is enough bandwidth for the vehicles to communicate with minimum competition, which increases the number of successful transmission. However when N continue to increase, the competition over the medium becomes more intense, the number of collision raises and thus the throughput lowers.

Figure5.13 shows the average end-to-end delay of a vehicle in the network. It illustrates and compares two different scenarios with two different values of the RSU service rate. It proves that the end-to-end delay behaves in accord with the RSU service time behaviour, as it displays greater values when the RSU service time inclines, and lower values when it declines. In both scenarios, our ASTC protocol demonstrates better performance as it adaptively decreases the communication end-to-end delay between the vehicles and the RSU.

5.8 Conclusion

In this chapter, we have analysed the effect of speed on the end-to-end delay in a V2G communication environment. We have taken into account the overhead delay caused by issuing the certificate and by processing and verifying the digital signature appended to the message. Our results showed that at high speeds, exchanging simple information between the EV and the charging station will no be affected.

We also proposed a new adaptive service time control in wireless vehicular network that aims to mitigate the effect of the queuing delay in the RSU. In our scenario we took into account all the factors that contribute in the delay measurement. The ASTC scheme have achieved the desired results, it demonstrates lower end-to-end delay and higher average throughput.

In the next chapter, we extend our work to a multi-hop network. We divide the network into

multiple clusters, organized in a hierarchical structure, and we propose tow distributed time synchronization mechanisms to ensure smooth reliable communications between the vehicles and the RSU.

Chapter 6

Distributed Time Synchronization for Large-Scale Vehicular Network

6.1 Introduction

The most common services used in the Intelligent Transportation System (ITS) is promoting traffic safety. To ensure the safety, these services should be highly reliable and should abide to strict communication delay boundaries. The performance of safety-related applications depends on the effectiveness of the Medium Access Control (MAC) protocol. IEEE 802.11p [8] is the protocol that defines the MAC sub-layer in the Vehicular Adhoc Network (VANET). This protocol proves high efficiency in small size networks [141] [142]. However it fails to provide the needed performance in high density vehicular networks because the communication reliability is reduced and the latency is increased due to high congestion, and the Quality of Service (QoS) support is affected due to intense competition. The main challenge that we are attempting to overcome in this chapter is how to design a new MAC mechanism for large-scale network to fulfil the basic requirements of the traffic safety-related services.

All vehicles fall in the communication range of one RSU, however due to the large size of the network, the RSU will not be able to process easily all the vehicle transmissions. In addition to that, it is very difficult to provide any service if a significant number of vehicles attempt to communicate with the RSU at the same time; the high number of packets would collide in the medium, the RSU will be overwhelmed with requests and it will not be able to forward all of them to the internet server. A denial of service state at the RSU will be reached in a very short period of time. Therefore, the network should be organized in way to alleviate these difficulties. Another problem that emerges with large-scale vehicular network is how to synchronize the communications among

the vehicles and the RSU. We have to devise a new synchronization mechanism among the vehicles in order to reduce the delay and increase the successful packet arrival rate and to promote QoS support. In this chapter we present two new distributed time synchronization mechanisms:

- Distributed Time Synchronization (DTS) mechanism for large-scale vehicular network.
- QoS-based Distributed Time Synchronization (QDTS) mechanism for high intensity vehicular network.

We summarize our contributions in this chapter as follows:

- We present cluster-based multi-layer architecture for large-scale vehicular network. Time Slots (TSs) are distributed on per-vehicle basis.
- We present a novel QoS-based distributed time synchronization mechanism. TS distribution enable the QoS support because it is performed based on the AC.
- We design a new time synchronization mechanism based on a distributed approach.
- This is a scalable approach, it prevents the single point of failure problem at the RSU, and it is most convenient for an extended network.
- We thoroughly evaluate the buffering delay in the vehicles.
- We develop a new analytical system to model the operation of this network.
- We develop multiple simulation scenarios.
- We carry out a comprehensive performance analysis taking into account the real values of the parameters set by the standard.

The remainder of this chapter is organized as follows. It is divided to two main sections DTS and QDTS. In each section we describe the proposed model, the model assumption, the analytical

model, the time synchronization mechanism, and the algorithms. These sections are followed by the simulation results and analysis. Finally, we conclude this work.

6.2 Related Work

In the literature, various multi-hop architectures have been proposed for vehicular networking. These architectures vary from IEEE802.11p-based networks, to hybrid architectures combining cellular technologies with Local Area Network (LAN) using Wireless Access for Vehicular Environment (WAVE) architecture [143] [144], to cluster-based VANET networks [145] [146].

In [147], a distributed asynchronous multichannel MAC scheme for large-scale VANETs have been proposed. It is a TDMA-based asynchronous multichannel MAC with distributed TDMA mechanism. This scheme provides concurrent transmissions on many service channels while enabling the broadcast of safety messages on the control channel. To mitigate the effect of the contention among the nodes, the model is introduced with a sublayer above the multichannel MAC mechanism.

In [148], the authors have developed a Clustering Based Multichannel MAC (CBMMAC) protocol. The aim of the research is to increase the throughput for non-real-time data communication, while providing a timely delivery of safety messages. It is very similar to MCTRP, the near-by vehicles moving in the same direction form a group called cluster. Each cluster elect a leader. The CH is the source of synchronization and it controls the cluster. The communication is done using the 7 channels of WAVE. These channels are divided into four groups: the Inter-Cluster Control (ICC) channel, Inter-Cluster Data channel (ICD), a Cluster-Range Control (CRC) channel and four Cluster-Range Data (CRD) channels. Each node in the cluster has two transceivers, the first one is used on the ICC channel and the second one is used on the CRC channel. The former uses an IEEE 802.11 -based contention while the latter uses contention-free TDMA method. The intra-cluster coordination is done on the CRC channel; it allows the allocation of real-time and non-real-time channel using TDMA. This protocol share with the previous protocol the same disadvantage in

relying an essential node to control the whole cluster, which represents a weak point of the design. Another disadvantage is the usage of the all seven channels within the cluster which may lead to high channel utilization and high collision levels especially when two groups are in close proximity.

6.3 Distributed Time Synchronization Mechanism

6.3.1 Model Description

To overcome the challenges due to the presence of a large-scale network, we propose re-organizing the architecture of the network. We partition the network into a combination of small network units, i.e clusters. identified by common characteristics such as velocity, direction, and position. Each cluster elects its own Cluster Head (CH), and the vehicles members (VM) of each cluster communicate directly with CH, not with the Road Side Unit (RSU). Next step would be to organize the CHs into multiple layers, and connect the low layer CHs with the high layer CHs. The last CH layer is connected directly with the RSU. The RSU resides on top of the architecture. So the final outcome of this re-organization process is the formation of multi-layer network composed of multiple clusters. Figure 6.1 shows our proposed architecture. It is a cluster-based mutli-layer architecture. Each layer is composed of multiple CHs. The process of cluster formations and the technique of CH election are out of the scope of this study.
We divide the communication fields into two:

- Intra-cluster communication field: it takes place within the cluster between the CH and the VMs: we denote it IntraField.
- Inter-cluster communication field: it takes place between the CHs residing at different layers: we denote it InterField.

Our proposed model is an extension of our previous proposed star topology architecture developed in [125]. The communication between the VMs and the CH is based on the contention among the

vehicles to gain access to the medium. In addition to that, in the MAC layer of each vehicle there are 4 ACs competing to access the channel. The communication protocol adopted in the IntraField is the IEEE802.11p protocol [8] designed precisely for vehicular communications.

Each CH collects the requests from their local VMs in order to forward them to the next CH located in the next layer. To do so, the CH is equipped with buffer to manage the order of the requests to be transmitted.

In the InterField, the CH of a lower layer communicates with a CH at a higher layer in order to reach the RSU. Each CH is collecting a sizeable amount of data, therefore the communication in the InterField should be free of data loss, otherwise a considerable volume of packets should be re-transmitted leading to a significant drop of performance. As a solution to this problem, we propose that the InterField communication is done using the TDMA technique which is considered a contention free mechanism. The time is divided into segments of time frame, each time frame is partitioned into multiple TSs. The CH at the layer n manages and allocates the required number of TSs for the CHs at the layer $n-1$. It is a decentralized, distributed technique of time synchronization, in which each CH executes the TS distribution process for the CH at the lower layer based on information collected at a previous stage, such as the amount of data transmitted by each CH and the number of CHs participating in the communication. In brief, the role of any intermediate CH is summarized in following main points:

- To receive the VMs transmissions in the IntraField.
- To forward all the transmissions coming from lower layer CHs in the InterField.
- To perform the proper time synchronization among the CHs in lower layer by properly distributing the TSs among the vehicles.
- To manage the buffer.

The target of the data transmitted by all the VMs is to reach the RSU. The RSU processes all the incoming requests, forward some them to a remote Internet server, or responds locally by sending

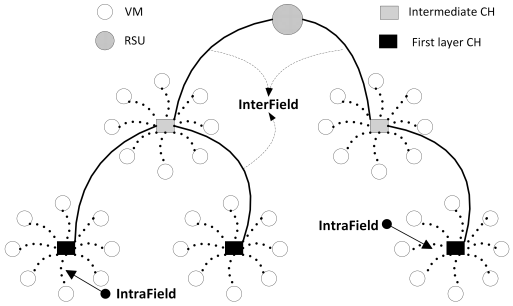

Figure 6.1: Cluster-based Multi-layer topology for vehicular network

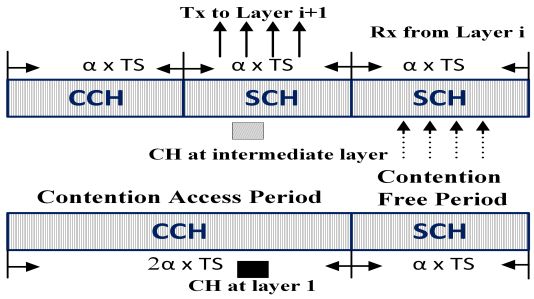

Figure 6.2: Superframe at layer 1 and at intermediate layers in DTS and QDTS

its reply to the VM via the CHs. Another important responsibility for the RSU, is managing the TS distribution among the CH in the next lower layer.

6.3.2 Time Synchronization Mechanism

A major problem to solve is the synchronization among the vehicles as they are communicating, to reduce the average end-to-end delay and increase the successful packets arrival rate. In order to achieve this goal, we divide the time into cycles of Superframes (SF). As per the IEEE 802.11p standard, there are two types of channels: Control Channel (CCH) dedicated for safety-related applications, and Service Channel (SCH) to accommodate all other types of applications. In a single channel mode, a vehicle alternates between one CCH and one SCH. According to the standard [8], the duration of both channels is $T_{CH} = T_{SH} = 50\,ms$. The concept of our proposed system is as the following:

- The SF is composed of one CCH and one SCH. Hence, its size (T_{SF}) is equal to the sum of one CCH and SCH: $T_{SF} = T_{CCH} + T_{SCH} = 100\,ms$ (see Figure 6.2).
- The CCH part is dedicated for the IntraField communication.
- The SCH part is dedicated for the InterField communication.
- The SCH of the first layer CHs is divided into α TS. All the TS in the SCH of the first layer CHs, are dedicated to transmitting data to the CHs in the upper layer.

- The size of the CCH in the CHs that occupy the intermediate layers is reduced by αTS, and the SCH size extends by αTS. The SCH is divided into two halves with the same size (α): One half is dedicated to receiving data from the CHs in the lower layer, the other half is reserved for data transmission to the CH in the upper layer (see Figure 6.2).

- The SCH part acts as a buffer at each CH. We assume that the packets arrival process to this buffer follows the Poisson distribution. The packets arrival rate is equal to the sum of packet transmitting rates of all CHs in the lower layer. The service rate is proportional the medium data transmission rate (R).

- The RSU receives all packets from the CHs at the immediate lower layer and process them. We assume that the RSU has the capability to accommodate all the packets received without buffering delay.

6.3.3 Model Assumption

Cluster formation mechanism is out of the scope of this chapter. However we assume that clusters are organized in a stable manner without having overlapped spaces. We also assume that the process of CH election is already performed [149].
In this proposed model, we assume the following:

- The MAC sub-layer of every vehicle receives the packets from the application layer at a rate of λ packets per second with Poisson distribution.

- All vehicles have the same transmission power potentials, thus all vehicles have the same communication range r which represents the radius of the cluster.

- All vehicles travel approximately at the same average speed. Therefore, mobility does not impact the communications among them.

- An error free medium in which packets are not dropped due to Bit Error Rate (BER).

- All messages have the same length L (in Bytes).
- There is no hidden node problem.
- The propagation delay is negligible compared with other delay values.

6.4 Analytical Model for DTS

The Buffer Delay (BD), in a CH, depends on the number of free available TSs when the tagged VM begins to transmit. If the number of busy TSs in the buffer is small , the BD of the incoming packet will be short. On the other hand, if many vehicles are engaged in the communication simultaneously, more timeslots in the buffer may be occupied which lead to a longer waiting period proportional to the number of busy TSs. The impact of the buffer delay can be greater if the number of busy TSs exceed the SF size (T_{SF}), in which case the tagged packet is forced to wait for a period of one or more SF cycles to transmit. A key point in this study is to estimate the number of occupied timeslots found once the tagged vehicle transmits.

Let p_i be the probability that a specified timeslot TS_i is selected for a vehicle v_i. The probability p_i is independent of all vehicles and all timeslots, therefore we assume that $p_1 = p_2 = ... = p_N = p$. Let θ_j is the probability that j vehicles are trying to access the same timeslot. Our goal is to calculate the average number of vehicles (η) that can select a given timeslot.

The probability θ_j is given as :

$$\theta_j = p^j \times (1-p)^{(N-j)} \tag{6.1}$$

Equation (6.1) means that only j vehicles are competing for the same timeslot and the remaining $N-j$ vehicles are not. To be more accurate, we have to calculate the probability that any j vehicles in the network are trying to take the same timeslot, therefore equation (6.1) should be multiplied by a combination of j out of N. The previous equation becomes:

$$\theta_j = \binom{j}{N} \times p^j \times (1-p)^{(N-j)} \tag{6.2}$$

The average number of vehicles that can access the channel in a given timeslot across the cluster can be calculated as the following:

$$\eta = \sum_{j=0}^{N} j \times \theta_j = \sum_{j=0}^{N} j \times \binom{j}{N} \times p^j \times (1-p)^{(N-j)} \tag{6.3}$$

Taking into account the binomial theorem, we can easily simplify equation (6.3) to the following:

$$\eta = p \times N \tag{6.4}$$

For detailed derivations of Eq. 6.3 and Eq. 6.4 refer to Appendix B.

Let α be the number of timeslots in a buffer. The probability p of selecting one timeslot is given as:

$$p = \frac{1}{\alpha} \tag{6.5}$$

However if a node needs to use multiple TSs (X), p becomes

$$p = \frac{X}{\alpha} \tag{6.6}$$

6.4.1 Average End-to-End Delay

We evaluate our proposed model by calculating the average end-to-end delay from the tagged VM to the sink (RSU). This metric depends on three main factor

- **Intra-cluster communication delay:** $D1$

  The calculation of $D1$ is fully explained and determined in [124]. At this level, we have N VMs communicating with one CH in a star topology. The calculation of D1 depends on the ACs internal competition, the backoff delay that takes place at the MAC sub-layer, and the transmission delay.

  $D1 = D_{BF} + D_{Suc} + D_{Col}$ [124] where, D_{BF}, D_{Suc}, and D_{Col} are the average backoff delay, average successful transmission delay, and average delay caused by one or multiple collisions respectively.

- **Buffering delay in each CH**

  It is the buffering delay that takes place in each CH explained in detail in the next section.

- **Inter-cluster communication delay** $D2$

  It is the transmission delay between the CHs from one layer to another.

The detailed algorithm for the average end-to-end delay is presented in Algorithm 6.1.

6.4.2 Average Buffering Delay

There are five main factors that affect BD:

- **Buffer size:** A buffer with few timeslots can cause a long delay especially if the number of the vehicles in the network is high. In a network with high density, vehicles have to restrain from transmitting their packets awaiting for free timeslots in the buffer.

- **Superframe size:** the size of the SF plays a major role in the performance of the network in terms of delay. In fact, even if there are enough free timeslots in the buffer, if T_{SF} is too short, the vehicle is forced to wait one or many cycles of SFs to complete its communication. On the other hand, if the SF is large to accommodate all transmissions, the buffering delay will be reduced significantly.

- **Availability of free timeslots:** If the packet of the tagged vehicle reaches the CH buffer and there are l TSs reserved by other vehicles, this packet should wait $l \times TS$ before it gets transmitted. The consequences of this factor could be significant if l is larger than the size of the SF.

- **Network size:** This a dominant factor, as extended networks are usually associated with immense amount of data transmissions which flood the buffer quickly.

Algorithm 1. Total Average Delay Estimation in DTS

// Initialization phase

read(N); // Number of VMs
read(α); // Buffer size in CH1
read($\phi[i]$); // Number of CHs at level i
read(T_{SF}); // Size of the SF in TS
read(A); // List of CHs on the path to the RSU
$n \longleftarrow A.legnth()$; // Number of CHs on the path to the RSU.
$TotalAveDelay \longleftarrow D1$;

// Calculation Of The Total Average Delay

for $(i \longleftarrow 1, i \leq n, i++)$ **Do**
  $Rat[i] \longleftarrow Quotient(\phi[i], \alpha)$
  $Rem[i] \longleftarrow Mod(\phi[i], \alpha)$
  if $Rat[i] \leq 1$ **Then**
    $\gamma[i] \longleftarrow \frac{\phi[i]+1}{2}$
    $BD[i] \longleftarrow \gamma[i] \times TS$
  else $BD[i] \longleftarrow Rat[i] \times T_{SF} + \frac{Rem[i]+1}{2} \times TS$
  endif
$TotalAveDelay \longleftarrow TotalAveDelay + BD[i]$
endfor

- **Service time:** With a rapid service, the buffer dispatches packets to the next CH or the RSU quickly, which clears the way for more vehicles to transmit their data. In our case the service time is directly proportional to the size of the frame (L in KB) and inversely proportional to the data transmission rate (R in Mbps). It is given as $\frac{L}{R}$.

In the best case scenario, the packet of the tagged vehicles arrives first to the CH, it waits one TS before being transmitted. If the packet arrives second, it waits two TSs then it proceeds to the next CH or to the sink. Following the same reasoning, a packet waits $l+1$ TSs before accessing the channel if there are l TSs already assigned to different vehicles (assuming that l is less than the size of the SF).

To calculate the average BD, we identify two cases:

- **Case 1:** $l \leq T_{SF}$.

  In this case the average BD is calculated using the following relation:

$$BD = \sum_{i=1}^{l} i \times p^i = \frac{l+1}{2} \tag{6.7}$$

- **Case 2:** $l > T_{SF}$..

  In this case the average BD is calculated using the following relation:

$$BD = Rat \times T_{SF} + \sum_{i=1}^{Rem} i \times Rem^{i} = Rat \times T_{SF} + \frac{Rem+1}{2} \tag{6.8}$$

  Where *Rat* and *Rem* are the quotient and the remainder of $\frac{\alpha}{T_{SF}}$

$$\alpha = Rat \times T_{SF} + Rem \tag{6.9}$$

6.5 QoS-based Distributed Time Synchronization

6.5.1 Model Description

In this model we adopt the same previous architecture, which based on braking down the big network into multiple small-scale networks. See Figure 6.1. The main difference between QDTS and DTS is that this mechanism promotes QoS support in the entire network. The QoS is guaranteed in the intra-cluster communication because we are using IEEE 802.11p protocol, which is equipped with 4 ACs with different priority levels (AC0 has the highest, AC3 has the lowest).The QoS support should also be guaranteed in the inter-cluster communication. For example, the packets arriving from AC0 should not wait long time in the buffer, and should be assigned a TS as soon as possible. In this section we develop three different QoS scenarios: In the first we assign a fixed number of TSs for each AC. In the second we give AC0 the absolute priority by assigning it all the TSs it requires. In the third scheme we use IEEE 802.11p in the inter-cluster communication instead of TDMA.

The main role of any intermediate CH in QDTS mechanism (in addition to those described in the DTS mechanism) is to manage the transmission, reception, buffering and synchronizing the data packets based on their ACs. Our proposed schemes do not take into account the velocity of the vehicles. In [141] we showed that even a vehicle travelling fast (100 km/h) needs 36 seconds to pass by an area covered by an RSU (1 km). Based on that, even with this high velocity, the

Algorithm 2. Total Average Delay Estimation in scenario SC1

// Initialization phase
read(N); // Number of VMs
read(α); // Buffer size in CH1
read($\phi[i]$); // Number of CHs at level i
read(T_{SF}); // Size of the SF in TS
read(A); // List of CHs on the path to the RSU
$n \longleftarrow A.legnth()$;
// Number of CHs on the path to the RSU.
// Number of TS allocated
for each AC in the buffer
$P[0] \longleftarrow \alpha \times 0.4$; $P[1] \longleftarrow \alpha \times 0.3$;
$P[2] \longleftarrow \alpha \times 0.2$; $P[3] \longleftarrow \alpha \times 0.1$;
// P_i is the number of TS
allocated in the buffer for AC_i
// Average delay per AC
$D[0] \longleftarrow D_{AC0}$; $D[1] \longleftarrow D_{AC1}$;
$D[2] \longleftarrow D_{AC2}$; $D[3] \longleftarrow D_{AC3}$;
//D_{ACi} is the InterField average delay of ACi

// Average delay calculation phase
for $(i \longleftarrow 1, i \leq n, i++)$ **Do** // i Number of layers
 for $(j \longleftarrow 0, j \leq 3, j++)$ **Do** // j Number of ACs
  $Rat[i][j] \longleftarrow Quotient(N[i][j], P[j])$
  $Rem[i][j] \longleftarrow Mod(N[i][j], P[j])$
// $N[i][j]$ is the number of packets
for the class AC_j at the layer i
  if $Rat[i][j] \leq 1$ **Then**
   $\gamma[i][j] \longleftarrow \frac{P[j]+1}{2}$
   $BD[i][j] \longleftarrow \gamma[i][j] \times TS$
  else
   $BD[i][j] \longleftarrow Rat[i][j] \times T_{SF} + \frac{Rem[i][j]+1}{2} \times TS$
  endif
 endfor
$D[j] \longleftarrow D[j] + BD[i][j]$
endfor

communication performance is not affected because it only takes few milliseconds to complete a transmission.

6.6 Analytical Model for QDTS

In our study we consider three different scenarios (SC1, SC2 and SC3) in all of which we evaluate the performance of all ACs in terms of average delay and average throughput.

Algorithm 3. Total Average Delay Estimation in scenario SC2

// Initialization phase
read(N); // Number of VMs
read(α); // Buffer size in CH1
read($\phi[i]$); // Number of CHs at level i
read(T_{SF}); // Size of the SF in TS
read(A); // List of CHs on the path to the RSU
$n \longleftarrow A.legnth()$; // Number of CHs on the path to the RSU.
// Number of TS needed for each AC at the first CH
for $(i \longleftarrow 0, i \leq 3, i++)$ **Do** // i Number of AC
read(P[i]); // $P[i]$ is the number of TS needed for AC_i
endof // Average delay per AC
$D[0] \longleftarrow D_{AC0}$; $D[1] \longleftarrow D_{AC1}$;
$D[2] \longleftarrow D_{AC2}$; $D[3] \longleftarrow D_{AC3}$;
//D_{ACi} is the InterField average delay of ACi

// Average delay calculation phase
for $(i \longleftarrow 1, i \leq n, i++)$ **Do** // i Number of layers
if $P[0] \leq \alpha$ **Then**
$\gamma[i][0] \longleftarrow \frac{P[0]+1}{2}$
if $P[1] \leq (\alpha - P[0])$ **Then**
$\gamma[i][1] \longleftarrow \frac{P[1]+1}{2}$
if $P[2] \leq (\alpha - (P[0]+P[1]))$ **Then**
$\gamma[i][2] \longleftarrow \frac{P[2]+1}{2}$
if $P[3] \leq (\alpha - (P[0]+P[1]+P[2]))$ **Then**
$\gamma[i][3] \longleftarrow \frac{P[3]+1}{2}$
else
$\gamma[i][3] \longleftarrow \left[1 + [Quotient(P[3], \alpha) + \frac{Mod(P[3],\alpha)+1}{2}]\right] \times TS$
else
$\gamma[i][2] \longleftarrow \left[1 + [Quotient(P[2], \alpha) + \frac{Mod(P[2],\alpha)+1}{2}]\right] \times TS$
else
$\gamma[i][1] \longleftarrow \left[1 + [Quotient(P[1], \alpha) + \frac{Mod(P[1],\alpha)+1}{2}]\right] \times TS$
else
$\gamma[i][0] \longleftarrow [Quotient(P[0], \alpha) + \frac{Mod(P[0],\alpha)+1}{2}] \times TS$
endif

for $(j \longleftarrow 0, j \leq 3, j++)$ **Do**
$D[j] \longleftarrow D[j] + BD[i][j]$
endfor
endfor

6.6.1 Scenario 1 (SC1)

In SC1, the CH divides the SCH channel into 4 portions x, y, z, and v dedicated for AC0, AC1, AC2 and AC3. Since AC0 possesses the highest priority among the other ACs, it should be granted the highest percentage of TS in the SF, followed by AC1, then AC2 and finally AC3. We assume that at the beginning of each SF the CH coordinates with the lower layer nodes, using CCH, to identify the type of packets that should be expected (to which AC they belong). The following TS distribution among the ACs is assumed in SC1: $x = 40\%\,\alpha$, $y = 30\%\,\alpha$, $z = 20\%\alpha$, *and* $v = 10\%\,\alpha$. In this scenario, we guarantee that the safety-related messages (highest priority) are allowed to pass through the layers faster than the those associated with less important services.

To calculate the average end-to-end delay experienced by an AC we need to calculate the sum of the delay that occurs in the IntraField ($D1$), the delay in the buffer (BD) and the delay in the InterField ($D3$). Due to the space limitation we show the delay calculation of AC0 only. Same approach can be applied on the other ACs.

$D1$ depends on the Backoff Delay (D_{BF}) that takes place in the MAC layer of the VM, the successful packet transmission delay (D_{Suc}) and the unsuccessful packet transmission delay due to a collision (D_{Col}). $D1 = D_{BF} + D_{Suc} + D_{Col}$. We explained in details the calculation of these delays in [125].

$D3$ is the transmission delay from one CH to another at higher layer. $D3$ can be expressed as the following: $D3 = L/R + \delta$, where L is the size of the packets in Bytes, R is the data rate in Mbps and δ is the propagation delay.

$D2$ depends on the buffer size. A larger buffer means that more vehicles (consequently ACs) are able to allocate the number of TSs they need which results in lower delay. It depends also on the network size and the superframe size (T_{SF}). If (T_{SF}) is small, the packets have to wait multiple cycles of SF before they are transmitted, however in the opposite case, the packets will be assigned the required TSs maybe in the first SF which reduce the buffering delay. As for the network size, it is clear that bigger networks create more demands which leads to longer delays in the buffer.

Assuming that the tagged VM sends an AC0 packet to the CH. If this packet arrives first, it waits only one TS before being forwarded. If it comes second, it waits 2 TSs before being transmitted. However if the packet arrives and all x TSs allocated for AC0 are occupied, it should wait for one or multiple full SF (depends on how many packets are ahead in the queue) before being transmitted. Same reasoning is followed if the AC0 of the tagged VMs required l TSs. If the number of available TSs is greater than l, then the data are transmitted in the current SF, hover if the number of TSs available is less than l, the data waits for the next SF to be transmitted.

Therefore, to calculate $D3$ we assume two cases:

- **Case 1**: The number of TS allocated for AC0 (x) is greater than the size required to transmit the data l.

  $D3$ in this case is determined as the following:

  $$D3 = \sum_{i=1}^{l} i \times p^i = \frac{l+1}{2} \tag{6.10}$$

  where p is the probability of selecting an available TS in the buffer. In the case of AC3 it is: $p = \frac{1}{x}$

- **Case 2**: The number of TS allocated for AC0 (x) is less than the size required to transmit the data l.

  $D3$ in this case is determined as the following:

  $$D3 = Rat \times T_{SF} + \sum_{i=1}^{Rem} i \times Rem^i = Rat \times T_{SF} + \frac{Rem+1}{2} \tag{6.11}$$

  where,

  $$x = Rat \times T_{SF} + Rem \tag{6.12}$$

The average buffer delay for the other classes can be calculated following the same method. The detailed algorithm is presented in Algorithm 6.2.

6.6.2 Scenario 2 (SC2)

In this scenario we give AC0 the absolute priority over the other ACs: At any moment a packet of AC0 arrives to the CH, it will have the preference by assigning it a TS instantly, even before the other packets (from the other ACs) that are already present in the buffer. AC1 follows AC0 in terms of priority, which means that at any moment the CH receives a packet associated to AC1, it allocates a TS for it immediately as long as all remaining packets in the buffer belong to AC2 and AC3. Same thing apply to AC2 and AC3. In another word, a packet belonging to AC3 will not be assigned a TS by the CH as long as a minimum of one packet belonging to the other ACs exists in the buffer. Similar to SC1, at the beginning of each SF, the CHs inquire about the packets type via CCH.

In SC2, the buffer delay of AC0 is minimized. Every packet will be transmitted in the current SF, it will never wait for a T_{SF} before being sent. However the buffer delay of AC2 and AC3 are increased, because their packets have to give up their spaces for the higher priority classes.

The buffer delay evaluation is similar to SC1 with different parameters. A detailed algorithm for SC2 is presented in Algorithm 6.3.

6.6.3 Scenario 3 (SC3)

In this scenario, the communication protocol in the InterField is based on the contentions among the CHs (IEEE 802.11p). Our objective is to set this scenario as the benchmark of our study. We need to compare our proposed time synchronization mechanism, which is based on a combination of contention-based within the clusters and contention free outside the clusters, with a fully IEEE 802.11p based network.

In SC3 $D1$ is very similar to $D2$, the only difference is the size of the vehicles involved in the communication in the InterField vs the IntraField. The buffering delay is based on first come first serve technique, a TS will be assigned to the arriving packets regardless of its AC.

Table 6.4: Summary of Notations in DTS and QDTS

Parameter	Value
N	Number of Nodes in a cluster.
α	Number of TS in SCH the first layer CH .
ϕ_i	Number of CH at layer i.
$BD[i]$	Average buffer delay in the CH at layer i.
BD	Buffer Delay.
$A[i]$	List of CHs on the path to the RSU.
γ_i	Average number of slots spent by a packet in a buffer.
θ_i	Probability that i vehicles are selecting TS_i.
η	Average number of vehicle trying to access the channel at a given time.
$P[i]$	Number of TS needed by AC_i.

Table 6.5: Simulation Parameters

Parameter	Value	Parameter	Value
Slot Time	13 μs	Transmission Power	20 dbm
SIFS period	32 μs	bandwidth	10 Mhz
Propagation delay	2 μs	Floor noise	-99 dbm
Data rate	6 Mbps	LL queue size	50 Packets
Packet size	1024 bits	SF	99 ms

6.7 Simulation Results and Analysis

We evaluate our proposed scenarios using Network Simulator 2 (NS2) and We validate the analytical model results using Matlab. In NS2, we build a network composed of three layers, each layer consists of various number of clusters. The head of the network is the RSU. The VMs speed is set between 60 to 80 Km/hour. The communication range of the RSU and the vehicles is set to 500 m. The total number of VMs vary from 5 to 50. We study the performance in terms of average throughput and average latency. We start our analysis with DTS scheme than we present the QDTS scheme results.

6.7.1 DTS Mechanism

In this section we analyse the performance of the DTS mechanism, we specifically interpret the average end-to-end delay and the average network throughput. We compare the results of our proposed mechanism with the standard IEEE 802.11p, and we prove that DTS outperforms IEEE

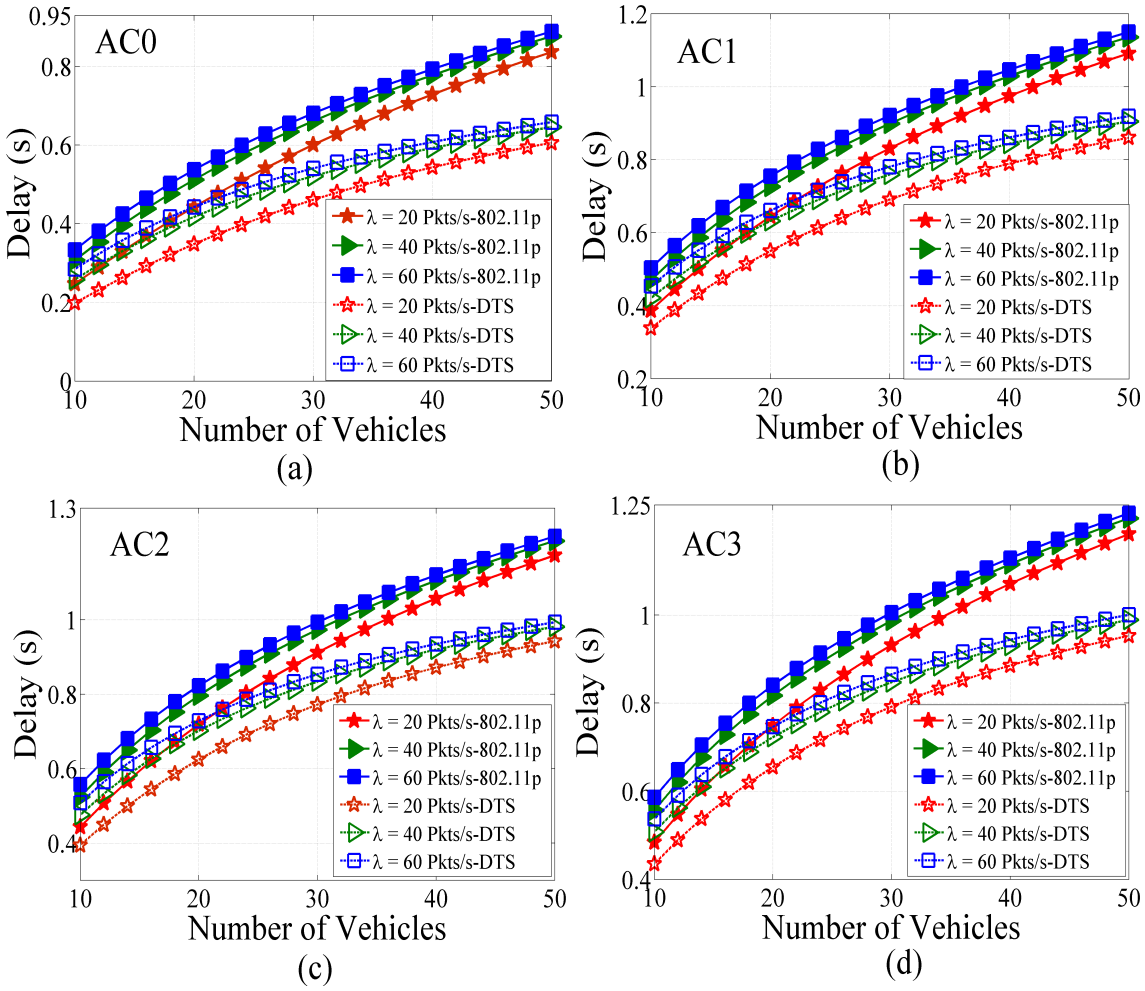

Figure 6.3: Average end-to-end delay for all access categories against the number of vehicles in DTS

802.11p in terms of both performance metrics. We use Matlab to evaluate our analytical model. Table 6.5 shows some of parameters, used in the simulation, set according the IEEE 802.11p standard.

Figure 6.3 shows the average end-to-end delay of the data transmitted from the tagged vehicle to the RSU, versus the number of vehicles, across all ACs for different values of λ. All these figures show that the delay increases as the network size increases. This is because, the buffer at each CH has a limited space shared by all VMs and CHs in the lower layers. Therefore, higher number of VMs in the clusters results in accumulated delays in every CH buffers on the path to the RSU. These figures also show that the average delay increases as the packet arrival rate increases. In fact,

more packets transmitted lead to greater latency in the CH buffers. In addition to that, we notice that the average delay of the higher priority class AC0 is lower than those of all other classes. That is because AC0 has more chances to access the medium and transmit packets compared to the other ACs. Finally, these figures show that DTS present better results than the IEEE 802.11p standard across all number packet arrival rate values and different network sizes. We notice that as the number of vehicles increases in the network, the delay of the DTS mechanism decreases more than the one of the IEEE 802.11p, and this is due to the increased contention among the vehicles in IEEE 802.11p which results in high collision rates among the packets.

Figure 6.4 shows the average throughput of the network. The average throughput is the sum of the average number of packets which arrive successfully to the RSU after passing through the intra-cluster sub-network and the CHs leading to the RSU. Figure 6.4 (b), (c) and (d) show that the average throughput in AC1, AC2 and AC3 declines as the number of VMs grows. This is due to the fact that adding more vehicles to the network increases the level of contention and cause extra packets collision. Figure 6.4 (a) shows that, in the case of AC0, the average throughput increases at the beginning then starts to decline as the number of VMs increments. The reason behind this behaviour is that AC0 has the preference to access the medium and no other AC compete with it during data transmission. Therefore, when the number of VMs is small, the level of external contention is low, and consequently more packets can pass through and reach the CH (and then the RSU) successfully. As the network extends, the level of contention rises and thus more packets fail to reach the CH due to collisions. We notice also that the average throughput of AC0 is greater than the one of the other ACs. Finally, these figures show that DTS mechanism enhances significantly the throughput compared to IEEE 802.11p.

6.7.2 QDTS Mechanism

We use Matlab to evaluate the performance of our system. Table 6.5 shows some of the parameters, used in the simulation, set according the IEEE 802.11p standard. The average end-to-end transmission delay, between the tagged vehicle and the RSU, against the packet arrival rate is il-

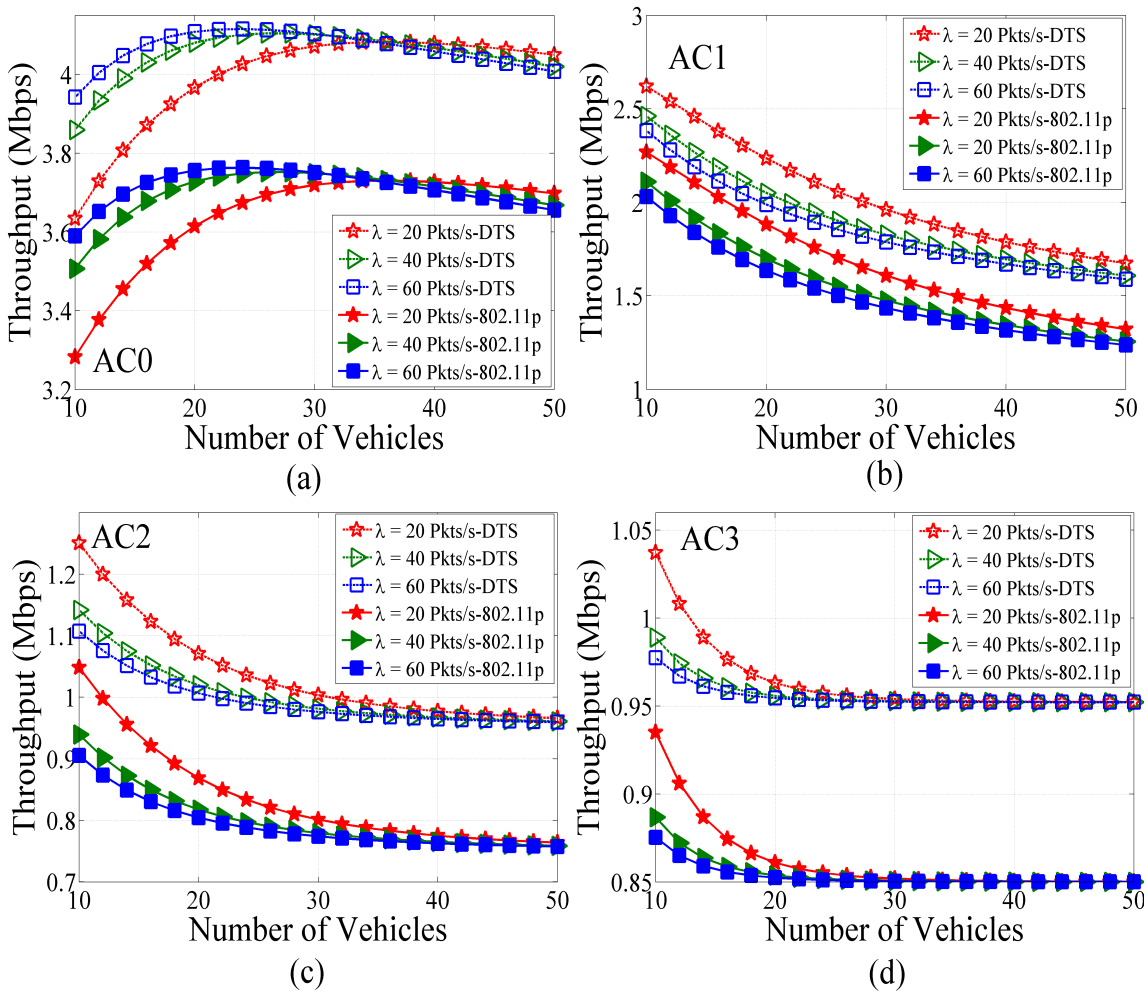

Figure 6.4: Average Throughput for all access categories against the number of vehicles in DTS

lustrated in Figure 6.5. This figure shows the delay results in three different scenarios (SC1, SC2 and SC3) for two cluster sizes (N=40 and N=60 vehicles). Across all ACs, the average delay tends to grow with increasing the number of packets generated at the application layer. In the InterField communication environment, the additional flow of packets, coming from the higher layers to the MAC layer, increases the transmission rate into the medium which rises the level of congestion and results in higher collision rate among the packets. The lost packets, due to collisions, need to be re-transmitted which cost a lot in terms of delay. In fact, in addition to the time already lost due to the transmission failure at the first attempt, each packet should be re-generated and inserted at the MAC queue, then passes through the backoff stage which doubles in size before being transmitted again. At the CH level, although there is no contention, increasing the number of packets

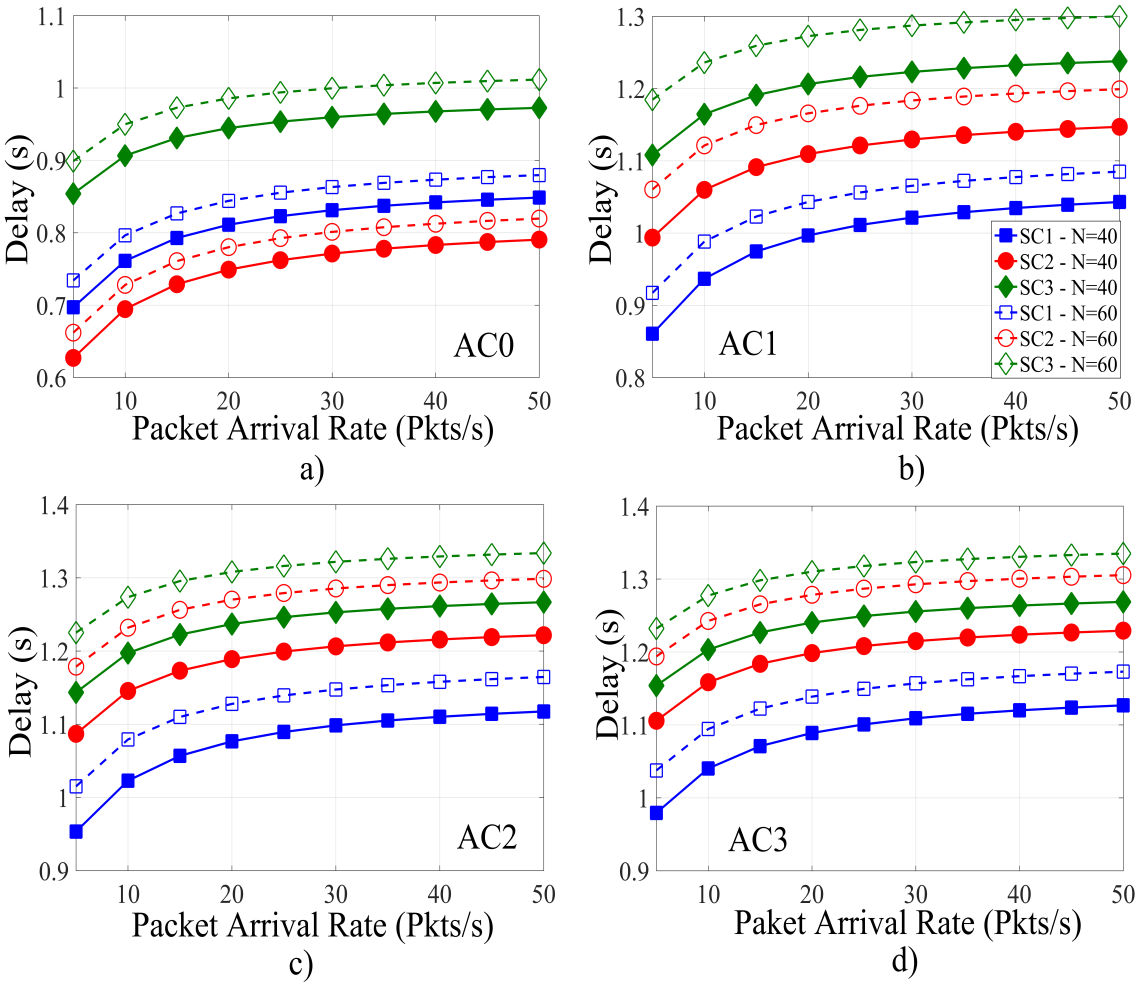

Figure 6.5: Average end-to-end delay for all access categories against the number of vehicles in QDTS

means accumulating these packets in the buffer. The buffer has a limited size, therefore the extra arriving packets to the CH will be scheduled in the next SF or even wait longer to be scheduled after multiple SF.

We notice also that as the number of packets generated increases, the average delay tends to converge toward a fixed value. This is because the medium in the InterField environment and the buffer at the CH level tend to reach their saturation level when the number of packets reaches a certain threshold.

This figure reveals also that the average end-to-end delay gets higher when the size of the cluster gets larger. In fact, as the number of vehicles increase in each cluster, higher packet collision prob-

ability increases in the InterField and higher latency is experienced in the buffer at the CHs in each layer of the architecture. Figure 6.5 shows that across all scenarios, AC0 has the lowest latency values, followed by AC1, then AC2 and finally AC3. This aligns with the fact that AC0 has the highest priority to access the medium in the intra-cluster environment; it does not experience any internal competition with the other ACs. On the other hand, each of the three remaining ACs has to compete before accessing the channel.

Figure 6.5 shows also that the performance of the ACs varies from one scenario to another. For instance, AC0 performs better in the scenario SC2 than in the scenario SC1, while the other ACs are at their best performance in the scenario SC1. In SC2, AC0 has the absolute priority at the CH level: whenever an AC0 flow of packets arrives to the CH, the CH insert them at the head of the queue and allocates immediately the required number of slots needed for them. The CH holds back all other packets coming from other ACs and put them at the end of the queue. However in SC1, whenever the 40% of TS allocated for AC0 are filled, the remaining incoming packets should wait for the next SF to be transmitted.

On the other hand, AC2 and AC3 are the lowest priority classes, therefore allocating a fixed percentage of the buffer size for them, allow them to experience fewer competitions and suffer less from extensive delays. Therefore, the performance of AC2 and AC3 , as shown in Figure 6.5, is more enhanced in the scenario SC1 than the other scenarios, because in SC2 and SC3 they have to wait till all the packets of AC0 and AC1 are transmitted before they take turn in the buffer. One last observation is that the AC2 and AC3 have close numerical values in the scenarios SC2 and SC3 for the same reasons just mentioned.

Figure 6.6 shows the average throughput of the different ACs against the packet arrival rate for two different network size (N=40 and N=60 vehicles) in three different scenarios: SC1, SC2 and SC3. The general appearance of the average throughput in all ACs is decreasing as the number of the generated packets increases. This is due to the intense competition and to the big number of collisions encountered by the rising number of packets being sent in the InterField. It is due

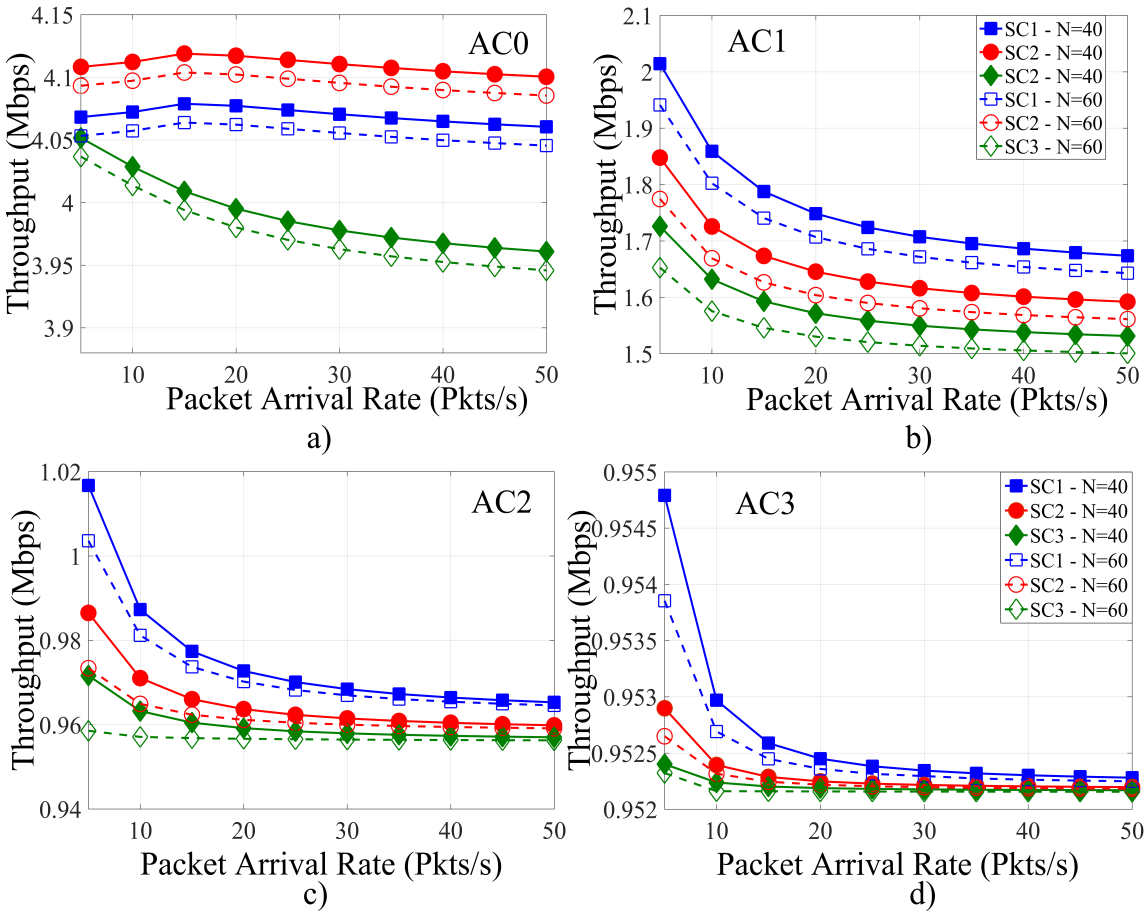

Figure 6.6: Average Throughput for all access categories against the number of vehicles in QDTS

also to the limited size of the buffer in the CH, which leads to longer waiting periods in the queue before a TS is reserved for each packet. Same reasoning can be used to prove that the network's performance in terms of throughput improves more with low size clusters than larger clusters, as less number of vehicles produces smaller amount of packets.

Given that AC0 has the superiority in terms of medium access, Figure 6.6 shows that AC0 outperforms all other ACs in all the scenarios and in both network dimensions. However we notice that AC0 achieves better outcomes in SC2 than in SC1. The reason behind this is that AC0 has unlimited access to the TS at the CH(s) in SC2, while it only gains 40% of the TS in SC1 and therefore additional packet should stay in the queue awaiting the next SF.

We notice also that the services using AC1, AC2 and AC3 would prefer the scenario SC1 over the scenario SC2, because in SC1 they guaranteed reservation of TS in each buffer, while they have to

wait before earning the required number of TS in the other scenarios.

6.8 Conclusion

The IEEE 802.11p standard is optimized to provide the best performance in a relatively small-size VANETs. In a dense scenario, where a large number of vehicles communicate with each other and with RSUs, this protocol may fail to provide the required services because of the high collision rates and long communication delays. In this chapter, we proposed to re-organize large networks by merging nearby vehicles into one cluster, and then establish a multi-layer topology formed by CHs. Two synchronization mechanisms have been proposed, the first one is designed to manage the packets transmitted by the vehicles without considering the AC class, while the second enable QoS support by treating each packet based on its AC class. Different scenarios have been developed.We modelled our proposed mechanism with an analytical system and then we conducted a comprehensive analysis to evaluate the performance. The results showed that in large-scale networks, our mechanism provides low average end-to-end delay and high average throughput values.

As a future work, we intend to add the mobility element to our analytical model, we plan to take into account additional factors that affect the reliability of the communication such as the transmission power/range of the vehicles, the hidden node problem, the status of the channel, and the handover between RSUs.

Chapter 7

Conclusions and Future Research

7.1 Conclusions

In this thesis, we provided an in-depth study of the IEEE 802.11p protocol as the de facto standard for today's Vehicular Ad hoc Network's (VANET) communications. The main characteristics and functionalities of this protocol and how they are related to the safety applications in VANET were described. While it managed to attract the attention due to its features and performance, we could still extend it to achieve improved performance.

By conducting an extensive survey study in the literature, Thorough understanding of the methodologies followed by the research community to enhance the operation of the IEEE 802.11p standard was acquired. this thesis also provided some suggestions on ways to enhance the capabilities of the standard.

In this thesis, multiple efficient, reliable, Quality of Service (QoS)-based IEEE 802.11p-based protocols were developed. We found that, in the context of a star network topology, a new adaptive approach should replace the existing deterministic approach established in the Enhanced Distributed Channel Access (EDCA) and Carrier Sense Multiple Access with Collision Avoidance (CSMA/CA) algorithms. The adaptive-based solution supports the reduction of the end-to-end delay and increase the network reliability. In the context of large-scale networks, in which a multi-layer cluster-based architecture is adopted, novel network management schemes must be put in place to alleviate the additional requirements for processing, buffering, and transmission delays.

We started our study in Chapter 2 where we have carried out a comprehensive performance analysis of the IEEE 802.11p protocol. We have proposed a Markov chain-based analytical model that depicts accurate representation of that protocol. We have taken into accounts the internal collision probability, the unsaturated traffic condition and the freezing probability. Then, we have

extended the proposed model by including a buffer at the entry point of each Access Category (AC) at the Medium Access Control (MAC) layer. We have validated our proposed model by simulating various scenarios and network conditions. From the results obtained we prove that the extended model has enhanced the overall performance of the IEEE 802.11p. We conclude that introducing a buffer before the backoff phase helps in reducing the delay caused by multiple retransmission attempts.

In chapter 3, We have proposed multiple IEEE 802.11p-based adaptive algorithms that can assist in improving the performance of the conventional protocol. The main idea is to replace the deterministic approach adopted by CSMA/CA in the EDCA algorithm with a probabilistic one that takes into account the status of the medium at the time of transmission. In the first part part, we have proposed two adaptive backoff algorithms ABA1 and ABA2. The function of the former is directly proportional to the collision probability, however the function of the latter is exponentially dependant on the collision probability. In the second part, we have presented two Arbitration Inter-Frame Space (AIFS) algorithms to promote the QoS support among the ACs in a vehicle. The first algorithm (SPA) provides strict priority assignment to the ACs, while the second algorithm (AAA) adaptively determines the value of the AIFSs according the congestion level in the medium. We conclude from the simulation results, that adjusting the backoff size and the AIFS values of each AC according to the congestion level in the medium, has a positive impact in terms of increasing the throughput and reducing the end-to-end delay.

In Chapter 4, we have presented a comprehensive analysis of the mobility impact on the end-to-end delay and throughput in Vehicle to Grid (V2G) communication scenarios. We have focused on situations where authentication is performed when essential information, such as payment data, is exchanged between the vehicles and the charging infrastructure. We have also studied the impact of security overhead on the Vehicular to Infrastructure (V2I) communications. We have proposed a new adaptive service time control scheme that aims to adaptively compensate the additional delay introduced in the Road Side Unit (RSU) queue, by changing the size of the buffer at the vehicle

MAC layer. From the results obtained, we conclude that the vehicle speed does not affect the safety-related applications even with the introduction of the security overhead. We also conclude that increasing the buffer size in the MAC layer assists in compensating the additional processing delay in the RSU.

In Chapter 5, we have proposed a distributed time synchronization mechanism and a QoS-based distributed time synchronization for cluster-based multi-layer large vehicular networks. In the former scheme, the cluster head simply distributes the time slots among the vehicles in its cluster, however in latter the cluster head takes into account the AC associated with packets before distributing the time slots. Two QoS-based schemes have been studied, the first one divides the buffer proportionally among the ACs, however in the second one the buffer is allocated first by the highest priority AC packets as long as they exist. As a conclusion, we see that dividing the network into small clusters and adopting two access control protocols (CSMA/CA and TDMA) instead of CSMA/CA alone, contribute in enhancing the performance in terms of latency and network throughput.

In accordance with the research results, it can be concluded that the IEEE 802.11p standard has to be upgraded to employ adaptive approaches that take the network most updated status into its consideration. The values of the Contention Window (CW), AIFS, Transmission Opportunity (TxOP), and other parameters in EDCA should be tuned adaptively as functions of the probability of collision in the medium in order to significantly impact the overall performance.

7.2 Future Research

Based on our research results, the future directions should focus on the following areas:

1. Implementing these enhanced algorithms on platforms and running real experiments in an actual vehicular network, and then evaluating and comparing the results with the theoretical ones. Additional variables may be included such as accounting for the vehicles velocity and see the impact on the performance of our proposed

algorithms.

2. Extending this study to take into account additional factor at the physical layer, such as the bit error rate and the modulation/demodulation schemes.

3. assessment of the impact of the proposed algorithms on the performance of a certain application that comes with specific set of requirements as this study did not focus on a specific application.

4. Study of the privacy and security implications of our proposed algorithms.

5. Developing a cross-layer architecture in which the MAC layer depends on the requirements of the application layer while the latter considers the factors of the MAC layer (Internal competition status, level of congestion in the medium etc..) before initiating the communication process.

Bibliography

[1] "National highway transportation safety administratino(NHSTA), https://crashstats.nhtsa.dot.gov/#/." [Accessed: 2017-02-25].

[2] "Ministry of Transportation, Statistics andData, https://www.tc.gc.ca/eng/motorvehiclesafety/resources-researchstats-menu-847.htm." [Accessed: 2017-02-24].

[3] "OECD territorial reviews: Toronto, Canada, http://www.oecd.org/gov/regional-policy/oecdterritorialreviewstorontocanada.htm." [Accessed: 2017-02-26].

[4] "Fixing America's Surface Transportation Act, https://www.fhwa.dot.gov/fastact/." [Accessed: 2017-02-26].

[5] J. B. Kenney, "Dedicated short-range communications (dsrc) standards in the united states," *Proceedings of the IEEE*, vol. 99, July 2011.

[6] "US Dinistry of transportation Research and Innovative Technology Administration, http://www.its.dot.gov/factsheets/dsrc_factsheet.htm.." [Accessed: 2017-02-25].

[7] "IEEE guide for wireless access in vehicular environments (wave) - architecture," *IEEE Std 1609.0-2013*, pp. 1–78, March 2014.

[8] "IEEE draft standard for amendment to standard [for] information technology-telecommunications and information exchange between systems-local and metropolitan networks-specific requirements-part ii: Wireless lan medium access control (mac) and physical layer (phy) specifications-amendment 6: Wireless access in vehicularenvironments," *IEEE Std P802.11p/D11.0 April 2010*, pp. 1–35, June 2010.

[9] I. Chantaksinopas, W. Lee, A. Prayote, and P. Oothongsap, "Delay-sensitive applications in vanet and seamless connectivity: The limitation of umts network," *Int. J. Comput. Sci. Netw. Sec*, vol. 12, pp. 54–61, oct 2012.

[10] G. Bianchi, "Performance analysis of the ieee 802.11 distributed coordination function," *IEEE Journal on Selected Areas in Communications*, vol. 18, pp. 535–547, March 2000.

[11] M. I. Hassan, H. L. Vu, and T. Sakurai, "Performance analysis of the ieee 802.11 mac protocol for dsrc safety applications," *IEEE Transactions on Vehicular Technology*, vol. 60, pp. 3882–3896, Oct 2011.

[12] D. Malone, K. Duffy, and D. Leith, "Modeling the 802.11 distributed coordination function in nonsaturated heterogeneous conditions," *IEEE/ACM Transactions on Networking*, vol. 15, pp. 159–172, Feb 2007.

[13] M. Torrent-Moreno, D. Jiang, and H. Hartenstein, "Broadcast reception rates and effects of priority access in 802.11-based vehicular ad-hoc networks," in *Proceedings of the 1st ACM International Workshop on Vehicular Ad Hoc Networks*, VANET '04, pp. 10–18, ACM, Oct 2004.

[14] X. Ma and X. Chen, "Delay and broadcast reception rates of highway safety applications in vehicular ad hoc networks," in *2007 Mobile Networking for Vehicular Environments*, pp. 85–90, May 2007.

[15] L. Mokdad, J. Ben-Othman, and P. Ballarini, "Stochastic models for ieee 802.11p," in *2016 IEEE Symposium on Computers and Communication (ISCC)*, pp. 74–78, June 2016.

[16] Y. Xie, I. W. H. Ho, and L. F. Xie, "Stochastic modeling and analysis of unicast performance in 802.11p vanets," in *2015 10th International Conference on Information, Communications and Signal Processing (ICICS)*, pp. 1–4, Dec 2015.

[17] M. Gholibeigi, M. Baratchi, H. van den Berg, and G. Heijenk, "Towards reliable multi-hop broadcast in vanets: An analytical approach," in *2016 IEEE Vehicular Networking Conference (VNC)*, pp. 1–8, Dec 2016.

[18] L. Liu, C. Wang, H. Zhang, and L. Wu, "Variable sch interval multichannel medium access control scheme with unsaturated channel in vanets," in *2016 IEEE International Conference on Communication Systems (ICCS)*, pp. 1–6, Dec 2016.

[19] A. F. M. S. Shah and N. Mustari, "Modeling and performance analysis of the ieee 802.11p enhanced distributed channel access function for vehicular network," in *2016 Future Technologies Conference (FTC)*, pp. 173–178, Dec 2016.

[20] M. A. Togou, L. Khoukhi, and A. S. Hafid, "Throughput analysis of the ieee802.11p edca considering transmission opportunity for non-safety applications," in *2016 IEEE International Conference on Communications (ICC)*, pp. 1–6, May 2016.

[21] J. Zheng and Q. Wu, "Performance modeling and analysis of the ieee 802.11p edca mechanism for vanet," *IEEE Transactions on Vehicular Technology*, vol. 65, pp. 2673–2687, April 2016.

[22] J. R. Gallardo, D. Makrakis, and H. T. Mouftah, "Performance analysis of the edca medium access mechanism over the control channel of an ieee 802.11p wave vehicular network," in *2009 IEEE International Conference on Communications*, pp. 1–6, June 2009.

[23] J. R. Gallardo, D. Makrakis, and H. T. Mouftah, "Mathematical analysis of edca's performance on the control channel of an ieee 802.11p wave vehicular network," *EURASIP J. Wirel. Commun. Netw.*, vol. 2010, pp. 5:1–5:10, Apr. 2010.

[24] J. He, Z. Tang, T. O'Farrell, and T. M. Chen, "Performance analysis of dsrc priority mechanism for road safety applications in vehicular networks," *Wirel. Commun. Mob. Comput.*, vol. 11, pp. 980–990, July 2011.

[25] M. Khatua and S. Misra, "D2d: Delay-aware distributed dynamic adaptation of contention window in wireless networks," *IEEE Transactions on Mobile Computing*, vol. 15, pp. 322–335, Feb 2016.

[26] Y. Kim, Y. H. Bae, D. S. Eom, and B. D. Choi, "Performance analysis of a mac protocol consisting of edca on the cch and a reservation on the schs for the ieee 802.11p/1609.4 wave," *IEEE Transactions on Vehicular Technology*, vol. PP, pp. 1–1, oct 2016.

[27] Q. Yang, S. Xing, W. Xia, and L. Shen, "Modelling and performance analysis of dynamic contention window scheme for periodic broadcast in vehicular ad hoc networks," *IET Communications*, vol. 9, pp. 1347–1354, jul 2015.

[28] C. Han, M. Dianati, R. Tafazolli, R. Kernchen, and X. Shen, "Analytical study of the ieee 802.11p mac sublayer in vehicular networks," *IEEE Transactions on Intelligent Transportation Systems*, vol. 13, pp. 873–886, June 2012.

[29] T. H. Luan, X. Ling, and X. S. Shen, "Provisioning qos controlled media access in vehicular to infrastructure communications," *Ad Hoc Netw.*, vol. 10, pp. 231–242, Mar. 2012.

[30] J. Misic, G. Badawy, and V. B. Misic, "Performance characterization for ieee 802.11p network with single channel devices," *IEEE Transactions on Vehicular Technology*, vol. 60, pp. 1775–1787, May 2011.

[31] W. Sun, H. Zhang, C. Pan, and J. Yang, "Analytical study of the ieee 802.11p edca mechanism," in *2013 IEEE Intelligent Vehicles Symposium (IV)*, pp. 1428–1433, June 2013.

[32] R. Woo, D. S. Han, and J.-H. Song, "Performance analysis for priority based broadcast in vehicular networks," in *2013 Fifth International Conference on Ubiquitous and Future Networks (ICUFN)*, pp. 51–55, July 2013.

[33] Y. Yao, L. Rao, X. Liu, and X. Zhou, "Delay analysis and study of ieee 802.11p based dsrc safety communication in a highway environment," in *2013 Proceedings IEEE INFOCOM*, pp. 1591–1599, April 2013.

[34] P. Wang, F. Wang, Y. J. F. Liu, and X. Wang, "Performance analysis of edca with strict priorities broadcast in ieee802.11p vanets," in *2014 International Conference on Computing*

Networking and Communications (ICNC), pp. 403–407, Feb 2014.

[35] A. Bohm and M. Jonsson, "Supporting real-time data traffic in safety-critical vehicle-to-infrastructure communication," in *2008 33rd IEEE Conference on Local Computer Networks (LCN)*, pp. 614–621, Oct 2008.

[36] J. Li and C. Chigan, "Delay-aware transmission range control for vanets," in *2010 IEEE Global Telecommunications Conference GLOBECOM 2010*, pp. 1–6, Dec 2010.

[37] S. Biswas and J. Miic, "A cross-layer approach to privacy-preserving authentication in wave-enabled vanets," *IEEE Transactions on Vehicular Technology*, vol. 62, pp. 2182–2192, Jun 2013.

[38] . Pual, C. Pereira, A. Aguiar, and J. Gross, "Experimental characterization and modeling of rf jamming attacks on vanets," *IEEE Transactions on Vehicular Technology*, vol. 64, pp. 524–540, Feb 2015.

[39] J. M. Chung, M. Kim, Y. S. Park, M. Choi, S. Lee, and H. S. Oh, "Time coordinated v2i communications and handover for wave networks," *IEEE Journal on Selected Areas in Communications*, vol. 29, pp. 545–558, March 2011.

[40] J. A. Fernandez, K. Borries, L. Cheng, B. V. K. V. Kumar, D. D. Stancil, and F. Bai, "Performance of the 802.11p physical layer in vehicle-to-vehicle environments," *IEEE Transactions on Vehicular Technology*, vol. 61, pp. 3–14, Jan 2012.

[41] M. Mierau, R. Kohrs, and C. Wittwer, "A distributed approach to the integration of electric vehicles into future smart grids," in *2012 3rd IEEE PES Innovative Smart Grid Technologies Europe (ISGT Europe)*, pp. 1–7, Oct 2012.

[42] A. Kovacs, D. Marples, R. Schmidt, and R. Morsztyn, "Integrating evs into the smart-grid," in *2013 13th International Conference on ITS Telecommunications (ITST)*, pp. 413–418, Nov 2013.

[43] J. Rezgui, S. Cherkaoui, and D. Said, "A two-way communication scheme for vehicles charging control in the smart grid," in *2012 8th International Wireless Communications and Mobile Computing Conference (IWCMC)*, pp. 883–888, Sept 2012.

[44] B. Ran, E. Negeri, N. Baken, and F. Campfens, "Last-mile communication time requirements of the smart grid," in *2013 Sustainable Internet and ICT for Sustainability (SustainIT)*, pp. 1–6, Oct 2013.

[45] M. Erol-Kantarci, J. H. Sarker, and H. T. Mouftah, "Communication-based plug-in hybrid electrical vehicle load management in the smart grid," in *2011 IEEE Symposium on Computers and Communications (ISCC)*, pp. 404–409, June 2011.

[46] A. Benslimane, T. Taleb, and R. Sivaraj, "Dynamic clustering-based adaptive mobile gateway management in integrated vanet - 3g heterogeneous wireless networks," *IEEE Journal on Selected Areas in Communications*, vol. 29, pp. 559–570, March 2011.

[47] S. Cspedes and X. Shen, "A framework for ubiquitous ip communications in vehicle to grid networks," in *2011 IEEE GLOBECOM Workshops (GC Wkshps)*, pp. 1231–1235, Dec 2011.

[48] E. Yaacoub, F. Filali, and A. Abu-Dayya, "Qoe enhancement of svc video streaming over vehicular networks using cooperative lte/802.11p communications," *IEEE Journal of Selected Topics in Signal Processing*, vol. 9, pp. 37–49, Feb 2015.

[49] C. M. Huang, C. C. Yang, and Y. C. Lin, "An adaptive video streaming system over a cooperative fleet of vehicles using the mobile bandwidth aggregation approach," *IEEE Systems Journal*, vol. 10, pp. 568–579, June 2016.

[50] A. T. Giang, A. Busson, A. Lambert, and D. Gruyer, "Spatial capacity of ieee 802.11p-based vanet: Models, simulations, and experimentations," *IEEE Transactions on Vehicular Technology*, vol. 65, pp. 6454–6467, Aug 2016.

[51] V. Shivaldova, M. Sepulcre, A. Winkelbauer, J. Gozalvez, and C. F. Mecklenbruker, "A model for vehicle-to-infrastructure communications in urban environments," in *2015 IEEE International Conference on Communication Workshop (ICCW)*, pp. 2387–2392, June 2015.

[52] T. M. Ma, "Improved scheme for the problem of anti-fading of dsrc systems in ieee 802.11p environments," *IET Communications*, vol. 10, pp. 632–640, April 2016.

[53] Y. Mao, F. Yan, and L. Shen, "Multi-round elimination contention-based multi-channel mac scheme for vehicular ad hoc networks," *IET Communications*, vol. 11, pp. 421–427, Feb 2017.

[54] C. Y. Chang, H. C. Yen, and D. J. Deng, "V2v qos guaranteed channel access in ieee 802.11p vanets," *IEEE Transactions on Dependable and Secure Computing*, vol. 13, pp. 5–17, Jan 2016.

[55] F. Borgonovo, A. Capone, M. Cesana, and L. Fratta, "Adhoc: a new, flexible and reliable mac architecture for ad-hoc networks," in *2003 IEEE Wireless Communications and Networking, WCNC 2003*, vol. 2, pp. 965–970, March 2003.

[56] K. Bilstrup, E. Uhlemann, E. G. Ström, and U. Bilstrup, "On the ability of the 802.11p mac method and stdma to support real-time vehicle-to-vehicle communication," *EURASIP J. Wirel. Commun. Netw.*, vol. 2009, Jan 2009.

[57] S. Moser, J. Wei, and F. Slomka, "Towards real-time media access in vehicular ad-hoc networks," in *2012 IEEE Wireless Communications and Networking Conference Workshops (WCNCW)*, pp. 388–392, April 2012.

[58] R. Barr, *An Efficient, Unifying Approach to Simulation Using Virtual Machines*. PhD thesis, Cornell University, Ithaca, NY, USA, 2004. AAI3128231.

[59] F. Yu and S. Biswas, "A self reorganizing mac protocol for inter-vehicle data transfer applications in vehicular ad hoc networks," in *10th International Conference on Information*

Technology (ICIT 2007), pp. 110–115, Dec 2007.

[60] N. Lu, Y. Ji, F. Liu, and X. Wang, "A dedicated multi-channel mac protocol design for vanet with adaptive broadcasting," in *2010 IEEE Wireless Communication and Networking Conference*, pp. 1–6, April 2010.

[61] T. Jiang, Y. Alfadhl, and K. K. Chai, "Efficient dynamic scheduling scheme between vehicles and roadside units based on ieee 802.11p/wave communication standard," in *2011 11th International Conference on ITS Telecommunications*, pp. 120–125, Aug 2011.

[62] M. Hadded, P. Muhlethaler, A. Laouiti, and L. A. Saidane, "A centralized tdma based scheduling algorithm for real-time communications in vehicular ad hoc networks," in *2016 24th International Conference on Software, Telecommunications and Computer Networks (SoftCOM)*, pp. 1–6, Sept 2016.

[63] Y. Kim, M. Lee, and T. J. Lee, "Coordinated multichannel mac protocol for vehicular ad hoc networks," *IEEE Transactions on Vehicular Technology*, vol. 65, pp. 6508–6517, Aug 2016.

[64] K. Liu, J. K. Y. Ng, V. C. S. Lee, S. H. Son, and I. Stojmenovic, "Cooperative data scheduling in hybrid vehicular ad hoc networks: Vanet as a software defined network," *IEEE/ACM Transactions on Networking*, vol. 24, pp. 1759–1773, June 2016.

[65] R. Zhang, X. Cheng, L. Yang, X. Shen, and B. Jiao, "A novel centralized tdma-based scheduling protocol for vehicular networks," *IEEE Transactions on Intelligent Transportation Systems*, vol. 16, pp. 411–416, Feb 2015.

[66] J. Li, H. Zhang, X. Cui, and Y. Xiong, "Analysis on the characteristics of timing synchronization samples of ieee 802.11p," in *2015 International Conference on Identification, Information, and Knowledge in the Internet of Things (IIKI)*, pp. 219–222, Oct 2015.

[67] V. Nguyen, T. Z. Oo, P. Chuan, and C. S. Hong, "An efficient time slot acquisition on the hybrid tdma/csma multichannel mac in vanets," *IEEE Communications Letters*, vol. 20, pp. 970–973, May 2016.

[68] D. N. M. Dang, H. N. Dang, V. Nguyen, Z. Htike, and C. S. Hong, "Her-mac: A hybrid efficient and reliable mac for vehicular ad hoc networks," in *2014 IEEE 28th International Conference on Advanced Information Networking and Applications*, pp. 186–193, May 2014.

[69] X. Jiang and D. H. C. Du, "Ptmac: A prediction-based tdma mac protocol for reducing packet collisions in vanet," *IEEE Transactions on Vehicular Technology*, vol. 65, pp. 9209–9223, Nov 2016.

[70] M. Hadded, P. Muhlethaler, A. Laouiti, R. Zagrouba, and L. A. Saidane, "Tdma-based mac protocols for vehicular ad hoc networks: A survey, qualitative analysis, and open research issues," *IEEE Communications Surveys Tutorials*, vol. 17, pp. 2461–2492, June 2015.

[71] R. S. Tomar, S. Verma, and G. S. Tomar, "Cluster based rsu centric channel access for vanets," in *Transactions on Computational Science XVII*, pp. 150–171, Springer, 2013.

[72] E. Dror, C. Avin, and Z. Lotker, "Fast randomized algorithm for hierarchical clustering in vehicular ad-hoc networks," in *2011 The 10th IFIP Annual Mediterranean Ad Hoc Networking Workshop*, pp. 1–8, June 2011.

[73] A. Upadhyay, M. Sindhwani, and S. K. Arora, "Cluster head selection for ccb-mac protocol by implementing high priority algorithm in vanet," in *2016 3rd International Conference on Electronic Design (ICED)*, pp. 107–112, Aug 2016.

[74] N. Shahin and Y. T. Kim, "An enhanced tdma cluster-based mac (etcm) for multichannel vehicular networks," in *2016 International Conference on Selected Topics in Mobile Wireless Networking (MoWNeT)*, pp. 1–8, April 2016.

[75] A. Yie, Y. Lee, and J. Ahn, "System for lte d2d communications," May 2015. EP Patent App. EP20,140,176,207.

[76] A. Bazzi, B. M. Masini, A. Zanella, and I. Thibault, "Beaconing from connected vehicles: Ieee 802.11p vs. lte-v2v," in *2016 IEEE 27th Annual International Symposium on Personal, Indoor, and Mobile Radio Communications (PIMRC)*, pp. 1–6, Sept 2016.

[77] G. e. m. Zhioua, N. Tabbane, H. Labiod, and S. Tabbane, "A fuzzy multi-metric qos-balancing gateway selection algorithm in a clustered vanet to lte advanced hybrid cellular network," *IEEE Transactions on Vehicular Technology*, vol. 64, pp. 804–817, Feb 2015.

[78] M. Ren, L. Khoukhi, H. Labiod, J. Zhang, and V. Veque, "A new mobility-based clustering algorithm for vehicular ad hoc networks (vanets)," in *NOMS 2016 - 2016 IEEE/IFIP Network Operations and Management Symposium*, pp. 1203–1208, April 2016.

[79] J. H. Kwon, C. Kwon, and E. J. Kim, "Neighbor mobility-based clustering scheme for vehicular ad hoc networks," in *2015 International Conference on Platform Technology and Service*, pp. 31–32, Jan 2015.

[80] E. Dror, C. Avin, and Z. Lotker, "Fast randomized algorithm for 2-hops clustering in vehicular ad-hoc networks," *Ad Hoc Networks*, vol. 11, pp. 2002–2015, sept 2013.

[81] Y. Chen, M. Fang, S. Shi, W. Guo, and X. Zheng, "Distributed multi-hop clustering algorithm for vanets based on neighborhood follow," *EURASIP Journal on Wireless Communications and Networking*, vol. 2015, pp. 1–12, apr 2015.

[82] S. Ucar, S. C. Ergen, and O. Ozkasap, "Multihop-cluster-based ieee 802.11p and lte hybrid architecture for vanet safety message dissemination," *IEEE Transactions on Vehicular Technology*, vol. 65, pp. 2621–2636, April 2016.

[83] S. Ucar, S. C. Ergen, and O. Ozkasap, "Vmasc: Vehicular multi-hop algorithm for stable

clustering in vehicular ad hoc networks," in *2013 IEEE Wireless Communications and Networking Conference (WCNC)*, pp. 2381–2386, April 2013.

[84] S. V. Bana and P. Varaiya, "Space division multiple access (sdma) for robust ad hoc vehicle communication networks," in *ITSC 2001. 2001 IEEE Intelligent Transportation Systems. Proceedings (Cat. No.01TH8585)*, pp. 962–967, Aug. 2001.

[85] J. J. Blum and A. Eskandarian, "A reliable link-layer protocol for robust and scalable inter-vehicle communications," *IEEE Transactions on Intelligent Transportation Systems*, vol. 8, pp. 4–13, March 2007.

[86] R. S. Tomar and S. Verma, "Enhanced sdma for vanet communication," in *2012 26th International Conference on Advanced Information Networking and Applications Workshops*, pp. 688–693, March 2012.

[87] M. Shemshaki and C. Mecklenbruker, "Antenna selection algorithm with improved channel predictor for vehicular environment," in *2014 IEEE 6th International Symposium on Wireless Vehicular Communications (WiVeC 2014)*, pp. 1–5, Sept 2014.

[88] S. Han, K. Zhao, L. Q. Yang, and X. Cheng, "Performance evaluation for multi-antenna vehicular communication based on ieee 802.11p standard," in *2016 International Conference on Computing, Networking and Communications (ICNC)*, pp. 1–5, Feb 2016.

[89] X. Xie, F. Wang, K. Li, P. Zhang, and H. Wang, "Improvement of multi-channel mac protocol for dense vanet with directional antennas," in *2009 IEEE Wireless Communications and Networking Conference*, pp. 1–6, April 2009.

[90] S. Jung, S. Lee, and K. Han, "A dmac protocol to improve spatial reuse by managing the nav table of the nodes in vanet," in *2009 Second International Conference on Computer and Electrical Engineering*, vol. 1, pp. 387–390, Dec 2009.

[91] K. T. Feng, "Lma: Location- and mobility-aware medium-access control protocols for vehicular ad hoc networks using directional antennas," *IEEE Transactions on Vehicular Technology*, vol. 56, pp. 3324–3336, Nov 2007.

[92] Y. Bi, K. H. Liu, L. X. Cai, X. Shen, and H. Zhao, "A multi-channel token ring protocol for qos provisioning in inter-vehicle communications," *IEEE Transactions on Wireless Communications*, vol. 8, pp. 5621–5631, November 2009.

[93] X. Shen, X. Cheng, R. Zhang, B. Jiao, and Y. Yang, "Distributed congestion control approaches for the ieee 802.11p vehicular networks," *IEEE Intelligent Transportation Systems Magazine*, vol. 5, pp. 50–61, winter 2013.

[94] J. Zhang, K. H. Liu, and X. Shen, "A novel overlay token ring protocol for inter-vehicle communication," in *2008 IEEE International Conference on Communications*, pp. 4904–4909, May 2008.

[95] A. Balador, C. T. Calafate, J. C. Cano, and P. Manzoni, "Dtb-mac: Dynamic token-based mac protocol for reliable and efficient beacon broadcasting in vanets," in *2015 12th Annual IEEE Consumer Communications and Networking Conference (CCNC)*, pp. 109–114, Jan 2015.

[96] A. Balador, A. Bhm, C. T. Calafate, and J. C. Cano, "A reliable token-based mac protocol for v2v communication in urban vanet," in *2016 IEEE 27th Annual International Symposium on Personal, Indoor, and Mobile Radio Communications (PIMRC)*, pp. 1–6, Sept 2016.

[97] A. Balador, A. Bohm, E. Uhlemann, C. T. Calafate, and J. C. Cano, "A reliable token-based mac protocol for delay sensitive platooning applications," in *2015 IEEE 82nd Vehicular Technology Conference (VTC2015-Fall)*, pp. 1–5, Sept 2015.

[98] M. Dixit, R. Kumar, and A. K. Sagar, "Vanet: Architectures, research issues, routing protocols, and its applications," in *2016 International Conference on Computing, Communication*

and Automation (ICCCA), pp. 555–561, April 2016.

[99] R. Mishra, A. Singh, and R. Kumar, "Vanet security: Issues, challenges and solutions," in *2016 International Conference on Electrical, Electronics, and Optimization Techniques (ICEEOT)*, pp. 1050–1055, March 2016.

[100] M. Azees, P. Vijayakumar, and L. J. Deborah, "Comprehensive survey on security services in vehicular ad-hoc networks," *IET Intelligent Transport Systems*, vol. 10, pp. 379–388, Jul 2016.

[101] E. A. M. Anita and J. Jenefa, "A survey on authentication schemes of vanets," in *2016 International Conference on Information Communication and Embedded Systems (ICICES)*, pp. 1–7, Feb 2016.

[102] C. A. Kerrache, C. T. Calafate, J. C. Cano, N. Lagraa, and P. Manzoni, "Trust management for vehicular networks: An adversary-oriented overview," *IEEE Access*, vol. 4, pp. 9293–9307, Dec 2016.

[103] M. J. Booysen, S. Zeadally, and G. J. van Rooyen, "Survey of media access control protocols for vehicular ad hoc networks," *IET Communications*, vol. 5, pp. 1619–1631, July 2011.

[104] P. Yang, J. Wang, Y. Zhang, Z. Tang, and S. Song, "Clustering algorithm in vanets: A survey," in *2015 IEEE 9th International Conference on Anti-counterfeiting, Security, and Identification (ASID)*, pp. 166–170, Sept 2015.

[105] C. Cooper, D. Franklin, M. Ros, F. Safaei, and M. Abolhasan, "A comparative survey of vanet clustering techniques," *IEEE Communications Surveys Tutorials*, vol. 19, pp. 657–681, Sept 2017.

[106] L. Chen and C. Englund, "Cooperative intersection management: A survey," *IEEE Transactions on Intelligent Transportation Systems*, vol. 17, pp. 570–586, Feb 2016.

[107] D. Jia, K. Lu, J. Wang, X. Zhang, and X. Shen, "A survey on platoon-based vehicular cyber-physical systems," *IEEE Communications Surveys Tutorials*, vol. 18, pp. 263–284, Mar 2016.

[108] "IEEE standard for telecommunications and information exchange between systems - lan/man specific requirements - part 11: Wireless medium access control (mac) and physical layer (phy) specifications: High speed physical layer in the 5 ghz band," *IEEE Std 802.11a-1999*, pp. 1–102, Dec 1999.

[109] "IEEE standard for information technology–local and metropolitan area networks–specific requirements–part 11: Wireless lan medium access control (mac) and physical layer (phy) specifications - amendment 8: Medium access control (mac) quality of service enhancements," *IEEE Std 802.11e-2005 (Amendment to IEEE Std 802.11, 1999 Edition (Reaff 2003)*, pp. 1–212, Nov 2005.

[110] G. Bianchi, "Ieee 802.11-saturation throughput analysis," *IEEE Communications Letters*, vol. 2, pp. 318–320, Dec 1998.

[111] Y. Xiao, "Enhanced dcf of ieee 802.11e to support qos," in *2003 IEEE Wireless Communications and Networking, 2003. WCNC 2003.*, vol. 2, pp. 1291–1296 vol.2, March 2003.

[112] I. Al-Anbagi, M. Erol-Kantarci, and H. T. Mouftah, "A reliable ieee 802.15.4 model for cyber physical power grid monitoring systems," *IEEE Transactions on Emerging Topics in Computing*, vol. 1, pp. 258–272, Dec 2013.

[113] H. A. Omar, W. Zhuang, A. Abdrabou, and L. Li, "Performance evaluation of vemac supporting safety applications in vehicular networks," *IEEE Transactions on Emerging Topics in Computing*, vol. 1, pp. 69–83, June 2013.

[114] K. M. Alam, M. Saini, and A. E. Saddik, "Toward social internet of vehicles: Concept, architecture, and applications," *IEEE Access*, vol. 3, pp. 343–357, 2015.

[115] X. Y. Tian, Y. H. Liu, J. Wang, W. W. Deng, and H. Oh, "Computational security for context-awareness in vehicular ad-hoc networks," *IEEE Access*, vol. 4, pp. 5268–5279, Aug 2016.

[116] C. Wu, X. Chen, Y. Ji, F. Liu, S. Ohzahata, T. Yoshinaga, and T. Kato, "Packet size-aware broadcasting in vanets with fuzzy logic and rl-based parameter adaptation," *IEEE Access*, vol. 3, pp. 2481–2491, Nov 2015.

[117] X. Li, B. J. Hu, H. Chen, G. Andrieux, Y. Wang, and Z. H. Wei, "An rsu-coordinated synchronous multi-channel mac scheme for vehicular ad hoc networks," *IEEE Access*, vol. 3, pp. 2794–2802, Dec 2015.

[118] X. Ma, J. Zhang, and T. Wu, "Reliability analysis of one-hop safety-critical broadcast services in vanets," *IEEE Transactions on Vehicular Technology*, vol. 60, pp. 3933–3946, Oct 2011.

[119] I.-S. Hwang and H.-H. Chang, "Performance assessment of ieee 802.11 e edcf using three-dimension markov chain model," *Applied Mathematical Sciences*, vol. 2, no. 3, pp. 139–151, 2008.

[120] J. Hu, G. Min, M. E. Woodward, and W. Jia, "A comprehensive analytical model for ieee 802.11e qos differentiation schemes under unsaturated traffic loads," in *2008 IEEE International Conference on Communications*, pp. 241–245, May 2008.

[121] Y. Xiao, "Performance analysis of ieee 802.11e edcf under saturation condition," in *2004 IEEE International Conference on Communications (IEEE Cat. No.04CH37577)*, vol. 1, pp. 170–174, June 2004.

[122] P. E. Engelstad and O. N. Osterbo, "Delay and throughput analysis of ieee 802.11e edca with starvation prediction," in *The IEEE Conference on Local Computer Networks 30th Anniversary (LCN'05)l*, pp. 647–655, Nov 2005.

[123] C. Han, M. Dianati, R. Tafazolli, and R. Kernchen, "Throughput analysis of the ieee 802.11p enhanced distributed channel access function in vehicular environment," in *2010 IEEE 72nd Vehicular Technology Conference - Fall*, pp. 1–5, Sept 2010.

[124] Y. Y. Nasrallah, I. Al-Anbagi, and H. T. Mouftah, "A quality of service model for ieee 802.11p communication protocol in a smart city," in *2014 Global Information Infrastructure and Networking Symposium (GIIS)*, pp. 1–3, Sept 2014.

[125] Y. Y. Nasrallah, I. Al-Anbagi, and H. T. Mouftah, "A realistic analytical model of ieee 802.11p for wireless access in vehicular networks," in *2014 International Conference on Connected Vehicles and Expo (ICCVE)*, pp. 1029–1034, Nov 2014.

[126] "The network simulator NS2, http://www.isi.edu/nsnam/ns/." [Accessed: 2017-02-25].

[127] K. A. Hafeez, L. Zhao, B. Ma, and J. W. Mark, "Performance analysis and enhancement of the dsrc for vanet's safety applications," *IEEE Transactions on Vehicular Technology*, vol. 62, pp. 3069–3083, Sept 2013.

[128] Q. Wu and J. Zheng, "Performance modeling of the ieee 802.11p edca mechanism for vanet," in *2014 IEEE Global Communications Conference*, pp. 57–63, Dec 2014.

[129] F. Kaabi, P. Cataldi, F. Filali, and C. Bonnet, "Performance analysis of ieee 802.11p control channel," in *2010 Sixth International Conference on Mobile Ad-hoc and Sensor Networks*, pp. 211–214, Dec 2010.

[130] A. Bohm and M. Jonsson, "Position-based data traffic prioritization in safety-critical, real-time vehicle-to-infrastructure communication," in *2009 IEEE International Conference on Communications Workshops*, pp. 1–6, June 2009.

[131] W. Alasmary and W. Zhuang, "The mobility impact in ieee 802.11p infrastructureless vehicular networks," in *2010 IEEE 72nd Vehicular Technology Conference - Fall*, pp. 1–5, Sept 2010.

[132] H. Liu, H. Ning, Y. Zhang, Q. Xiong, and L. T. Yang, "Role-dependent privacy preservation for secure v2g networks in the smart grid," *IEEE Transactions on Information Forensics and Security*, vol. 9, pp. 208–220, Feb 2014.

[133] Y. Zhang, S. Gjessing, H. Liu, H. Ning, L. T. Yang, and M. Guizani, "Securing vehicle-to-grid communications in the smart grid," *IEEE Wireless Communications*, vol. 20, December 2013.

[134] J. Petit, "Analysis of ecdsa authentication processing in vanets," in *2009 3rd International Conference on New Technologies, Mobility and Security*, pp. 1–5, Dec 2009.

[135] J. Petit and Z. Mammeri, "Analysis of authentication overhead in vehicular networks," in *WMNC2010*, pp. 1–6, Oct 2010.

[136] I. Al-Anbagi and H. T. Mouftah, "A qos scheme for charging electric vehicles in a smart grid environment," in *2014 IEEE 80th Vehicular Technology Conference (VTC2014-Fall)*, pp. 1–5, Sept 2014.

[137] H. Oh and C. k. Kim, "A robust handover under analysis of unexpected vehicle behaviors in vehicular ad-hoc network," in *2010 IEEE 71st Vehicular Technology Conference*, pp. 1–7, May 2010.

[138] "IEEE standard for wireless access in vehicular environments–security services for applications and management messages - redline," *IEEE Std 1609.2-2016 (Revision of IEEE Std 1609.2-2013) - Redline*, pp. 1–884, March 2016.

[139] K. Papagiannaki, S. Moon, C. Fraleigh, P. Thiran, and C. Diot, "Measurement and analysis of single-hop delay on an ip backbone network," *IEEE Journal on Selected Areas in Communications*, vol. 21, pp. 908–921, Aug 2003.

[140] "ANSI. public key cryptography for the financial services industry:the elliptic curve digital

signature algorithm. ansi x9.62," 1998. [Online; https://www.security-audit.com/files/x9-62-09-20-98.pdf].

[141] Y. Y. Nasrallah, I. Al-Anbagi, and H. T. Mouftah, "Mobility impact on the performance of electric vehicle-to-grid communications in smart grid environment," in *2015 IEEE Symposium on Computers and Communication (ISCC)*, pp. 764–769, July 2015.

[142] Y. Y. Nasrallah, I. Al-Anbagi, and H. T. Mouftah, "Adaptive service time control in wireless access for vehicular environment," in *2015 IEEE International Conference on Ubiquitous Wireless Broadband (ICUWB)*, pp. 1–5, Oct 2015.

[143] H. Abid, T. C. Chung, S. Lee, and S. Qaisar, "Performance analysis of lte smartphones-based vehicle-to-infrastrcuture communication," in *2012 9th International Conference on Ubiquitous Intelligence and Computing and 9th International Conference on Autonomic and Trusted Computing*, pp. 72–78, Sept 2012.

[144] G. Araniti, C. Campolo, M. Condoluci, A. Iera, and A. Molinaro, "Lte for vehicular networking: a survey," *IEEE Communications Magazine*, vol. 51, pp. 148–157, May 2013.

[145] L. Zhang, H. Elsayed, and E. Barka, "A novel location service protocol in multi-hop clustering vehicular ad hoc networks," in *2011 International Conference on Innovations in Information Technology*, pp. 386–391, April 2011.

[146] B. Hassanabadi, C. Shea, L. Zhang, and S. Valaee, "Clustering in vehicular ad hoc networks using affinity propagation," *Ad Hoc Netw.*, vol. 13, pp. 535–548, Feb. 2014.

[147] C. Han, M. Dianati, R. Tafazolli, X. Liu, and X. Shen, "A novel distributed asynchronous multichannel mac scheme for large-scale vehicular ad hoc networks," *IEEE Transactions on Vehicular Technology*, vol. 61, pp. 3125–3138, Sept 2012.

[148] H. Su and X. Zhang, "Clustering-based multichannel mac protocols for qos provisionings over vehicular ad hoc networks," *IEEE Transactions on Vehicular Technology*, vol. 56,

pp. 3309–3323, Nov 2007.

[149] E. Souza, I. Nikolaidis, and P. Gburzynski, "A new aggregate local mobility (alm) clustering algorithm for vanets," in *2010 IEEE International Conference on Communications*, pp. 1–5, May 2010.

Appendix A

Derivations for Chapter 3

In this appendix we derive the equations that determine the stationary probability of any state at stage 0, the stationary probability of the remaining state, and the equation of $b_{0,0}$.

Derivation 1. Stationary probability of a state k at stage 0 ($b_{0,k}$)

From Eq. 3.6 and Eq. 3.7 we can build the following system of equations: beginequation

$$\begin{cases} b_{0,0} = b_{0,1} + \frac{1}{W_0} \times \left(\left(1 - p_c\right) \times \left(\sum_{i=0}^{i=M+f-1} b_{i,0} \right) + b_{M+f,0} \right) \\ b_{0,1} = b_{0,2} + \frac{1}{W_0} \times \left(\left(1 - p_c\right) \times \left(\sum_{i=0}^{i=M+f-1} b_{i,0} \right) + b_{M+f,0} \right) \\ . \\ . \\ b_{0,W_{0-1}} = \frac{1}{W_0} \times \left(\left(1 - p_c\right) \times \left(\sum_{i=0}^{i=M+f-1} b_{i,0} \right) + b_{M+f,0} \right) \end{cases} \tag{A.1}$$

The sum of all equations in Eq. A results in:

$$\begin{aligned} b_{0,0} &= W_0 \times \frac{1}{W_0} \times \left(\left(1 - p_c\right) \times \left(\sum_{i=0}^{i=M+f-1} b_{i,0} \right) + b_{M+f,0} \right) \\ \Leftrightarrow b_{0,0} &= \left(\left(1 - p_c\right) \times \left(\sum_{i=0}^{i=M+f-1} b_{i,0} \right) + b_{M+f,0} \right) \end{aligned} \tag{A.2}$$

The sum of k equations in Eq. A results in:

$$\begin{aligned} b_{0,0} &= b_{0,k} + k \times \frac{1}{W_0} \times \left(\left(1 - p_c\right) \times \left(\sum_{i=0}^{i=M+f-1} b_{i,0} \right) + b_{M+f,0} \right) \\ \Leftrightarrow b_{0,0} &= b_{0,k} + k \times \frac{1}{W_0} \times b_{0,0} \\ \Leftrightarrow b_{0,k} &= \frac{W_0 - k}{W_0} \times b_{0,0} \end{aligned} \tag{A.3}$$

Derivation 2. Stationary probability of any state $b_{i,k}$ where $i \neq 0$

From Eq. 3.9 and Eq. 3.10 we can build the following system of equations:

$$\begin{cases} b_{i,0} = b_{i,1} + b_{i-1,0} \times \frac{p_c}{W_i} \\ b_{i,1} = b_{i,2} + b_{i-1,0} \times \frac{p_c}{W_i} \\ . \\ . \\ b_{i,W_{i-1}} = b_{i-1,0} \times \frac{p_c}{W_i} \end{cases} \tag{A.4}$$

The sum of all the equations results in: $b_{i,0} = b_{i-1,0} \times p_c$, And hence we obtain the equation

$$b_{i,0} = b_{0,0} \times p_c^i. \tag{A.5}$$

The sum of k equations in Eq. A.4 results in:

$$\begin{aligned} b_{i,0} = b_{i,k} + k \times b_{i-1,0} \times \frac{p_c}{W_i} = b_{i,k} + k \times \frac{b_{i,0}}{p_c} \times \frac{p_c}{W_i} \\ \Leftrightarrow b_{i,k} = b_{i,0} \times \frac{W_i - k}{W_i} \Leftrightarrow b_{i,k} = \frac{W_i - k}{W_i} \times p_c^i \times b_{0,0}. \end{aligned} \tag{A.6}$$

Derivation 3. Stationary probability $b_{0,0}$

The sum of all the stationary probabilities of all the model's state is normally equal to one: $\sum_{i=0}^{M+f} \sum_{k=0}^{W_i-1} b_{i,k} + b_I = 1$

b_I is determined in Eq. 3.13 and Eq. 3.14. In this section, we derive the remaining part of the equation.

$$\sum_{i=0}^{M+f} \sum_{k=0}^{W_i-1} b_{i,k} = \sum_{i=0}^{M+f} \sum_{k=0}^{W_i-1} b_{i,0} \times \frac{W_i - k}{W_i} = \sum_{i=0}^{M+f} b_{i,0} \sum_{k=0}^{W_i-1} \frac{W_i - k}{W_i} \tag{A.7}$$

We calculate first the second sum of Eq. A.7.

$$\begin{aligned}
&\sum_{k=0}^{W_i-1} \frac{W_i-k}{W_i} = \frac{1}{W_i} \times \sum_{k=0}^{W_i-1} (W_i-k) \\
&= \frac{1}{W_i} \times \Big[W_i + (W_i-1) + (W_i-2) + ... + (W_i-(W_i-1)) \Big] \\
&= \frac{1}{W_i} \times \Big[\big(\underbrace{W_i + W_i + ... + W_i}_{W_i} \big) - \big(1+2+3+....+W_i-1 \big) \Big] \\
&= \frac{1}{W_i} \times \Big[W_i^2 - \sum_{k=1}^{W_i-1} k \Big] = \frac{1}{W_i} \times \Big[W_i^2 - \frac{W_i \times (W_i-1)}{2} \Big] = \frac{W_i+1}{2}
\end{aligned} \tag{A.8}$$

Taking into account Eq. A.8, Eq. A.5, $W_i = 2^i \times W_0$ if $i \leq M$ and $W_i = W_M$ if $M+1 \leq i \leq M+f$, the equation Eq. A.7 becomes:

$$\begin{aligned}
\sum_{i=0}^{M+f} \sum_{k=0}^{W_i-1} b_{i,k} &= \frac{b_{0,0}}{2} \times \Big[\sum_{i=0}^{M+f} (p_c^i + p_c^i \times W_i) \Big] = \frac{b_{0,0}}{2} \times \Big[\sum_{i=0}^{M+f} p_c^i + \sum_{i=0}^{M+f} (p_c^i \times W_i) \Big] \\
&= \frac{b_{0,0}}{2} \times \Big[\sum_{i=0}^{M+f} p_c^i + \sum_{i=0}^{M} (p_c^i \times 2^i \times W_0) + \sum_{i=M+1}^{M+f} (p_c^i \times W_M) \Big] \\
&= \frac{b_{0,0}}{2} \times \Big[\frac{1-p_c^{M+f+1}}{1-p_c} + W_0 \times \big(\frac{1-(2 \times p_c)^{M+1}}{1-2 \times p_c} \big) + W_M \times \big(\frac{p_c^{M+1} - p_c^{M+f+1}}{1-p_c} \big) \Big]
\end{aligned} \tag{A.9}$$

Appendix B

Derivations for Chapter 6

In this appendix we show the detailed derivation of the average number of vehicles that can access the channel in a given timeslot formulated in Eq. 6.3 and Eq. 6.4.

We start with a list of formulas and derivations that we need in our derivations.

Formula 1. The combinations formula

$$\binom{N}{k} = \frac{N!}{(k!) \times (N-k)!)} = \frac{1 \times 2 \times 3... \times (N-1) \times N}{(1... \times (k-1) \times k)(1 \times 2 \times 3.... \times (N-k+1) \times (N-k)} \tag{B.1}$$

Formula 2. The second combinations formula

We can formulate $\binom{N}{k}$ as function of $\binom{N-1}{k-1}$ from Eq. B.1.

$$\begin{aligned} \binom{N}{k} &= \frac{N}{k} \times \left(\frac{1 \times 2 \times 3... \times (N-1)}{(1... \times (k-1))(1 \times 2 \times 3.... \times (N-k+1) \times (N-k)}\right) \\ \Leftrightarrow \binom{N}{k} &= \binom{N-1}{k-1} \times \frac{N}{k} \end{aligned} \tag{B.2}$$

Formula 3. The binomial formula

$$(X+Y)^n = \sum_{k=0}^{n} \binom{n}{k} \times X^{n-k} \times Y^k \tag{B.3}$$

Detailed Derivation of η

We apply Formula 1. and Formula 2. on Eq. 6.3, we get the following:

$$\begin{aligned}
\eta &= \sum_{j=0}^{N} j \times \theta_j = \sum_{j=0}^{N} j \times \binom{N}{j} \times p^j \times (1-p)^{(N-j)} \\
&= \sum_{j=1}^{N} j \times \binom{N-1}{j-1} \times \frac{N}{j} \times p^j \times (1-p)^{(N-j)} \\
&= 1 \times \binom{N-1}{0} \times \frac{N}{1} \times p \times (1-p)^{(N-1)} + 2 \times \binom{N-1}{1} \times \frac{N}{2} \times p^2 \times (1-p)^{(N-2)} + ...+ \\
&+ (N-1) \times \binom{N-1}{N-2} \times \frac{N}{N-1} \times p^{(N-1)}) \times (1-p) + N \times \binom{N-1}{N-1} \times \frac{N}{N} \times p^N. \\
&= p \times N \times \left[\binom{N-1}{0} \times (1-p)^{(N-1)} + \binom{N-1}{1} \times p \times (1-p)^{(N-2)} + ... \binom{N-1}{N-1} \times p^{(N-1)} \right]
\end{aligned} \tag{B.4}$$

We apply Formula 3. on Eq. B.4 and we get Eq. 6.4

$$\begin{aligned}
\eta &= p \times N \times \left[\binom{N-1}{0} \times (1-p)^{(N-1)} + \binom{N-1}{1} \times p \times (1-p)^{(N-2)} + ... \binom{N-1}{N-1} \times p^{(N-1)} \right] \\
&= p \times N \times \left[p + (1-p) \right]^{(N-1)} \\
&\Leftrightarrow \eta = p \times N.
\end{aligned} \tag{B.5}$$